

Distributed MAC Protocol for Networks with Multipacket Reception Capability and Spatially Distributed Nodes

by

Guner Dincer CELIK

Submitted to the Department of Electrical Engineering and Computer Science

in partial fulfillment of the requirements for the degree of

Master of Science in Electrical Engineering and Computer Science

at the

MASSACHUSETTS INSTITUTE OF TECHNOLOGY

May 2007

© Massachusetts Institute of Technology 2007. All rights reserved.

Author
Department of Electrical Engineering and Computer Science
May 11, 2007

Certified by
Eytan Modiano
Associate Professor
Thesis Supervisor

Accepted by
Arthur C. Smith
Chairman, Department Committee on Graduate Students

Distributed MAC Protocol for Networks with Multipacket Reception Capability and Spatially Distributed Nodes

by

Guner Dincer CELIK

Submitted to the Department of Electrical Engineering and Computer Science
on May 11, 2007, in partial fulfillment of the
requirements for the degree of
Master of Science in Electrical Engineering and Computer Science

Abstract

The physical layer of future wireless networks will be based on novel radio technologies such as Ultra-Wideband (UWB) and Multiple-Input Multiple-Output (MIMO). One of the important capabilities of such technologies is the ability to capture a few packets simultaneously. This capability has the potential to improve the performance of the MAC layer. However, we show that in networks with spatially distributed nodes, reusing MAC protocols originally designed for narrow-band systems (e.g., CSMA/CA) is inefficient. It is well known that when networks with spatially distributed nodes operate with such MAC protocols, the channel may be captured by nodes that are near the destination. We show that when the physical layer enables multi-packet reception, the negative implications of reusing the legacy protocols include not only such unfairness but also a significant throughput reduction. We present a number of simple alternative backoff mechanisms that attempt to overcome the throughput reduction phenomenon. We evaluate the performance of these mechanisms via exact analysis, approximations, and simulation, thereby demonstrating that they usually outperform the legacy backoff mechanisms. We then discuss the implications of the results on developing realistic MAC protocols for networks with a multi-packet reception capability and in particular for UWB networks.

Thesis Supervisor: Eytan Modiano

Title: Associate Professor

Acknowledgments

I am profoundly thankful to my advisor, Prof. Eytan Modiano, and Post Doc. Assoc. Gil Zussman for their support in this work, for their guidance that helped me continue my research in the right direction and for their friendly mood that makes it enjoyable to work with them.

I also would like to thank my family for their endless moral support throughout my career.

Finally, this work was supported in part by ONR under grant N000140610064, and by a grant from Draper Laboratory.

Contents

1	Introduction	17
2	Related Work	23
3	System Description and Assumptions	29
3.1	Backward Protocol	32
4	Examples	33
4.1	Aloha with Two Distances: Example 1	33
4.2	Aloha with Two Distances: Example 2	36
4.3	Backward Protocol with Random Distances and Single Capture: Example 3	37
5	Protocol Analysis	41
5.1	Random Locations Without Fading	41
5.2	Deterministic Locations - Without Fading	46
5.2.1	Exact Model With Nodes at One of Two Different Locations	46
5.2.2	Basic Approximate Model	61
5.2.3	Enhanced Approximate Model	65
5.3	Deterministic Locations-With Fading	79
5.4	Random Locations With Fading	82
5.4.1	Approximating $p_c(r)$ Using $\tau(r)$	83
5.4.2	Approximating $p_c(r)$ Using Jensen's Inequality	85
6	New Protocols	89

6.1	Backward Model with Forced Idle Periods	90
6.2	Backward Model with Dynamic Contention Windows	94
7	Performance Evaluation and Simulations	97
7.1	Deterministic Locations Without Fading	98
7.2	Random Locations Without Fading	102
7.3	Random Locations With Fading Simulation	103
7.4	Backward Model with Forced Idle Periods	107
7.5	Backward Model with Dynamic Contention Windows	108
8	Conclusion and Future Work	115
A	Analytical solution of (4.3) and (4.4) in the case of two nodes	117
B	The Transition Probabilities of The 1-Dimensional Markov Chain of Section	
	5.2.1	119
C	Edmundson-Madansky Inequality	121

List of Figures

1-1	An example scenario where 1 nearby node captures the channel (since its signal is greater) and blocks 4 faraway nodes. The transmitting nodes are indicated with arrows. This is a very inefficient use of the network resources if the maximum number of simultaneously received transmissions in the network is greater than 1, i.e., if the receiver is capable of receiving multiple packets at a time.	18
3-1	The Single User State Diagram, <i>S</i> : Success, <i>I</i> : Idle, <i>F</i> : Failure, <i>AS</i> : After Success, <i>AF</i> : After Failure.	32
4-1	Simple spatial distribution.	34
4-2	Throughput plot for the system in Example-1 for $n_1 = 1, n_2 = 3$ and $z = 0.2$	36
4-3	Throughput plot for the system in Example-2 for $n_1 = 2, n_2 = 6$ and $z = 0.2$	37
4-4	The transmission probability and the throughput as a function of distance under the forward ($p_{ts} = 0.2$ and $p_{tf} = 0.05$) and the backward ($p_{ts} = 0.05$ and $p_{tf} = 0.2$) backoff mechanisms for $\alpha = 2$ and uniform distribution of 12 nodes on a disk.	39
5-1	System Markov Chain in Example-2, Case-a. ss: both nodes are successful, sf: node-1 is successful and node-2 is failed in its last attempt.	43
5-2	System Markov Chain in Example-2, Case-b.	43
5-3	The comparison of the transmission probability and the throughput of the exact and the approximate analysis for $\alpha = 2, p_{ts} = 0.2$ and $p_{tf} = 0.05$ (i.e., for the forward model case) and uniform distribution of 2 nodes on a disk.	46
5-4	The Markov Chain for the analysis in Section 5.2.1 for $n_1 = 6, n_2 = 10$ and $z = 0.2$. Note that only some of the transition probabilities of the state $(n_1, n_2) = (4, 6)$ are shown.	48

5-5	Throughput plot for deterministic locations case with $r_1 = 1, r_2 = 2, n_1 = 1, n_2 = 5$ and $z = 0.2$	58
5-6	Throughput of the faraway nodes for deterministic locations case with $r_1 = 1, r_2 = 2, n_1 = 1, n_2 = 5$ and $z = 0.2$	58
5-7	Throughput plot for deterministic locations case with $r_1 = 1, r_2 = 2, n_1 = 2, n_2 = 10$ and $z = 0.2$	59
5-8	Throughput of the faraway nodes for $n_1 = 2, n_2 = 10$ and $z = 0.2$	59
5-9	Throughput plot for deterministic locations case with $r_1 = 1, r_2 = 2, n_1 = 6, n_2 = 10$ and $z = 0.2$	60
5-10	Throughput of the faraway nodes for deterministic locations case with $r_1 = 1, r_2 = 2, n_1 = 6, n_2 = 10$ and $z = 0.2$	60
5-11	Throughput plot for $n_1 = 1, n_2 = 5$ and $z = 0.2$ using the Basic Approximate Model. . .	62
5-12	Throughput plot for deterministic locations case with $r_1 = 1, r_2 = 2, n_1 = 2, n_2 = 10$ and $z = 0.2$ using the Basic Approximate Model.	63
5-13	Throughput plot for deterministic locations case with $r_1 = 1, r_2 = 2, n_1 = 6, n_2 = 10$ and $z = 0.2$ using the Basic Approximate Model.	65
5-14	Network Structure, Enhanced Approximate Model.	66
5-15	Throughput plot for deterministic locations case with $r_1 = 1, r_2 = 2, n_1 = 1, n_2 = 5$ and $z = 0.2$ using the Enhanced Approximate Model.	75
5-16	Throughput plot for deterministic locations case with $r_1 = 1, r_2 = 2, n_1 = 2, n_2 = 10$ and $z = 0.2$ using the Enhanced Approximate Model.	75
5-17	Throughput plot for deterministic locations case with $r_1 = 1, r_2 = 2, n_1 = 6, n_2 = 10$ and $z = 0.2$ using the Enhanced Approximate Model.	76
5-18	Throughput plot for deterministic locations case with $r_1 = 1, r_2 = 2, r_3 = 4, n_1 = 1, n_2 = 2, n_3 = 4$ and $z = 0.2$ using the Enhanced Approximate Model.	77
5-19	Throughput plot of the users at distance 2 for deterministic locations case with $r_1 = 1, r_2 = 2, r_3 = 4, n_1 = 1, n_2 = 2, n_3 = 4$ and $z = 0.2$ using the Enhanced Approximate Model.	77

5-20	Throughput plot of the users at distance 4 for deterministic locations case with $r_1 = 1$, $r_2 = 2$, $r_3 = 4$, $n_1 = 1$, $n_2 = 2$, $n_3 = 4$ and $z = 0.2$ using the Enhanced Approximate Model.	77
5-21	Throughput plot for the case of deterministic locations with fading in the channel. The number of nodes at distances $r_1 = 1$, $r_2 = 2$ and $r_3 = 3$ are $n_1 = 1$, $n_2 = 3$, $n_3 = 9$ respectively, and $z = 0.2$	82
5-22	Throughput plot for random node locations case with fading in the channel for $n = 10$ and $z = 0.2$ using the Jensen's Inequality approximation to the average of $p_{c,k}(r)$	84
5-23	The upper and lower bounds to $\overline{p_{c,k}(r)}$ as a function of distance, r for $n = 10$ nodes in the system and $z = 0.2$. The figure corresponds to $\bar{k} = 5$	86
5-24	Throughput plot for random node locations case with fading in the channel for $n = 10$ and $z = 0.2$ using the Jensen's Inequality approximation to the average of $p_{c,k}(r)$	87
6-1	Throughput plot for deterministic locations case (no fading) with $r_1 = 1$, $r_2 = 2$, $n_1 = 5$, $n_2 = 15$ and $z = 0.2$ using the original model.	91
6-2	Throughput plot of the users at distance 1 for deterministic locations case (no fading) with $r_1 = 1$, $r_2 = 2$, $n_1 = 5$, $n_2 = 15$ and $z = 0.2$ using the original model.	91
6-3	Throughput plot of the users at distance 2 for deterministic locations case (no fading) with $r_1 = 1$, $r_2 = 2$, $n_1 = 5$, $n_2 = 15$ and $z = 0.2$ using the original model.	91
6-4	The single user state diagram for the <i>Backward Model with Forced Idle Periods</i> . This figure corresponds to having nodes stay idle for 1 slot after a successful transmission. <i>S</i> : Success, <i>I</i> : Idle, <i>F</i> : Failure, <i>WAS</i> : Wait After Success, <i>AF</i> : After Failure, <i>TAW</i> : Transmit After Waiting. The transition labeled by "a" occurs with probability 1.	92
7-1	Comparison of the total network throughput in the simulation model and in the exact model for deterministic node locations and without fading in the channel where TP-Sim stands for throughput obtained by simulation and TP-Exact that from the exact analysis. We utilized $n_1 = 1$, $n_2 = 5$, $r_1 = 1$, $r_2 = 2$, $z = 0.2$ and $t = 100K$	98

7-2	Comparison of the aggregate throughput of the distance-2 users in the simulation model and in the exact model for deterministic node locations and without fading in the channel where TP-Sim stands for throughput obtained by simulation and TP-Exact that from the exact analysis. We utilized $n_1 = 1, n_2 = 5, r_1 = 1, r_2 = 2, z = 0.2$ and $t = 100K$	99
7-3	Comparison of the total network throughput in the simulation model and in the exact model for deterministic node locations and without fading in the channel where TP-Sim stands for throughput obtained by simulation and TP-Exact that from the exact analysis. We utilized $n_1 = 1, n_2 = 5, r_1 = 1, r_2 = 2, z = 0.2$ and $t = 1000k$	99
7-4	Comparison of the aggregate throughput of the distance-2 users in the simulation model and in the exact model for deterministic node locations and without fading in the channel where TP-Sim stands for throughput obtained by simulation and TP-Exact that from the exact analysis. We utilized $n_1 = 1, n_2 = 5, r_1 = 1, r_2 = 2, z = 0.2$ and $t = 1000k$	99
7-5	Comparison of the total network throughput in the simulation model and in the exact model for deterministic node locations and without fading in the channel where TP-Sim stands for throughput obtained by simulation and TP-Exact that from the exact analysis. We utilized $n_1 = 2, n_2 = 10, r_1 = 1, r_2 = 2, z = 0.2$ and $t = 100K$	100
7-6	Comparison of the total network throughput in the simulation model and in Enhanced Approximate Model for deterministic node locations and without fading in the channel where TP-Sim stands for throughput obtained by simulation and TP-App. that from the approximate model. We utilized $n_1 = 1, n_2 = 2, n_3 = 4, r_1 = 1, r_2 = 2, r_3 = 4, z = 0.2$ and $t = 100K$	101
7-7	Comparison of the aggregate throughput of the distance-2 users in the simulation model and in Enhanced Approximate Model for deterministic node locations and without fading in the channel where TP-Sim stands for throughput obtained by simulation and TP-App. that from the approximate model. We utilized $n_1 = 1, n_2 = 2, n_3 = 4, r_1 = 1, r_2 = 2, r_3 = 4, z = 0.2$ and $t = 100K$	101

7-8	Comparison of the aggregate throughput of the distance 4 users in the simulation model and in Enhanced Approximate Model for deterministic node locations and without fading in the channel where TP-Sim stands for throughput obtained by simulation and TP-App. that from the approximate model. We utilized $n_1 = 1, n_2 = 2, n_3 = 4, r_1 = 1, r_2 = 2, r_3 = 4, z = 0.2$ and $t = 100K$	101
7-9	Total network throughput when there are 10 uniformly distributed nodes on a plane (no fading) with $z = 0.2, t = 100K$ and 40 iterations.	102
7-10	Total network throughput when there are 20 uniformly distributed nodes on a plane (no fading) with $z = 0.2, t = 100K$ and 40 iterations.	102
7-11	Total network throughput when there are 40 uniformly distributed nodes on a plane (no fading) with $z = 0.2, t = 100K$ and 40 iterations.	103
7-12	Total network throughput when there are 10 uniformly distributed nodes on a disk with fading in the system for $z = 0.2, t = 100K$ and 40 iterations.	104
7-13	Total network throughput when there are 20 uniformly distributed nodes on a disk with fading in the system for $z = 0.2, t = 100K$ and 40 iterations.	104
7-14	Total network throughput when there are 50 uniformly distributed nodes on a disk with fading in the system for $z = 0.2, t = 100K$ and 40 iterations.	104
7-15	Total network throughput when there are 100 uniformly distributed nodes on a disk with fading in the system for $z = 0.2, t = 100K$ and 40 iterations.	105
7-16	Total network throughput when there are 10 uniformly distributed nodes on a disk with fading in the system for $z = 0.1, t = 100K$ and 40 iterations.	106
7-17	Total network throughput when there are 10 uniformly distributed nodes on a disk with fading in the system for $z = 0.3, t = 100K$ and 40 iterations.	106
7-18	Total network throughput when there are 10 uniformly distributed nodes on a disk with fading in the system for $z = 0.5, t = 100K$ and 40 iterations.	106
7-19	Total network throughput when there are 10 uniformly distributed nodes on a disk with fading in the system for $z = 0.7, t = 100K$ and 40 iterations.	107
7-20	Total network throughput of the <i>Backward Model with Forced Idle Periods</i> for $r_1 = 1, r_2 = 2, n_1 = 5, n_2 = 15, z = 0.2$ and $t = 100K$ in the case where nodes stay idle for 2 slots after each successful transmission.	108

7-21	Throughput of the nodes at distance 1 for <i>Backward Model with Forced Idle Periods</i> for $r_1 = 1, r_2 = 2, n_1 = 5, n_2 = 15, z = 0.2$ and $t = 100K$ in the case where nodes stay idle for 2 slots after each successful transmission.	108
7-22	Throughput of the nodes at distance 2 for <i>Backward Model with Forced Idle Periods</i> for $r_1 = 1, r_2 = 2, n_1 = 5, n_2 = 15, z = 0.2$ and $t = 100K$ in the case where nodes stay idle for 2 slots after each successful transmission.	109
7-23	Total network throughput of the <i>Backward Model with Forced Idle Periods</i> for $r_1 = 1, r_2 = 2, n_1 = 5, n_2 = 15, z = 0.2$ and $t = 100K$ in the case where nodes stay idle for 8 slots after each successful transmission.	109
7-24	Throughput of the nodes at distance 1 for <i>Backward Model with Forced Idle Periods</i> for $r_1 = 1, r_2 = 2, n_1 = 5, n_2 = 15, z = 0.2$ and $t = 100K$ in the case where nodes stay idle for 8 slots after each successful transmission.	109
7-25	Throughput of the nodes at distance 2 for <i>Backward Model with Forced Idle Periods</i> for $r_1 = 1, r_2 = 2, n_1 = 5, n_2 = 15, z = 0.2$ and $t = 100K$ in the case where nodes stay idle for 8 slots after each successful transmission.	110
7-26	Total network throughput for <i>Backward Model with Dynamic Contention Windows</i> for $r_1 = 1, r_2 = 2, n_1 = 1, n_2 = 5, z = 0.2$ and $t = 100K$	110
7-27	Total throughput of the nodes at distance 1 for <i>Backward Model with Dynamic Contention Windows</i> for $r_1 = 1, r_2 = 2, n_1 = 1, n_2 = 5, z = 0.2$ and $t = 100K$	111
7-28	Total throughput of the nodes at distance 2 for <i>Backward Model with Dynamic Contention Windows</i> for $r_1 = 1, r_2 = 2, n_1 = 1, n_2 = 5, z = 0.2$ and $t = 100K$	111
7-29	Total network throughput of the <i>Backward Model with Dynamic Contention Windows</i> for $r_1 = 1, r_2 = 2, n_1 = 2, n_2 = 10, z = 0.2$ and $t = 100K$	112
7-30	Total throughput of the nodes at distance 1 for <i>Backward Model with Dynamic Contention Windows</i> for $r_1 = 1, r_2 = 2, n_1 = 2, n_2 = 10, z = 0.2$ and $t = 100K$	112
7-31	Total throughput of the nodes at distance 2 for <i>Backward Model with Dynamic Contention Windows</i> for $r_1 = 1, r_2 = 2, n_1 = 2, n_2 = 10, z = 0.2$ and $t = 100K$	113
7-32	Total network throughput of the <i>Backward Model with Dynamic Contention Windows</i> for $r_1 = 1, r_2 = 2, r_3 = 3, n_1 = 1, n_2 = 3, n_3 = 9, z = 0.2$ and $t = 100K$	113

7-33	Throughput of the node at distance 1 for <i>Backward Model with Dynamic Contention Windows</i> for $r_1 = 1, r_2 = 2, r_3 = 3, n_1 = 1, n_2 = 3, n_3 = 9, z = 0.2$ and $t = 100K$	113
7-34	The aggregate throughput of the nodes at distance 2 for <i>Backward Model with Dynamic Contention Windows</i> for $r_1 = 1, r_2 = 2, r_3 = 3, n_1 = 1, n_2 = 3, n_3 = 9, z = 0.2$ and $t = 100K$	114
7-35	The aggregate throughput of the nodes at distance 3 for <i>Backward Model with Dynamic Contention Windows</i> for $r_1 = 1, r_2 = 2, r_3 = 3, n_1 = 1, n_2 = 3, n_3 = 9, z = 0.2$ and $t = 100K$	114
A-1	The transmission probability obtained analytically and numerically as a function of distance for $p_{ts} = 0.2, p_{tf} = 0.05, \alpha = 1$ and uniform distribution of 2 nodes on a line. . . .	118

Chapter 1

Introduction

Future communication technologies such as UWB, MIMO or existing spread spectrum systems such as code division multiple access (CDMA) have fundamental differences from the corresponding narrowband or single antenna systems. Although some medium-access control (MAC) protocols for UWB have been proposed [10, 14, 16, 20, 26, 39], they do not take into account the special characteristics of the system such as multipacket reception capability. In this thesis we focus on fundamental aspects of MAC layer design for multipacket reception networks with spatially distributed nodes.

In wideband communications the information is spread over a very wide bandwidth using time hopping or spreading codes at the transmitter [57]. In a packet based network, this spreading enables the receiver to demodulate multiple packets at a time. The same result is observed in MIMO systems by the use of multiple antennas at the receiver. This capability of multipacket reception introduces new challenges in designing MAC protocols [18, 59].

The basic underlying assumption in legacy MAC protocols (e.g., slotted aloha) is that any concurrent transmission of two or more users causes all transmitted packets to be lost [4]. However, this model does not reflect the actual situation in many practical wireless networks where some information can be received correctly from a simultaneous transmission of several packets. Therefore, this assumption has been subjected to some improvements in literature. The first improvement is called the *capture effect*: The packet with the strongest power level can be received successfully (captured) in the presence of con-

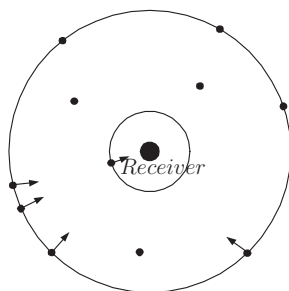


Figure 1-1: An example scenario where 1 nearby node captures the channel (since its signal is greater) and blocks 4 faraway nodes. The transmitting nodes are indicated with arrows. This is a very inefficient use of the network resources if the maximum number of simultaneously received transmissions in the network is greater than 1, i.e., if the receiver is capable of receiving multiple packets at a time.

tending transmissions if its power level is sufficiently high. It occurs in networks with single packet reception capability where packets arrive at the common receiver with different power levels due to near-far effect, shadowing or fading. The effect of capture on Aloha [1, 2, 27, 28, 30, 52, 53, 61] and on IEEE 802.11 protocol (Carrier Sense Multiple Access-Collision Avoidance (CSMA/CA)) [22, 23, 36, 44] has been studied extensively in the literature and new MAC protocols for channels with capture have been proposed [11]. Hajek *et al.* [25] provided asymptotic results on the capture probability in the limit of infinite number of users. The other major improvement to the original model, known as *multipacket reception capability*, assumes that a subset of the collided packets can be received successfully. The impact of the multipacket reception capability on MAC protocols has received limited attention to date. Ghez *et al.* [18, 19] proposed a channel model for networks with multipacket reception capability and studied stability properties of slotted aloha in such a setting. Peh *et al.* [45] revisited the model of [18] and proposed improvements in retransmission control schemes by utilizing additional feedback. Tong *et al.* have proposed MAC protocols based on multipacket reception capability [37, 38, 59, 60] using the channel model suggested in [18]. The protocols developed in [59, 60] maximize the per-slot throughput by controlling the set of users who are allowed to transmit in each slot. However, these protocols require a centralized controller and hence are impractical for large distributed networks. Nguyen *et al.* [43] considered the SNR model for capture and derived expressions for capture probability for both narrowband (single capture) and wideband (multiple packet reception) communication systems. Furthermore, new MAC algorithms for multipacket reception channels were proposed in [7, 31, 48, 49].

Note that there are other solutions rather than designing a MAC protocol specific to this setting, yet each of them has its own disadvantages. First, using power control schemes where nodes are allowed to choose the power level with which to send their packets has been proposed in [29, 33, 40, 53] for the single capture case and in [34] for the multipacket reception case. However, power control mechanisms require sophisticated feedback and complex transmitters that can adjust the transmit power level dynamically. Hence expensive transmitters are needed which might be a problem for networks with large number of nodes. Moreover, for more realistic network settings such as multi-hop networks with many receivers, every node can send to a subset of the receivers and adjusting the power level according to different feedback from different receivers makes the design more complicated. A second alternative is to use Time Division Multiple Access (TDMA) technique. Applying TDMA schemes directly to multipacket reception channel not only causes excessive delays but also results in very inefficient usage of channel resources since the receiver can capture multiple packets at a time, hence allowing some contention is in fact preferred. Optimal scheduling algorithms for TDMA networks with multipacket reception capability have been studied in [9, 54], however, they require a centralized controller together with an advanced feedback mechanism making it difficult to utilize them in large network settings such as multihop networks.

Multipacket reception capability in networks with *spatially distributed nodes* calls for new MAC protocols as well. However, previous work in this field mostly do not take into account the spatial distribution of the nodes, which, as we explain shortly, results in very inefficient utilization of the channel and unfairness when existing MAC protocols are used in this network setting. It is well-known that existing MAC protocols (e.g., IEEE 802.11) are unfair and may starve some of the nodes [3, 5, 17, 41]. The reason for this is that if a node has a successful transmission, IEEE 802.11 gives a higher transmission probability to that node and a lower probability to the failed node. Consequently, successful users continue to capture the channel and the failed users continue to transmit with low probability, resulting in starvation of some of the nodes in the network. This fairness phenomenon is even more pronounced in networks with spatially distributed nodes since the distant users have weaker signals than nearby users due to the severe attenuation of the signal power with

distance. Consequently, packets belonging to distant users are lost with higher probability. Furthermore, when there is *multipacket reception* capability in a network with spatially distributed nodes, unfairness amounts to very inefficient usage of the channel resources. For example consider that an IEEE 802.11 type protocol is applied to such a network and consider the collision of a nearby user and 4 distant users as shown in Fig. 1-1. In a typical scenario, the packet of the nearby node is received successfully and the others are lost since the power level of the nearby user is much greater than that of the distant users. Once the faraway node senses the collision, it increases its contention window (i.e., decreases its transmission probability) and the successful nearby node decreases its contention window (increases its transmission probability) continuing to capture the channel. Thus even the less frequent transmissions of the remote users will be unsuccessful leading to their complete starvation. This means that, one user might dominate the network and starve several distant users. Hence unfairness in multipacket reception channels with spatially distributed nodes may lead to very low overall network throughput. The above example suggests that a fair protocol in such a network should give a greater chance to distant users in order to prevent their starvation in the network. Moreover, under most spatial distributions the number of remote nodes is considerably greater than that of nearby nodes and hence allowing a higher transmission probability to distant users can increase the network throughput. This is the main idea of this work where we design and analyze a distributed MAC protocol for networks with multipacket reception capability and spatially distributed nodes. Our protocol is simple to operate and easy to extend to more complicated network structures. We start with a single receiver, single hop system in this thesis, however, ultimately we aim at extending this protocol to multi-hop settings.

A simple alternative scheme to what has been done in CSMA/CA type traditional algorithms would have the node use a high transmission probability following a collision and a low transmission probability following a success. This simple scheme will be referred to as the *backward model*. We propose the *Backward Protocol* inspired by this idea and show by some motivating examples in Chapter 4, that the *Backward Protocol* gives greater chances to distant nodes and achieves better performance than the traditional mechanisms which employ the *forward model* (i.e., having large transmission probability after a success

and a low transmission probability after a failure).

We develop comprehensive analysis of the protocol in various settings. We start with an analysis of the case where the nodes are randomly distributed on a plane without fading in the channel. Next, we analyze the protocol when the node locations are deterministic and there is no fading in the channel. We give exact analysis together with approximations that enable us to extend the results to more sophisticated networks (i.e., more allowed distances from the receiver and more users) with high accuracy. We utilize approximation techniques to analyze the cases where there is multipath fading in the channel both when the node locations are deterministic and when they are random. We show by numerical analysis that the *Backward Protocol* gives more fair results in all of the cases and better throughput results in most of the cases described above.

In addition to the exact and the approximate analysis of the protocol under different scenarios, we provide simulation results for the network settings where the approximate models no longer hold and we compare the effect of different parameters in the model. Finally, based on the results obtained from these simple mechanisms, we attempt at developing more realistic MAC protocols for networks with multipacket reception capability and spatially distributed nodes.

The main contributions of our work are the following. We propose the *Backward Protocol* that is a dynamic MAC protocol designed for networks with multipacket reception capability and spatially distributed nodes. We show by analysis and simulations that the *Backward Protocol* deals with the severe fairness problem due to the near-far effect and it achieves higher throughput values than traditional back-off mechanisms in most cases considered. Finally, we provide various approximations that are accurate and useful in analyzing the performance of the network for more complicated settings.

The organization of the thesis is as follows. We begin with the previous work in this field and describe what has been done in literature in a similar context in Chapter 2. In Chapter 3, we give the system description and assumptions used for the channel, the feedback, and the users. We also describe the *Backward Protocol* in a detailed manner in this chapter. In Chapter 4, we give some motivating examples which suggest that the proposed scheme functions better than existing MAC protocols in terms of throughput and fairness.

In Chapter 5, we analyze the proposed protocol in various different settings. In Chapter 6 two new protocols which are improved versions of the original protocol are considered. Finally, extensive simulation results are presented in Chapter 7.

Chapter 2

Related Work

The related work regarding the effect of capture on MAC protocols starts with the work of Roberts [50] who introduced the so called perfect capture model as the packet of the user with the largest received power is correctly demodulated out of a collision of many packets. He also suggested the vulnerability circle model for capture which assumes that a packet transmitted from distance r is successfully received if no other packet is generated within a circle of radius αr . Metzner [40] studied the perfect capture model for Aloha protocol with power control and computed the optimal probabilities (optimal in the sense that it maximizes the throughput) with which transmitters should use the available power levels. Abramson analyzed the Aloha protocol under vulnerability circle model in [1] and Shacham [53] studied perfect capture model in Aloha protocol with multiple transmit power levels. Kuperus and Arnbak [28] considered the SNR model for capture and termed it *capture ratio*, which assumes that a packet is correctly received if its received power exceeds the total interference power by more than a threshold factor z (hence the name SNR model), and derived probability of capture in a channel with Rayleigh fading. Arnbak and Van Blitterswijk [2] extended the results in [28] for a channel with combined near-far effect and Rayleigh fading. Cidon, Kodesh and Sidi [11] introduced and analyzed different MAC protocols to exploit the capture effect and discussed the power control idea in such a setting. Lau and Leung [30] considered various spatial distributions and provided a comparison of the vulnerability circle and the SNR models. A more detailed review of the work in this field until 1993 can be found in Linnartz's book [32], where he also analyzed

many cases for the SNR model.

Then the subsequent works of Zorzi and Rao [61], and Krishna and Lemaire [27] extended the results in [32] about MAC protocols with capture and derived expressions for the capture probability when there are n contending transmissions, C_n , using the SNR model. Moreover, Zorzi and Rao [61] provided stability results for ALOHA protocol with capture, which states that the protocol is stable if the arrival rate to the system, λ is less than C_∞ where C_∞ is the capture probability in the limit of infinitely many transmissions. They also proposed a retransmission control scheme to stabilize unstable systems. Some corrections to this work was suggested in [42], followed by the reply [62]. As mentioned in the previous section, Lemaire, Krishna, and Zorzi in [29] and Luo and Ephremides in [33] proposed a power control scheme for networks with capture, where the nodes have discrete transmit power levels. Lemaire *et al.* [29] determined the optimal transmit probabilities for the power levels together with the optimal values of the power levels themselves for maximizing the capture probabilities. Luo and Ephremides [33] showed that the single power level system achieves optimal throughput when some decodability threshold value (i.e., SNR of each packet is above a certain level) for received packets is satisfied. Zorzi [63] extended the throughput analysis in [61] to the case where there is diversity, Rayleigh fading and shadowing in the system. Finally, Sant and Sharma [52] analyzed stability properties of slotted aloha from queuing theory perspective when there is capture effect and fading in the system.

Bianchi [6] analyzed IEEE 802.11 (CSMA/CA) protocol with finite number of users assumption. Hadzi-Velkov and Spasenovski [22–24] extended [6] to the case where there is capture in the channel under various settings (with and without Rayleigh fading and diversity in the channel). Manshaei *et al.* [36] extended the previous results on IEEE 802.11 with capture to the case where the nodes have different distances in the network. Nyandoro *et al.* [44] analyzed IEEE 802.11 protocol with capture and showed that the probability of successful reception increases when nodes use one of the two different power levels according to their service class. As pointed out in the introduction, there are many work on fairness and throughput starvation in IEEE 802.11 (CSMA/CA) type protocols [3,5,17,41], however, they are not aimed at multipacket reception channels and the fairness issue due to

the near-far effect is not addressed in most of them.

Ghez *et al.* studied the effect of multi-packet reception on Aloha protocol in [18] where they generalized the collision channel model by modeling the number of successfully received packets in each slot as a random variable which depends only on the number of transmissions on that slot. They derived the maximum stable throughput of Aloha channel under these assumptions. They extended the analysis, provided stability results also for the case in which the retransmission probabilities can be varied as a function of the channel history and presented a protocol that stabilizes the general system in [19]. Peh *et al.* [45] revisited the model of [18] and proposed improvements in retransmission control schemes by utilizing additional feedback. Tong *et al.* [37, 38, 56, 59, 60] used the model of [18] and extended the analysis in various directions. In particular, Zhao and Tong [59, 60] designed new MAC protocols based on multipacket reception capability that maximizes the expected number of successfully received packets per slot by controlling the set of users who are allowed to transmit in each slot depending on the channel history and the QoS constraints of the users. Hajek *et al.* [25] provided asymptotic results on the capture probability in the limit of infinite number of users. Chan and Berger [8] analyzed an extension of CSMA protocol (assuming nodes can sense the power level in the channel and hence the number of packets currently being transmitted) in multipacket reception networks using the channel model suggested in [18]. Likhanov *et al.* [31] presented and analyzed new algorithms for multipacket reception networks based on collision resolution technique. Yu *et al.* [58] provided conditions on spatial distribution function of nodes for stability of Aloha protocol in multipacket reception channel. Nguyen *et al.* [43] considered the SNR model for capture and derived expressions for capture probability for both narrowband (single capture) and wideband (multiple packet reception) communication systems.

Different approaches to the multi-access control in multipacket reception networks include a cross layer design protocol in [49] by exchanging parameters between physical and MAC layer. A similar approach was studied in [48] for the MIMO multiple access channel both from physical layer and MAC layer perspectives giving formulations for a cross layer optimization to maximize throughput. A MAC protocol for a spread spectrum multihop network which dynamically adjusts its behavior according to channel feedback

was described in [7]. Luo and Ephremides extended [33] to multipacket reception networks [34] and showed that the single-power-level-system achieves optimal throughput if SNR levels of packets are above some threshold. Extensions of TDMA type schemes to multipacket reception channels have been proposed, e.g., in [9] optimal scheduling (for maximum throughput) of transmissions on multiple independent channels is studied. A dynamic slot allocation scheme in multipacket reception channel using antenna arrays is proposed in [54]. Coupechoux *et al.* [12] analyzed the performance of slotted aloha on multihop multipacket reception network setting as well as discussing new issues on the design of MAC layer in such a setting [13]. Finally, Mackenzie and Wicker [35] presented a game theoretic analysis of the model of Ghez *et al.*

Moreover, recently there has been some interest [15] in UWB MAC layer which aims to address specific properties of the UWB physical layer suggested in [57]. Optimal scheduling and routing problems in UWB physical layer are studied in [47, 55]. Radunovic and Boudec [46] showed that due to the distinct characteristics of UWB-Impuls Radio (UWB-IR), reusing medium access control (MAC) protocols originally designed for narrow-band systems may be inefficient. A few aspects of the UWB MAC layer have been studied in for example [16, 39]. In [10, 14, 20, 26] optimization problems that attempt to address the particular properties of the physical layer are formulated and the results of these optimizations are used as a basis for a MAC protocol design.

These previous work specific to UWB is different from what is in this thesis in that they are explicitly based on UWB physical layer whereas we propose a more general MAC protocol that can work on all multipacket reception channels with spatially distributed nodes (e.g., CDMA, UWB etc.). Furthermore, we study the problem from a more fundamental point of view and obtain analytical results while the above mentioned works mostly evaluate the performance of some heuristic idea using simulations.

Furthermore, most of the above previous work on MAC layer design for general multipacket reception channels did not assume a spatial distribution of the nodes on the network. In the cases where a spatial distribution was considered, the throughput reduction due to near far effect and the starvation of distant nodes were not taken into account. Furthermore, in most cases the effect of capture or the multipacket reception capability on the existing

MAC protocols (Aloha mostly) were studied. The new protocols suggested for multipacket reception channel required a centralized controller and sophisticated feedback mechanisms making the protocol computationally complex and impractical for distributed networks. However a new MAC protocol design that will exploit the multipacket reception capability and remedy the fairness problem when the nodes are spatially distributed is necessary and this is the topic of this thesis.

Chapter 3

System Description and Assumptions

Consider a system where users are communicating to a receiver with possibly different distances from it. The receiver can be a base station as in cellular networks or an access point as in multi-hop wireless networks. We assume single destination, single-hop system in this thesis, however, our ultimate objective is to extend the protocol to multi-hop networks. Therefore, we assume the receiver does not control the transmissions of the users and we design a distributed protocol which will be explained in details shortly. We assume a signal transmitted from a user at distance r is attenuated according to $Kr^{-\beta}$ where β is called the power loss law exponent which is a constant typically taking values between 2 and 6 depending on the characteristics of the environment and K is the attenuation constant. Under these assumptions, the received power $P_R(i)$ of node i which is at distance r from the receiver is of the form

$$P_R(i) = R_i^2 K r^{-\beta} P_T(i) + N \quad (3.1)$$

where R_i is a Rayleigh distributed random variable with unit power, independent and identically distributed (i.i.d.) for every user (R_i^2 is an exponentially distributed random variable of unit mean). We carry out the analysis both with and without Rayleigh fading and hence R_i is assumed to be 1 when there is no fading in the system. $P_T(i)$ is the transmit power of user i which is assumed to be constant P_T in this work and N represents the effect of additive noise.

We utilize the well-known SNR model for capture (also known as the power capture

model) used in [21, 25, 30, 32, 43, 58, 61] (termed as the physical model in [21]) whereby given n simultaneous transmissions, the packet of user i is captured if

$$SNR(i) = \frac{P_R(i)}{N + \left\{ \sum_{j \neq i} P_R(j) \right\}} > z \quad (3.2)$$

which can be rewritten as

$$P_R(i) > z \left\{ \sum_{j \neq i} P_R(j) \right\} + zN \quad (3.3)$$

The additive noise power level is much smaller than the received power level and for practical purposes it will be neglected in the analysis. z is the power ratio threshold and depends on the physical layer and the receiver parameters. For single packet reception narrow-band systems z is in the range $1 \leq z \leq 10$, whereas for wide-band multi-packet reception systems (e.g., direct-sequence spread-spectrum systems like CDMA, UWB) z is in the range $z < 1$ allowing multiple packets to be received simultaneously [25, 42]. Except an example in Section 4.3 where we analyze a single packet capture system, we assume that z is less than 1 in this work, consistent with the multipacket reception capability.

We also utilize the classical vulnerability circle model suggested in [50] and [1], which was also used by Gupta and Kumar [21] under the name “the protocol model”. This model assumes a transmission from distance r is successful as long as there is no simultaneous transmission within the disk of radius αr . Note that, α is assumed to be greater than 1 and hence this model, in its original form, is useful for single packet reception networks. We utilize the vulnerability circle model only in a motivating example and also we demonstrate in Section 5.1 that this model can be derived from the power capture model for the case of two nodes as mentioned in [27].

We define the throughput, S , of the system as the average number of successfully received packets per unit time. Using (3.3), we define the parameter c as the maximum number of simultaneously successful transmissions. The event where the maximum number of

packets is captured will occur if there are c equal received-power packets at the receiver¹. It is easy to see from (3.3) that c is equal² to $\lceil 1/z \rceil$.

We analyze our protocol under different network scenarios, for example when the node locations are deterministic or randomly distributed. When random node locations are considered, the distance r of a node from the receiver is assumed to be uniformly distributed on a disk of radius 1 at the center of which the receiver is located, namely, the pdf of a node's distance from the receiver is given by,

$$f_r(r) = 2r \quad \forall r \ 0 \leq r \leq 1 \quad (3.4)$$

There are a few issues with utilizing this density as we discuss next. First, as pointed out in [43], when node distances from the receiver are less than 1, (3.1) implies a power gain which is not realistic. However, as far as the capture equation (3.3) is concerned, the ratio of the powers and hence the ratio of the distances of nodes from the receiver is important in the model. Furthermore, suppose a genie tells us the distance of the closest user to the receiver. Then, dividing every node's distance by this minimum distance gives received powers without positive gain and the results, of course, do not change. Therefore, using the distribution in (3.4) would not affect the capture probabilities. A second issue with this model is that when the number of nodes in the network becomes very large (i.e., in the limit as n tends to ∞) at least one of the users gets very close to the receiver having infinite power at the receiver. However, we are interested in finite number of users in this thesis which does not have the outlined problem.

We utilize the classical assumptions that can be found in [4], some of which can be relaxed under certain conditions. We assume the transmission is at packet level where all packets have the same length so that packet transmission time is fixed. Time is divided into slots during which at most one packet can be transmitted. A simple immediate 0,1,e (idle, successful, error) feedback mechanism is assumed whereby the receiver sends an acknowledgment/error (i.e, 1 or e) to the user if its attempt in the previous slot was suc-

¹If there are different power levels at the receiver, the weak users will have less chance of being captured and they might also prevent strong users from having successful transmissions.

²In [25], the capture equation 3.3 is defined with an equality, therefore c is given as $1 + \lfloor 1/z \rfloor$.

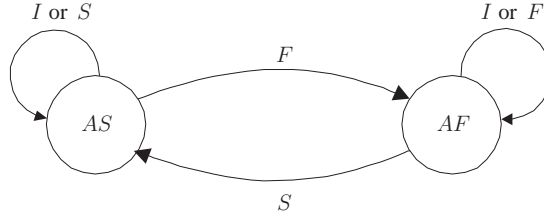


Figure 3-1: The Single User State Diagram, S : Success, I : Idle, F : Failure, AS : After Success, AF : After Failure.

cessful/failed. We assume saturated nodes, i.e., there is always a packet to send at each node and new arrivals join the unsuccessful packets.

3.1 Backward Protocol

In this section we introduce the basic protocol by describing the single user state diagram shown in Fig. 3-1. We define two probabilities p_{ts} and p_{tf} , the probability of transmission in the current slot after a successful transmission in the previous attempt (AS : *After Success*) and after a failed transmission in the previous attempt (AF : *After Failure*) respectively. As a result, every user chooses one of these probabilities to transmit at the beginning of each slot according to their success history in the previous slot. In the event of an idle in the previous slot, nodes keep their state for the next transmission. This state diagram is markovian³ and is used to keep track of the transmission history of each node. Consequently, nodes react differently if they succeeded or failed in the previous attempt and this captures, in a very simplistic sense, the dynamic protocol idea applied in IEEE 802.11 protocols. Decreasing the contention window after a successful attempt in IEEE 802.11 corresponds to a high p_{ts} value in our protocol and increasing the contention window after a failed attempt in IEEE 802.11 corresponds to a low p_{tf} value in our protocol. As mentioned before, we refer to these protocols as the *forward models* and whenever we have an operating point for which $p_{tf} > p_{ts}$ we refer to the resulting scheme as the *backward model* and the resulting protocol as the *Backward Protocol*.

³It is markovian since given the probability assignment in the current slot, the future of the system is independent of what happened in the past.

Chapter 4

Examples

In this section, we give motivating examples which help develop some intuition as to why the *Backward Protocol* is preferable in the multipacket reception channel with spatially distributed nodes. In the examples we assume that there is no fading in the system, therefore the random variable R_i in (3.3) is equal to 1. We start with two Aloha type examples where nodes can be located at one of the two possible distances from the receiver and have transmission probabilities that depend only on their distance. In the next example, we analyze the *Backward Protocol* using an approximate method together with the vulnerability circle model in a general network setting where nodes can be at a random distance from the receiver which is at the center of a disk.

4.1 Aloha with Two Distances: Example 1

Consider a simple arrangement of users on a disk as shown in Fig. 4-1. The number of users at distances $r_1 = 1$ and $r_2 = 2$ are n_1 and n_2 respectively. The nodes at distance 1 transmit with probability (w.p.) p_1 and those at distance-2 w.p. p_2 . It is easy to show using (3.3) that for a node at distance 2 to be successful when there is a transmission from distance 1, we need $(\frac{r_1}{r_2})^\beta > z$. Therefore, for the values of $z = 0.2$ and $\beta = 4$ assumed throughout this section, nodes at distance 2 cannot be successful¹ if there is a

¹Note that this conclusion is not valid for small enough values of z for given r_1 and r_2 . However, for a given z value we can always choose some practical r_1 and r_2 values so that $(\frac{r_1}{r_2})^\beta > z$ is not satisfied. Also

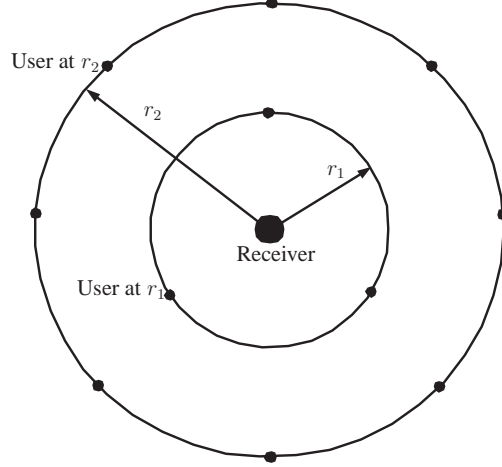


Figure 4-1: Simple spatial distribution.

transmission from distance 1. Furthermore, transmissions from distance 2 have no effect on the capture of nodes at distance 1 unless there are total c transmissions from distance 1 and 2^β from distance 2. When there are c transmitted packets from distance 1 and 2^β from distance 2, the total interference observed by the packet of a user at distance 1 becomes $(c - 1)KP_T + 2^\beta KP_T 2^{-\beta} = cKP_T$. Multiplying this by $z = 1/c$ results in an equality in (3.3) and hence the packet from distance-1 fails. Now assume $n_1 \leq c$ and $n_2 \leq c < 2^\beta$ for this example². Since $n_1 \leq c$ and $n_2 < 2^\beta$, nodes at distance 1 are always successful and nodes at distance 2 fail only if there is a transmission from distance 1.

Observation 1 *As long as $n_2 \geq n_1$, throughput (S) is maximum at $(p_1, p_2) = (0, 1)$ and is equal to n_2 . Furthermore, the maximum S value is produced by a unique (p_1, p_2) combination if $n_2 > n_1$.*

note that, $z = 0.2$ is a practical assumption [25].

²In fact, a nearby node may fail if there are $c - 1$ transmissions from distance 1 and $2^{\beta+1}$ transmissions from distance 2, but with our assumption that $n_2 < 2^\beta$, we do not need to worry about these cases.

Proof: $S = n_1 p_1 + (1 - p_1)^{n_1} n_2 p_2$. $\frac{\partial S}{\partial p_2} = n_2 (1 - p_1)^{n_1} \geq 0$, therefore, S is an increasing function of p_2 , and hence, the maximum S is at $p_2 = 1$. As a result;

$$\begin{aligned} S &\leq n_1 p_1 + (1 - p_1)^{n_1} n_2 \\ &\leq n_2 (p_1 + (1 - p_1)^{n_1}) \\ &\leq n_2 \end{aligned} \tag{4.1}$$

where in (4.1) we used the fact that $n_1 \leq n_2$.

We get this maximum throughput of $S = n_2$ at $(p_1, p_2) = (0, 1)$. Note that this maximum point is not unique if $n_1 = n_2$, i.e., $p_1 = 1$ (independent of p_2) also gives $S = n_2$. However, if $n_2 > n_1$, there is only one maximum value for S and its at the point $(p_1, p_2) = (0, 1)$. \square

The resulting throughput plot for $n_1 = 1$ and $n_2 = 3$ for all values of p_1 and p_2 is in Fig. 4-2. In this example we use $z = 0.2$ which corresponds to $c = 5$, satisfying $n_1 < c$ and $n_2 < c$. We see from the figure that the throughput of the system takes its maximum at the end point $(p_1, p_2) = (0, 1)$ giving throughput of 1 for each faraway nodes and 0 for the nearby node. This suggest that giving a higher probability of transmission to distant users might yield a higher throughput.

Moreover, we can find the fair point in the plot, i.e., the point which gives the same throughput to all the nodes for $n_1 = 1$ and $n_2 = 3$. The throughput equation is given by $S = p_1 + (1 - p_1)3p_2$, where nearby throughput is equal to p_1 and faraway throughput per node is $(1 - p_1)p_2$. Equating the two we get, $p_1 = (1 - p_1)p_2$, yielding $S = 4p_1$. Notice that $p_2 = p_1/(1 - p_1)$ which means that the fair point requires $p_2 \geq p_1$. Furthermore, $p_2 \leq 1$ requires $p_1/(1 - p_1) \leq 1$ and hence $p_1 \leq 0.5$ yielding $S = 4p_1 \leq 2$ with equality for the point $(p_1, p_2) = (0.5, 1)$. As a result, the point producing the highest throughput value that is divided evenly between the users is $(p_1, p_2) = (0.5, 1)$. Therefore, in this example we see that not only the highest throughput but also the fair point with highest throughput is obtained by giving more chances to faraway nodes.

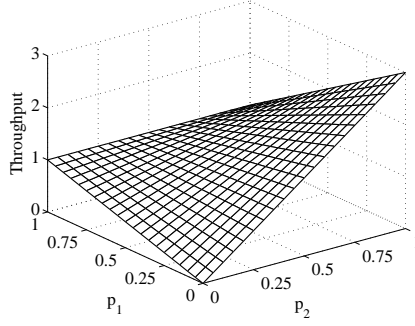


Figure 4-2: Throughput plot for the system in Example-1 for $n_1 = 1$, $n_2 = 3$ and $z = 0.2$.

4.2 Aloha with Two Distances: Example 2

Now consider the same settings as in the previous example but this time with $n_1 = 2$ and $n_2 = 6$ in Fig. 4-1. When we choose $z = 0.2$ and hence $c = 5$ as in the previous example, nodes at distance 1 are still successful all the time, however nodes at distance 2 can fail if there is a transmission from distance 1 or if all 6 of the distance-2 nodes transmit simultaneously.

Observation 2 Throughput S is maximum at $p_1 = 0$ and the maximum value is given by

$$\max_{p_2} \sum_{i=0}^c i \binom{6}{i} p_2^i (1 - p_2)^{6-i} \quad (4.2)$$

Proof:

$$S = 2p_1 + (1 - p_1)^2 \underbrace{\sum_{i=0}^c i \binom{6}{i} p_2^i (1 - p_2)^{6-i}}_{f_2(p_2)}$$

Define

$$C \triangleq \max_{p_2} f_2(p_2)$$

Then, $S = 2p_1 + (1 - p_1)^2 C = C + p_1(2 - C(2 - p_1))$, which takes its maximum value of C at $p_1 = 0$ as long as $C > \frac{2}{2-p_1}$. Now it is enough to show that for at least one value of p_2 , $f_2(p_2)$ is greater than 2. For $p_2 = 0.5$, $f_2(p_2) = 2.9 > 2$. \square

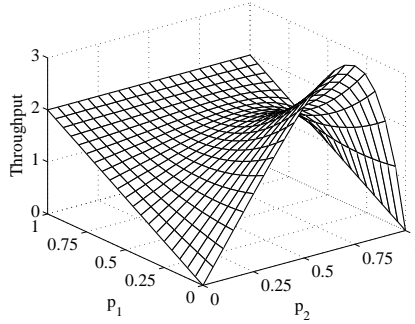


Figure 4-3: Throughput plot for the system in Example-2 for $n_1 = 2, n_2 = 6$ and $z = 0.2$.

The resulting throughput plot for all values of p_1 and p_2 is in Fig. 4-3. These examples show that giving higher probability of transmission to the faraway users can potentially result in higher throughput values in the multipacket reception channel. The crucial point of the analysis in the examples is assuming $n_2 > n_1$, which is reasonable for many spatial distribution of nodes, for example for a uniform distribution of users on a disk, the number of users increase linearly with the distance from the center of the disk where the receiver is located.

4.3 Backward Protocol with Random Distances and Single Capture: Example 3

We utilize the *Backward Protocol* in this section where there are n nodes randomly distributed on a plane and there is single capture capability at the receiver. We assume the classical vulnerability circle model suggested in [1], [21] and [50], i.e., a transmission from distance r is successful as long as there is no simultaneous transmission within the disk of radius αr . Note that, α is assumed to be greater than 1 in this example and hence there is only single capture in the system. In Section 5.1, we will also demonstrate that the vulnerability circle model can be derived from the power capture model for the case of two nodes as mentioned in [27].

Now we introduce an approximate model which will be revisited in Section 5.2.2 in a more detailed fashion under the name *basic approximate model*. We assume that at each

transmission attempt, regardless of the number of retransmissions suffered, a packet transmitted by a node at distance r is lost with constant and independent probability³ $p_d(r)$. Note that $p_d(r)$ is the probability that a node at distance r fails *given that* it has transmitted. In general, the probability that a packet is lost depends on other transmissions, however, if the number of nodes is large, we expect the approximate results to be close to the exact values. In fact, in Section 5.1, we develop an exact analysis for two nodes and show that the results obtained by the approximate model are very close to those of the exact model even for a small number of nodes.

It can be seen that, regarding the single user state machine in Fig. 3-1, a node changes its state from *After Success* to *After Failure* if it attempts and fails in the current slot, i.e., with probability $p_{ts}p_d$. Similarly, a node changes its state from *After Failure* to *After Success* if it attempts and succeeds in the current slot, i.e., with probability $p_{tf}(1 - p_d)$. The steady state probabilities of the corresponding Markov Chain for a node at distance r can easily be found to be;

$$p_{AS} = \frac{p_{tf}(1-p_d(r))}{p_{ts}p_d(r)+p_{tf}(1-p_d(r))}$$

$$p_{AF} = \frac{p_{ts}p_d(r)}{p_{ts}p_d(r)+p_{tf}(1-p_d(r))}$$

Next, we can obtain the overall transmission probability, given by

$$\tau(r) = p_{ts}p_{AS} + p_{tf}p_{AF} = \frac{p_{ts}}{1 - p_d(r) + \frac{p_{ts}}{p_{tf}}p_d(r)} \quad (4.3)$$

The probability that a transmission from a node at distance r fails is the probability that there is at least 1 node transmitting from within the circle of radius αr among $n - 1$ other nodes in the network. This probability is given by

$$p_d(r) = 1 - \left(1 - \int_0^{\alpha r} \tau(x)f_r(x)dx\right)^{n-1} \quad (4.4)$$

Where $f_r(x)$ is defined by (3.4). Now for any n and any $f_r(r)$, (4.3) and (4.4) can be solved

³This is usually done in the analysis of IEEE 802.11 without the dependence on r (e.g., [6]) and with the dependence on r in [36].

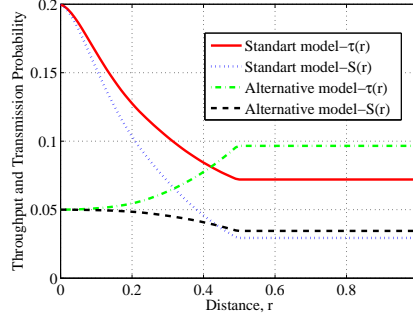


Figure 4-4: The transmission probability and the throughput as a function of distance under the forward ($p_{ts} = 0.2$ and $p_{tf} = 0.05$) and the backward ($p_{ts} = 0.05$ and $p_{tf} = 0.2$.) backoff mechanisms for $\alpha = 2$ and uniform distribution of 12 nodes on a disk.

numerically as a system of non-linear equations⁴. Once $\tau(r)$ and $p_d(r)$ are obtained, $S(r)$ can be easily found by

$$S(r) = \tau(r)(1 - p_d(r)) \quad (4.5)$$

Finally the overall throughput is given as

$$S = n \int_r S(r) f_r(r) dr \quad (4.6)$$

Now for $n = 12$, $\alpha = 2$ and $f_r(r) = 2r \quad \forall r \in (0, 1)$, Fig. 4-4 presents the values of $\tau(r)$ and $S(r)$ for the *forward model* (for $p_{ts} = 0.2$ and $p_{tf} = 0.05$) and the *backward model* (for $p_{ts} = 0.05$ and $p_{tf} = 0.2$). It can be seen that under the *backward model*, the transmission probabilities $\tau(r)$ of the distant nodes are higher than the transmission probabilities of the nearby nodes. Furthermore, comparing the two models, we see that the transmission probabilities of the distant nodes in the *backward model* are higher than those of the *forward model*. This leads to a system that is more fair than the *forward model* and that provides similar capture probabilities to the nodes regardless of their location. The throughput as a function of distance does not decay much in the *backward model*, whereas in the *forward model*, the throughput of faraway nodes is significantly less than that of nearby nodes and since the number of distant nodes is significantly larger than the number of nearby nodes, we expect the overall throughput of both systems to be similar;

⁴Note that (4.3) and (4.4) can be solved analytically in the case of two nodes. It is done to verify the numerical analysis and the solution is given in Appendix A for $f_r(r) = 1 \quad r \in [0, 1]$ and $\alpha = 1$.

for instance, for the example of Fig. 4-4, the throughput of the *forward model* is 0.4617 and that of the *backward model* is 0.4343.

In the light of these examples, even in a single capture channel, the *backward model* achieves more fair results for distant users and can potentially provide better throughput characteristics than the *forward model*. We naturally expect this to hold even more strongly with multipacket reception capability.

Chapter 5

Protocol Analysis

In this section we analyze the *backward protocol* for various different settings. We first develop an exact analysis of the *Backward Protocol* when nodes are randomly distributed on a disk and there is no multipath fading in the channel. The analysis enables us to verify the approximation we used in Section 3.1. Then we move on to a case where the node locations are known in advance. We introduce a more powerful approximation that can be utilized only in deterministic node locations case and use it to extend our analysis to networks with more users and more possible distances from the receiver than the exact analysis. Next we consider the above cases when there is multipath fading in the system. We utilize previous approximate models to both the deterministic node locations with fading and random node locations with fading cases and get analytical results. We show by numerical analysis that the *backward model* yields more fair results in all the cases and greater throughput in most of the cases compared to the *forward model*.

5.1 Random Locations Without Fading

In this section we develop an exact analysis using Markov Chains for the case where the node locations are random and there is no fading in the system. Our objective is to show that the approximate results used in the third motivating example in Sec. 3.1 are very close to the exact results even for a small number of nodes in the network. The approximation we used was that regardless of the success history, a packet from a user at distance r is

lost with constant and independent probability $p_d(r)$. Then using the state diagram of Fig. 3-1, we derived the average probability of transmission $\tau(r)$ as a function of $p_d(r)$ and formulated the throughput equation of our protocol. The exact analysis, however, requires using Markov Chains whose states denote whether each user is in *After Failure* or *After Success* state. An example of such a Markov Chain for $n = 2$ is shown in Fig. 5-1. If there are n nodes in the system, the number of states is at most 2^n . Since the analysis becomes extremely cumbersome for $n > 2$, we analyze the protocol for the case of 2 nodes. Namely, consider two nodes at distances r_1 and r_2 which are i.i.d. random variables distributed according to some density function $f_r(r)$ on a disk. Denote a node at distance r_1 as node-1 and that at r_2 as node-2. For this simple case of two transmitters, we can convert (3.3), and hence the capture model, into a simpler form as follows¹. The capture equation $P_{R,1} > zP_{R,2}$ simplifies to $r_1^{-\beta} > zr_2^{-\beta}$. Then we obtain $r_2 > \sqrt[\beta]{z} r_1$. Defining α as $\alpha \triangleq \sqrt[\beta]{z}$, we get user-1 is successful if $r_2 > \alpha r_1$. As a result, a transmission from distance r_1 is successful as long as there is no other transmission up to distance αr_2 , i.e., the vulnerability circle model of [1] used in Section 4.3 is another form of the power capture equation (3.3) for the case of 2 nodes. Note that here again we assume $\alpha \geq 1$ and hence $z \geq 1$, which in return means that there is only single capture in the channel, as in Section 4.3.

Case-a: $\alpha r_1 < r_2$:

In this case, node-1 is successful whenever it transmits since node-2 cannot interfere with node-1, therefore, node-1 uses the probability p_{ts} for transmission, whereas node-2 chooses p_{ts} or p_{tf} in each slot depending on its success history in its last transmission attempt. In order for node-2 to succeed, node-1 has to be silent. Now, based on the single user state diagram of Fig. 3-1, we can develop a system Markov Chain, shown in Fig. 5-1, that keeps track of the success history of both users in their last attempt.

It is easy to see that the Markov Chain of Fig. 5-1 is time-homogenous, irreducible and aperiodic, therefore the steady state probabilities exist and can be found easily by solving

¹This result also appears in [27].

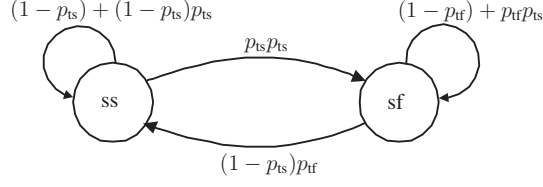


Figure 5-1: System Markov Chain in Example-2, Case-a. ss: both nodes are successful, sf: node-1 is successful and node-2 is failed in its last attempt.

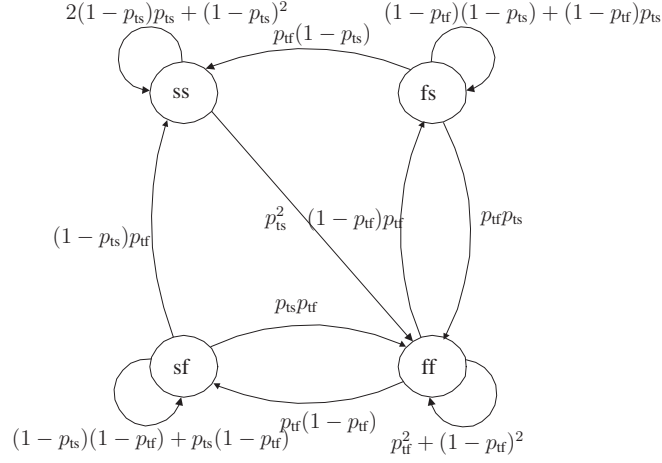


Figure 5-2: System Markov Chain in Example-2, Case-b.

the global balance equations.

$$p_{ss}^a = \frac{(1-p_{ts})p_{tf}}{(1-p_{ts})p_{tf} + p_{ts}^2}$$

$$p_{sf}^a = \frac{p_{ts}^2}{(1-p_{ts})p_{tf} + p_{ts}^2}$$

As mentioned above, the probability of transmission for node-1 (i.e., the nearby node) is always p_{ts} and for node-2 (the distant node) it is given by $(p_{ss}^a p_{ts} + p_{sf}^a p_{tf})$. Finally the throughput of node-1 is p_{ts} and that of node-2 is given by

$$S^a = p_{ss}^a p_{ts} (1 - p_{ts}) + p_{sf}^a p_{tf} (1 - p_{ts}) \quad (5.1)$$

Case-b: $r_1 < r_2 < \alpha r_1$:

Now both node-1 and node-2 can fail, resulting in the system Markov Chain shown in Fig. 5-2. By solving the global balance equations, we can find the steady state probabilities:

$$\begin{aligned}
p_{ff}^b &= \left(1 + \frac{2(1-p_{tf})p_{tf}(1-p_{ts})}{p_{ts}^2} + 2(1-p_{tf}) \right)^{-1} \\
p_{fs}^b &= p_{sf}^b = p_{ff}^b(1-p_{tf}) \\
p_{ss}^b &= p_{ff}^b \frac{2(1-p_{tf})p_{tf}(1-p_{ts})}{p_{ts}^2}
\end{aligned}$$

The average probability of transmission of each node is:

$$p_T^b = p_{ss}^b p_{ts} + p_{sf}^b p_{ts} + p_{fs}^b p_{tf} + p_{ff}^b p_{tf}$$

The average throughput obtained by each of the nodes is

$$S^b = p_{ss}^b p_{ts}(1-p_{ts}) + p_{sf}^b p_{ts}(1-p_{tf}) + p_{fs}^b p_{tf}(1-p_{ts}) + p_{ff}^b p_{tf}(1-p_{tf})$$

In order to obtain the probability of transmission, $\tau(r)$, and the throughput, $S(r)$, as a function of r , we average over case-a and case-b. We denote node-1, node-2 as n_1, n_2 respectively and work on specific locations of n_1 . We divide the averaging into two cases $0 < r_1 < \frac{1}{\alpha}$ and $\frac{1}{\alpha} \leq r_1 < 1$ since in the first case n_2 can be in the area corresponding to $[\alpha r_1, 1]$ whereas in the second case the probability of n_2 being in this interval is zero.

For $0 < r_1 < \frac{1}{\alpha}$:

In this case $\tau(r_1)$ and $S(r_1)$ take three different expressions depending on the interval to which n_2 belongs. If r_2 is in the interval $[\alpha r_1, 1]$, n_2 is outside the vulnerability circle of n_1 , hence case-a applies. If r_2 is inside the interval $[\frac{r_1}{\alpha}, \alpha r_1]$, both are in each other's vulnerability circle, therefore case-b applies. Finally if r_2 is in the interval $[0, \frac{r_1}{\alpha}]$, n_1 is outside the vulnerability circle of n_2 , hence case-a applies again but this time roles of n_1 and n_2

are interchanged. In a more compact form, the $\tau(r_1)$ and $S(r_1)$ are given by;

$$\tau(r_1) = P(n_2 \in [\alpha r_1, 1])p_{ts} + P(n_2 \in [\frac{r_1}{\alpha}, \alpha r_1])p_T^b + \quad (5.2)$$

$$P(n_2 \in [0, \frac{r_1}{\alpha}]) (p_{ss}^a p_{ts} + p_{sf}^a p_{tf}) = (1 - \alpha^2 r_1^2) p_{ts} + (\alpha^2 r_1^2 - \frac{r_1^2}{\alpha^2}) p_T^b + \frac{r_1^2}{\alpha^2} (p_{ss}^a p_{ts} + p_{sf}^a p_{tf})$$

$$S(r_1) = (1 - \alpha^2 r_1^2) p_{ts} + (\alpha^2 r_1^2 - \frac{r_1^2}{\alpha^2}) S^b + \frac{r_1^2}{\alpha^2} S^a \quad (5.3)$$

For $\frac{1}{\alpha} \leq r_1 < 1$:

Similar reasoning to previous case yields;

$$\tau(r_1) = P(n_2 \in [\frac{r_1}{\alpha}, 1])p_T^b + P(n_2 \in [0, \frac{r_1}{\alpha}]) (p_{ss}^a p_{ts} + p_{sf}^a p_{tf}) = \quad (5.4)$$

$$(1 - \frac{r_1^2}{\alpha^2}) p_T^b + \frac{r_1^2}{\alpha^2} (p_{ss}^a p_{ts} + p_{sf}^a p_{tf})$$

$$S(r_1) = (1 - \frac{r_1^2}{\alpha^2}) S^b + \frac{r_1^2}{\alpha^2} S^a \quad (5.5)$$

Thus, averaging over the distribution of node locations in (3.4), we get the overall throughput as

$$S = 2 \int_0^{1/\alpha} \left[(1 - \alpha^2 r^2) p_{ts} + (\alpha^2 r^2 - \frac{r^2}{\alpha^2}) S^b + \frac{r^2}{\alpha^2} S^a \right] 2r dr + \int_{1/\alpha}^1 \left[(1 - \frac{r^2}{\alpha^2}) S^b + \frac{r^2}{\alpha^2} S^a \right] 2r dr$$

From Fig. 5-3, we see that for 2 nodes, the *approximate* results of Section 4.3 are very close to the *exact* results. Intuitively, as the number of nodes in the system increases, the dependencies between the nodes should decrease and hence the approximate results should get closer to the exact results. Therefore we expect the plots in Fig. 4-4, which show the better performance of the *backward model* over the *forward model*, to be very close to exact values.

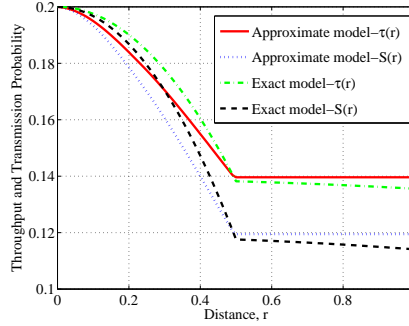


Figure 5-3: The comparison of the transmission probability and the throughput of the exact and the approximate analysis for $\alpha = 2$, $p_{ts} = 0.2$ and $p_{tf} = 0.05$ (i.e., for the forward model case) and uniform distribution of 2 nodes on a disk.

5.2 Deterministic Locations - Without Fading

In this section, we first develop the exact analysis of the case where nodes are allowed to be at one of the two distances from the receiver. Then, we extend the results to more complicated network settings using approximate analysis. The underlying protocol is as described in Section 3.1, i.e., a node successful in its previous attempt uses the probability p_{ts} , and a node that failed in its last attempt uses the probability p_{tf} for transmission in the current slot. If a node was idle in the previous slot, it continues to use the same probability it used during the previous slot.

5.2.1 Exact Model With Nodes at One of Two Different Locations

We assume the network setting of Fig. 4-1, i.e., there are two possible distances from the receiver denoted by r_1 and r_2 with n_1 and n_2 nodes at those distances respectively. Consider the *Backward Protocol* as described in Section 3.1 applied to this setting. We analyze this model using a two dimensional² Markov Chain whose states (i, j) are the number of failed users at distance $r_1 = 1$ and that at distance $r_2 = 2$. An example of such a Markov Chain is shown in Fig. 5-4 for $n_1 = 6$ and $n_2 = 10$. Note that only some of the transition probabilities of the state $(4, 6)$ are shown in the figure and they are referenced throughout

²Note that together with the assumption that $n_2 \leq 2^\beta$, this Markov Chain is 1 dimensional if $n_1 \leq c$. This is because we see from (3.3) that in order for a user at distance 1 to fail, we need either more than c transmissions from distance 1 or c transmissions from distance 1 and more than 2^β transmissions from distance 2. As a result, for $n_1 \leq c$, the 2-dimensional Markov Chain collapses to a 1-dimensional Markov Chain and this 1-dimensional Markov Chain is given in Appendix B.

this section. The number of states in the Markov Chain is $(n_1 + 1)(n_2 + 1)$. Similar to the case in Section 4.1, the analysis is carried out for all n_1 values and for $n_2 < 2^\beta$. The restriction on n_2 simplifies the analysis substantially since considering (3.3), the nodes at distance 2 can make a node at distance 1 fail only if the number of transmissions from distance 1 is c and there are more than 2^β transmissions from distance 2, which is excluded from the analysis by the restriction on n_2 . As a result, a transmission from distance 1 fails only if there are more than c transmissions from distance 1. Furthermore, we assume $(\frac{r_1}{r_2})^\beta > z$ is not satisfied which is the condition for a distance-2 user to be successful in the presence of a distance-1 transmission as discussed in Section 4.1. Hence, a transmission from distance 2 is successful as long as there is no transmission from distance 1 and the number of transmissions from distance 2 is not more than c . Next, we give the transition probabilities of this Markov Chain. In order to be able to describe this Markov Chain better, we group the transition probabilities according to the *amount of increase or decrease* from the current state to the next state. There are three cases in each dimension, i.e., whether the state increases, decreases or doesn't change, making a total of nine different cases to consider.

Denoting the probability of going from the current state (i, j) to the next state (l, m) by $P_{(i,j) \rightarrow (l,m)}$ we have;

Case 1: $l < i$ and $m < j$

$$s \triangleq i - l \text{ and } k \triangleq j - m$$

In this case we have s successful transmissions from the i users at distance 1 that are in the failed state and k successful transmissions from the j users at distance 2 that are in the failed state. Therefore,

$$P_{(i,j) \rightarrow (l,m)} = 0$$

This is due to the fact that a transmission from distance 1 would cause any transmissions from distance 2 to fail.

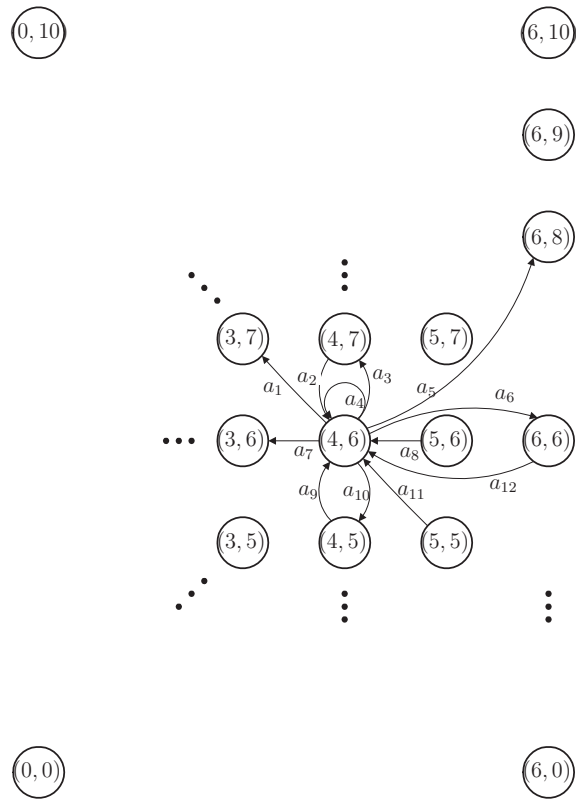


Figure 5-4: The Markov Chain for the analysis in Section 5.2.1 for $n_1 = 6$, $n_2 = 10$ and $z = 0.2$. Note that only some of the transition probabilities of the state $(n_1, n_2) = (4, 6)$ are shown.

Case 2: $l > i$ and $m < j$

$$s \triangleq l - i \text{ and } k \triangleq j - m$$

In this case there are s failed transmissions from the $n_1 - i$ users at distance 1 that are not in the failed state and k successful transmissions from the j users at distance 2 that are in the failed state.

$$P_{(i,j) \rightarrow (l,m)} = 0$$

The reasoning in this case is exactly the same as Case 1.

Case 3: $l > i$ and $m > j$

$$s \triangleq l - i \text{ and } k \triangleq m - j$$

In this case, the number of failed users at distance 1 increases by s (s failed transmissions from the $n_1 - i$ users at distance 1 that are not in the failed state) and that at distance 2 by k (k failed transmissions from the $n_2 - j$ users at distance 2 that are not in the failed state). If $l \leq c$, then the transition probability is 0 because any number of transmissions less than or equal to c from distance 1 is successful. If $l \geq c + 1$ and the increase amount in the first dimension s is less than or equal to c , then there has to be s transmissions from the $n_1 - i$ users at distance 1 that are not in the failed state and at least $c + 1 - s$ transmissions from the failed users at distance 1. This is required since we need more than c transmissions from distance 1 in order to have failure (this is not necessary if $s \geq c + 1$ since all $c + 1$ transmissions will be failed anyway. We see this in the last part of the formula where there is no term for failed users at distance 1). Since $l > i$, we know that at least 1 transmission from distance 1 has occurred and hence any number of transmissions from distance 2 will fail. We need k transmissions from the successful users at distance 2 in order to increase

the second dimension of the state by k . Hence,

$$P_{(i,j) \rightarrow (l,m)} = \begin{cases} 0 & \text{if } l \leq c \\ \binom{n_1 - i}{s} p_{\text{ts}}^s (1 - p_{\text{ts}})^{n_1 - i - s} \binom{n_2 - j}{k} p_{\text{ts}}^k (1 - p_{\text{ts}})^{n_2 - j - k} & \\ \cdot \sum_{v=c+1-s}^i \binom{i}{v} p_{\text{tf}}^v (1 - p_{\text{tf}})^{i-v} & \text{if } s \leq c \text{ and } l \geq c + 1 \\ \binom{n_1 - i}{s} p_{\text{ts}}^s (1 - p_{\text{ts}})^{n_1 - i - s} \binom{n_2 - j}{k} p_{\text{ts}}^k (1 - p_{\text{ts}})^{n_2 - j - k} & \text{if } s \geq c + 1 \end{cases}$$

An example of this case with $l \leq c$ in Fig. 5-4 is the zero transition probability from the state (4, 6) to the state (5, 7). Another example of this case with $s \leq c$ and $l \geq c + 1$ is the nonzero transition probability a_5 from the state (4, 6) to the state (6, 8).

Case 4: $l < i$ and $m > j$

$$s \triangleq i - l \text{ and } k \triangleq m - j$$

In this case, there are s successful transmissions from the i users at distance 1 in the failed state and k failed transmissions from the $n_2 - j$ users at distance 2 that are not in the failed state. If $s \geq c + 1$ the transition probability is zero, because the maximum amount of simultaneously successful transmissions in the channel is c . If $s \leq c$, then we need s transmissions from the failed users at distance 1 (i.e., users transmitting with the probability p_{tf}) and we allow up to $c - s$ transmissions from the successful users at distance 1. This second contribution sums up to 1 if $n_1 - i$ is less than or equal to $c - s$. Finally, similar to Case 3, since there is some transmission from distance 1, all the transmissions from distance

2 will fail and therefore, we need k transmissions from successful users at distance 2.

$$P_{(i,j) \rightarrow (l,m)} = \begin{cases} 0 & \text{if } s \geq c + 1 \\ \binom{i}{s} p_{\text{tf}}^s (1 - p_{\text{tf}})^{i-s} \binom{n_2 - j}{k} p_{\text{ts}}^k (1 - p_{\text{ts}})^{n_2 - j - k} \\ \cdot \sum_{v=0}^{c-s} \binom{n_1 - i}{v} p_{\text{ts}}^v (1 - p_{\text{ts}})^{n_1 - i - v} & \text{if } s \leq c \text{ and } n_1 - i \geq c - s \\ \binom{i}{s} p_{\text{tf}}^s (1 - p_{\text{tf}})^{i-s} \binom{n_2 - j}{k} p_{\text{ts}}^k (1 - p_{\text{ts}})^{n_2 - j - k} & \text{if } s \leq c \text{ and } n_1 - i < c - s \end{cases}$$

In Fig. 5-4, a_{11} is an example of this case for $s \leq c$ and $n_1 - i < c - s$.

Case 5: $l = i$ and $m < j$

$$k \triangleq j - m$$

In this case, the state stays constant in the first dimension and decreases by k in the second dimension. This means that there are k successful transmissions from the j users at distance 2 that are in the failed state. We apply the same logic that we used for the distance-1 users in Case 4 to the distance-2 users here and note that in order to have success from distance 2, we need to have no transmission from distance 1.

$$P_{(i,j) \rightarrow (l,m)} = \begin{cases} 0 & \text{if } k \geq c + 1 \\ (1 - p_{\text{ts}})^{n_1 - i} (1 - p_{\text{tf}})^i \binom{j}{k} p_{\text{tf}}^k (1 - p_{\text{tf}})^{j-k} \\ \cdot \sum_{v=0}^{c-k} \binom{n_2 - j}{v} p_{\text{ts}}^v (1 - p_{\text{ts}})^{n_2 - j - v} & \text{if } k \leq c \text{ and } n_2 - j \geq c - k \\ (1 - p_{\text{ts}})^{n_1 - i} (1 - p_{\text{tf}})^i \binom{j}{k} p_{\text{tf}}^k (1 - p_{\text{tf}})^{j-k} & \text{if } k \leq c \text{ and } n_2 - j < c - k \end{cases}$$

For instance, in Fig. 5-4, a_{10} is an example of the case for $k \leq c$ and $n_2 - j \geq c - k$ and a_2 for $k \leq c$ and $n_2 - j < c - k$.

Case 6: $l < i$ and $m = j$

$$s \triangleq i - l$$

In this case the state does not change in the second dimension and decreases by s in the first. Consequently, we need s successful transmissions from the i failed users at distance 1 and no transmissions from the $n_2 - j$ users at distance 2 that are not in the failed state. Cases 6 and 7 can be understood in a similar fashion to what we did in the previous cases.

$$P_{(i,j) \rightarrow (l,m)} = \begin{cases} 0 & \text{if } s \geq c + 1 \\ \binom{i}{s} p_{\text{tf}}^s (1 - p_{\text{tf}})^{i-s} (1 - p_{\text{ts}})^{n_2-j} & \\ \cdot \sum_{v=0}^{c-s} \binom{n_1-i}{v} p_{\text{ts}}^v (1 - p_{\text{ts}})^{n_1-i-v} & \text{if } s \leq c \text{ and } n_1 - i \geq c - s \\ \binom{i}{s} p_{\text{tf}}^s (1 - p_{\text{tf}})^{i-s} (1 - p_{\text{ts}})^{n_2-j} & \text{if } s \leq c \text{ and } n_1 - i < c - s \end{cases}$$

In Fig. 5-4, a_{12} and a_7 are examples for this case for $s \leq c$ and $n_1 - i < c - s$.

Case 7: $l > i$ and $m = j$

$$s \triangleq l - i$$

In this case, there are s failed transmissions from the i users at distance 1 that are at the failed state and we need no transmissions from the $n_2 - j$ users at distance 2 in order not to change the second dimension of the state.

$$P_{(i,j) \rightarrow (l,m)} = \begin{cases} 0 & \text{if } l \leq c \\ \binom{n_1-i}{s} p_{\text{ts}}^s (1 - p_{\text{ts}})^{n_1-i-s} (1 - p_{\text{ts}})^{n_2-j} & \\ \cdot \sum_{v=t+1-s}^i \binom{i}{v} p_{\text{tf}}^v (1 - p_{\text{tf}})^{i-v} & \text{if } s \leq c \text{ and } l \geq c + 1 \\ \binom{n_1-i}{s} p_{\text{ts}}^s (1 - p_{\text{ts}})^{n_1-i-s} (1 - p_{\text{ts}})^{n_2-j} & \text{if } s \geq c + 1 \end{cases}$$

An example for this case for $l \leq c$ is the zero transmission probability from the state (3, 6) to the state (4, 6) in Fig. 5-4. For the case $s \leq c$ and $l \geq c+1$, a_6 is an example in the figure.

Case 8: $l = i$ and $m > j$

$$k \triangleq m - j$$

In this case the state stays constant in the first dimension and increases by k in the second, i.e., we need k unsuccessful transmissions from distance 2. We divide the event into three disjoint events in order to understand the formula better.

$$P_{(i,j) \rightarrow (l,m)} = P_1 + P_2 + P_3$$

where P_1 is the probability of the event denoting the case where there is no transmission from distance 1. Similar to what we did for users at distance 1 in Case 3 or Case 7, if $m \leq c$, then the transition probability is 0 because there is no transmission from distance 1 and hence any number of transmissions less than or equal to c from distance 2 is successful. If $m \geq c + 1$ and the increase amount in the second dimension k is less than or equal to c , then there has to be k transmissions from the $n_2 - j$ users at distance 2 that are not in the failed state and at least $c + 1 - k$ transmissions from the failed users at distance 2. This is required since we need more than c transmissions from distance 2 in order to have failure. Note that these transmissions from the failed users at distance 2 are not necessary if $k \geq c + 1$, since all $c + 1$ transmissions will be failed anyway. We see this in the last part of the formula where there is no term for failed users at distance 2.

P_2 stands for the event where there is no transmission from the failed users at distance 1 and from 1 up to c transmissions from the successful users at distance 1 so that all the transmissions from distance 1 will be successful and the first dimension of the state will not change. Since there is at least 1 transmission from close-by users, any transmission from faraway nodes will be unsuccessful and hence we need k transmissions from the successful users at distance 2 as shown below in the formula for P_2 .

P_3 is the probability of the event denoting the case where there is no transmission from the successful users at distance 1 and greater than c transmissions from the failed users so

that all the transmissions from distance 1 will be failed and the state in the first dimension will not change. Similar to P_2 , since there are some transmissions from nearby nodes, the k transmissions from the $n_2 - j$ users at distance 2 that are not in the failed state will be failed and the second dimension of the state will increase by k .

$$P_1 = \begin{cases} 0 & \text{if } m \leq c \\ (1 - p_{ts})^{n_1 - i} (1 - p_{tf})^i \binom{n_2 - j}{k} p_{ts}^k (1 - p_{ts})^{n_2 - j - k} \cdot \sum_{v=c+1-k}^j \binom{j}{v} p_{tf}^v (1 - p_{tf})^{j-v} & \text{if } k \leq c \text{ and } m \geq c + 1 \\ (1 - p_{ts})^{n_1 - i} (1 - p_{tf})^i \binom{n_2 - j}{k} p_{ts}^k (1 - p_{ts})^{n_2 - j - k} & \text{if } k \geq c + 1 \end{cases}$$

$$P_2 = \begin{cases} (1 - p_{tf})^i \binom{n_2 - j}{k} p_{ts}^k (1 - p_{ts})^{n_2 - j - k} \sum_{v=1}^{n_1 - i} \binom{n_1 - i}{v} p_{ts}^v (1 - p_{ts})^{n_1 - i - v} & \text{if } n_1 - i \leq c \\ (1 - p_{tf})^i \binom{n_2 - j}{k} p_{ts}^k (1 - p_{ts})^{n_2 - j - k} \sum_{v=1}^c \binom{n_1 - i}{v} p_{ts}^v (1 - p_{ts})^{n_1 - i - v} & \text{if } n_1 - i \geq c + 1 \end{cases}$$

$$P_3 = \begin{cases} 0 & \text{if } i \leq c \\ (1 - p_{ts})^{n_1 - i} \binom{n_2 - j}{k} p_{ts}^k (1 - p_{ts})^{n_2 - j - k} \sum_{v=c+1}^i \binom{i}{v} p_{tf}^v (1 - p_{tf})^{i-v} & \text{if } i > c \end{cases}$$

In Fig. 5-4, a_3 is an example for this case. In a_3 , P_1 and P_2 are nonzero but P_3 is zero.

Case 9: $l = i$ and $m = j$

This is the most complicated case where the state does not change in either dimension. Therefore the associated event is divided into 4 disjoint events.

$$P_{(i,j) \rightarrow (l,m)} = P_1 + P_2 + P_3 + P_4$$

where P_1 is the probability associated with the event where there is no transmission from either distance 1 users or the failed users at distance 2. Therefore, in order for the state to

stay constant, we need c or fewer transmissions from the $n_2 - j$ users at distance 2 that are not in the failed state so that all of them will be successful.

P_2 is the probability of the event in which we do not have any transmissions from distance 1 and this time also no transmissions from the $n_2 - j$ users at distance 2 that are not in the failed state. As a result, we need all transmissions from distant users in the failed state to be unsuccessful and hence we need more than c transmissions from them.

P_3 is the probability of the event denoting the case where there is no transmission from failed users at distance 1 and less than c transmissions from the distance-1 users that are not in the failed state so that they will be successful and the first dimension of the state stays constant. In order for the second dimension not to change, we need no transmissions from the $n_2 - j$ users at distance 2 that are not in failed state because otherwise, they will fail and increase the second dimension of the state.

Finally P_4 is the probability of the event where there is no transmission from the distance-1 users that are not in the failed state and more than c transmissions from the failed users at distance 1 so that all of them will be unsuccessful and the first dimension of the state will stay constant. Similar to P_3 , we need no transmissions from the $n_2 - j$ users at distance 2 that are not in the failed state.

$$P_1 = \begin{cases} (1 - p_{ts})^{n_1 - i} (1 - p_{tf})^i (1 - p_{tf})^j & \text{if } n_2 - j \leq c \\ (1 - p_{ts})^{n_1 - i} (1 - p_{tf})^i (1 - p_{tf})^j \sum_{v=0}^c \binom{n_2 - j}{v} p_{ts}^v (1 - p_{ts})^{n_2 - j - v} & \text{if } n_2 - j \geq c + 1 \end{cases}$$

$$P_2 = \begin{cases} 0 & \text{if } j \leq c \\ (1 - p_{ts})^{n_1 - i} (1 - p_{tf})^i (1 - p_{ts})^{n_2 - j} \sum_{v=c+1}^j \binom{j}{v} p_{tf}^v (1 - p_{tf})^{j-v} & \text{if } j \geq c + 1 \end{cases}$$

$$P_3 = \begin{cases} (1 - p_{\text{tf}})^i (1 - p_{\text{ts}})^{n_2 - j} \sum_{v=1}^{n_1 - i} \binom{n_1 - i}{v} p_{\text{ts}}^v (1 - p_{\text{ts}})^{n_1 - i - v} & \text{if } n_1 - i \leq c \\ (1 - p_{\text{tf}})^i (1 - p_{\text{ts}})^{n_2 - j} \sum_{v=1}^c \binom{n_1 - i}{v} p_{\text{ts}}^v (1 - p_{\text{ts}})^{n_1 - i - v} & \text{if } n_1 - i \geq c + 1 \end{cases}$$

$$P_4 = \begin{cases} 0 & \text{if } i \leq c \\ (1 - p_{\text{ts}})^{n_1 - i} (1 - p_{\text{ts}})^{n_2 - j} \sum_{v=c+1}^i \binom{i}{v} p_{\text{tf}}^v (1 - p_{\text{tf}})^{i - v} & \text{if } i \geq c \end{cases}$$

In Fig. 5-4 a_4 is an example of this case and in a_4 , P_1 , P_2 and P_3 are nonzero but P_4 is zero.

Note that as explained at the beginning of this section, for $n_1 \leq c$ this Markov Chain collapses to a 1-dimensional Markov Chain whose states denote the number of failed users at distance 2 only. The transition probabilities³ of the 1-dimensional Markov Chain are given in Appendix B.

Furthermore, even for the simpler case of 1 allowed distance of the nodes from the receiver, i.e., the case where every user has the same distance from the receiver (for instance $n_1 = 0$), the 1-dimensional Markov Chain reduces to another Markov Chain whose states denote the number of failed users in the system, which was analyzed in [51] in slotted aloha section with finite number of users.

Once the steady state probabilities, denoted by $p(i, j)$, are obtained, we calculate the

³The formulation of this 1-dimensional Markov Chain can be obtained from the original (two dimensional) Markov Chain by letting $i = 0$ and $l = 0$. Only the cases 5 ($l = i$ and $m < j$), 8 ($l = i$ and $m > j$) and 9 ($l = i$ and $m = j$) are relevant since $i = l = 0$ has to be satisfied.

throughput of the system as;

$$\begin{aligned}
S = & \sum_{i=0}^{n_1} \sum_{j=0}^{n_2} \left(p(i, j) \left\{ \sum_{v=0}^{\min(c, i)} \binom{i}{v} p_{\text{tf}}^v (1 - p_{\text{tf}})^{i-v} \sum_{d=0}^{\min(c-v, n_1-i)} (d+v) \binom{n_1-i}{d} p_{\text{ts}}^d (1 - p_{\text{ts}})^{n_1-i-d} + \right. \right. \\
& \left. \left. + (1 - p_{\text{ts}})^{n_1-i} (1 - p_{\text{tf}})^i \left[\sum_{v=0}^{\min(c, j)} \binom{j}{v} p_{\text{tf}}^v (1 - p_{\text{tf}})^{j-v} \sum_{d=0}^{\min(c-v, n_2-j)} (d+v) \binom{n_2-j}{d} p_{\text{ts}}^d (1 - p_{\text{ts}})^{n_2-j-d} \right] \right\} \right) \quad (5.6)
\end{aligned}$$

Note that the first two summations goes through all the states of the Markov Chain. Given that the state of the system is (i, j) , the following two summations denote the throughput coming from the nearby nodes and the last two summations denote the aggregate throughput of the faraway nodes. Since users at distance-2 can not be successful simultaneously with users at distance-1, the total throughput equation can be considered separately for nearby and faraway users as described above. Given any state (i, j) , i.e., i failed users at distance 1 and j at distance 2, we consider the cases that result in success and multiply the probabilities of these events with the number of successful users in those events to get the total throughput of the system for given p_{ts} and p_{tf} values. In particular, we first explain the throughput expression of the nearby nodes given that the state is (i, j) . The probability of v transmissions from the i distance-1 users at failed state and d transmissions from the $n_1 - i$ distance-1 users at successful state is given by

$$\binom{i}{v} p_{\text{tf}}^v (1 - p_{\text{tf}})^{i-v} \binom{n_1-i}{d} p_{\text{ts}}^d (1 - p_{\text{ts}})^{n_1-i-d} \quad (5.7)$$

This quantity is multiplied by the number of transmissions $d + v$ to get the throughput. The two summations associated with v and d are such that $v + d$ is always less than or equal to c . The reason for this condition is the fact that the receiver cannot capture more than c packets at a time. The same reasoning is applied to the throughput equation of the distance-2 nodes together with the fact that in order to have successful transmissions from faraway nodes, we need to have no transmissions from the nearby nodes.

As we see from the 3-dimensional throughput plot for $n_1 = 1$ and $n_2 = 5$ in Fig.

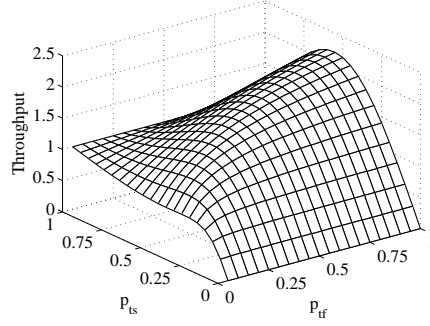


Figure 5-5: Throughput plot for deterministic locations case with $r_1 = 1$, $r_2 = 2$, $n_1 = 1$, $n_2 = 5$ and $z = 0.2$.

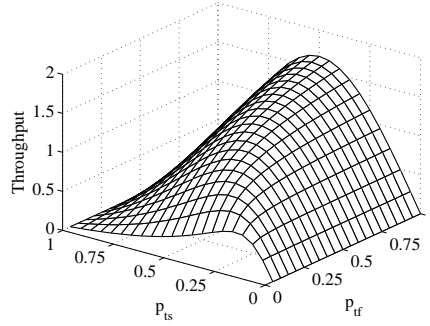


Figure 5-6: Throughput of the faraway nodes for deterministic locations case with $r_1 = 1$, $r_2 = 2$, $n_1 = 1$, $n_2 = 5$ and $z = 0.2$.

5-5, the maximum throughput of 2.195 is obtained for $(p_{ts}, p_{tf}) = (0.55, 1.00)$. We see that at the point where the throughput is maximum, p_{tf} is larger than p_{ts} , suggesting that the *backward model* is better than the *forward model* for this case. Fig. 5-6 shows the total throughput obtained in this case by the nodes at distance $r_2 = 2$. We see that distant nodes have very low throughput in the *forward model*, i.e., when p_{ts} is larger than p_{tf} , and they get significant throughput in the *backward model*, i.e., when p_{tf} is larger than p_{ts} . Furthermore, the maximum overall throughput case, i.e., $(p_{ts}, p_{tf}) = (0.55, 1.00)$, yields a total throughput of 1.645 for faraway nodes and 0.55 for the nearby node, suggesting that the *Backward Protocol* gives enough chances for distant nodes and hence prevents the throughput starvation of them in this case.

Fig. 5-7 shows the 3-dimensional throughput plot for $n_1 = 2$ and $n_2 = 10$. The maximum throughput value of 2.051 is obtained for $(p_{ts}, p_{tf}) = (0.25, 0.50)$, which is also in favor of the *backward model*. The throughput of the faraway users at $(p_{ts}, p_{tf}) = (0.25, 0.50)$

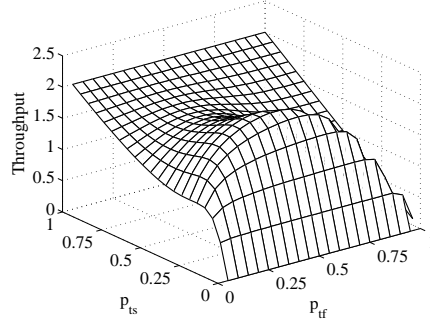


Figure 5-7: Throughput plot for deterministic locations case with $r_1 = 1$, $r_2 = 2$, $n_1 = 2$, $n_2 = 10$ and $z = 0.2$.

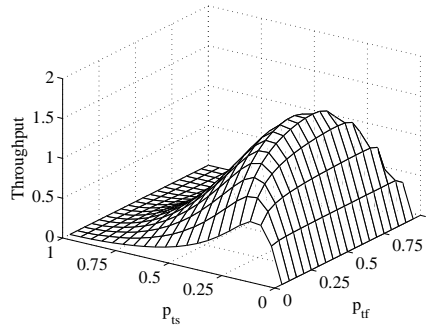


Figure 5-8: Throughput of the faraway nodes for $n_1 = 2$, $n_2 = 10$ and $z = 0.2$.

is 1.551 suggesting a similar conclusion to the $n_1 = 1$ and $n_2 = 5$ case. The 3-dimensional throughput plot of the faraway users is shown in Fig. 5-8 from which we can clearly see that the *backward model* gives higher throughput to distant users and hence is better than the *forward model* in terms of fairness.

Finally, in Fig. 5-9, the plot for $n_1 = 6$, $n_2 = 10$ is shown. Contrary to the previous cases, the maximum throughput is obtained for large values of p_{ts} and small values of p_{tf} . This is due to the fact that c , the maximum number of successful transmissions at a time is; $c = \lceil 1/0.2 \rceil = 5$. Since $n_1 = 6$, there are enough users at distance 1 to successfully capture the channel most of the time. This gives a large throughput value for large values of p_{ts} as expected, however, as we see in Fig. 5-10, the throughput of the faraway users is almost zero for large p_{ts} values and hence operating the protocol with a large p_{ts} value causes throughput starvation of the distant nodes. Instead, we see that in order to let distant nodes have some throughput, we need to have a small p_{ts} value and a moderate p_{tf} value. However, doing this will not utilize the available capacity effectively, as the throughput

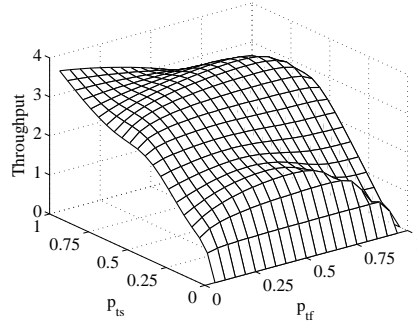


Figure 5-9: Throughput plot for deterministic locations case with $r_1 = 1$, $r_2 = 2$, $n_1 = 6$, $n_2 = 10$ and $z = 0.2$.

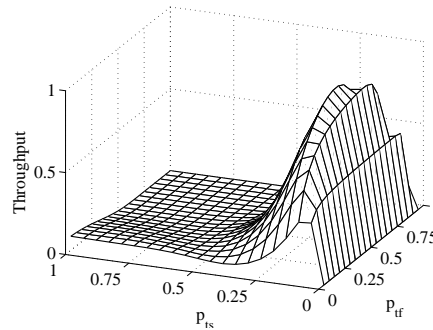


Figure 5-10: Throughput of the faraway nodes for deterministic locations case with $r_1 = 1$, $r_2 = 2$, $n_1 = 6$, $n_2 = 10$ and $z = 0.2$.

obtained out of the system will be low. As a result another solution to the problem might be needed if the number of nearby nodes becomes comparable to c . In Chapter 6 we will consider alternative protocols that will attempt to deal with this issue.

As is clear from the complexity of the above analysis involving just two locations, the analysis of the case with deterministic locations and without fading is quite complicated and cumbersome. Therefore, we develop approximate models that allow us to consider greater number of locations for the nodes. We verify the approximations by comparing the approximate results with the exact results presented in this section for the cases of two allowed distances from the receiver. However, for the verification of the case for three or more possible distances from the receiver, we develop a simulation model which is explained in details in Chapter 7. Note that, we also verify the simulation model by comparing the simulation results with the exact results of this section, i.e., for the case of two allowed distances from the receiver. These comparisons can be found in Figs 7-1, 7-2, 7-3, 7-4,

and 7-5. We see from these figures that the simulation model follows the exact results very closely.

5.2.2 Basic Approximate Model

This approximate model was introduced in Section 4.3; where we assumed that a packet transmitted by a user at distance r fails with constant and independent probability $p_d(r)$, regardless of its or any other user's success history. We expect this model to be reasonably accurate when the number of nodes in the network increases. This is because with a small number of nodes, the dependence among users is large and we showed already in Section 5.1 that even with just two nodes, the approximate results are very close to the exact results. Now we apply this approximation for the current case with users at one of two possible distances from the receiver and no fading. We use the notation τ_1 , τ_2 , p_{d1} and p_{d2} for $\tau(1)$, $\tau(2)$, $p_d(1)$ and $p_d(2)$. In addition, we still keep the assumption that $n_2 < 2^\beta$, which ensures us that the distance-1 users operate totally independently from nodes at distance 2.

Case 1: $n_1 \leq c$ and $n_2 \leq c$

Similar to the Aloha with Two Distances example in Section 4.1, nodes at distance 1 do not fail in this case (hence they transmit with probability p_{ts} always) and those at distance 2 fail only if there is a simultaneous transmission from distance 1. As a result, for nodes at distance $r_1 = 1$;

$$p_{d1} = 0 \quad \text{and} \quad \tau_1 = p_{ts} \quad (5.8)$$

The faraway nodes fail if there is at least one transmission from nearby nodes. Therefore,

$$p_{d2} = 1 - (1 - \tau_1)^{n_1} \quad (5.9)$$

$$\text{and from (4.3)} \quad \Rightarrow \tau_2 = \frac{p_{ts}}{1 - p_{d2} + \frac{p_{ts}}{p_{tf}} p_{d2}} = \frac{p_{ts}}{1 - (1 - (1 - p_{ts})^{n_1}) + \frac{p_{ts}}{p_{tf}} (1 - (1 - p_{ts})^{n_1})} \quad (5.10)$$

Note that p_{d2} is the probability that a packet from a node at distance 2 is lost *given that* the node has transmitted. Looking at the equations of p_{d2} and τ_2 , we see that they are functions of p_{ts} and p_{tf} only and hence given p_{ts} and p_{tf} they are constants independent of one another.

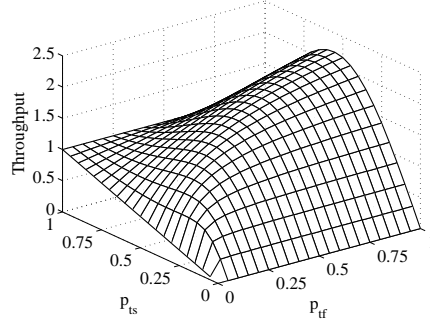


Figure 5-11: Throughput plot for $n_1 = 1$, $n_2 = 5$ and $z = 0.2$ using the Basic Approximate Model.

The throughput is also a function of p_{ts} and p_{tf} only and is given by;

$$S = n_1\tau_1 + (1 - \tau_1)^{n_1}n_2\tau_2 = n_1p_{ts} + n_2(1 - p_{ts})^{n_1} \frac{p_{ts}}{(1 - p_{ts})^{n_1} + \frac{p_{ts}}{p_{tf}}(1 - (1 - p_{ts})^{n_1})} \quad (5.11)$$

In (5.11), the $n_1\tau_1$ term denotes the throughput of the nearby nodes and $(1 - \tau_1)^{n_1}n_2\tau_2$ denotes that of the faraway nodes.

Fig. 5-11 shows the throughput plot for the case of $n_1 = 1$ and $n_2 = 5$. We see that the throughput values are exactly the same as those obtained from the exact model in the previous section. This is expected since when n_1 and n_2 are both less than or equal to c , the variables in two locations are constants independent of each other given p_{ts} and p_{tf} . Therefore, the approximation that a packet transmitted by a node at distance r is lost with constant and independent probability $p_d(r)$ is exact in this case. Namely for $n_1 = 1$ and $n_2 = 5$, $p_{d1} = 0$ and $p_{d2} = 1 - (1 - p_{ts})^{n_1} = p_{ts}$.

Regarding the Markov Chain analysis of this case in the previous section, when $n_1 \leq c$, the nearby users are always successful, hence the Markov Chain is 1-dimensional in this case. Since nodes at distance 2 fail only if there is a transmission from distance 1, $p_{d2} = 1 - (1 - p_{ts})^{n_1}$ is a constant, independent of the state of the Markov Chain. As a result, the case of $n_1 \leq c$ and $n_2 \leq c$ can be formulated exactly without a Markov Chain analysis.

Case 2: $n_1 \leq c$ and $n_2 > c$

As explained in Aloha with Two Distances example in Section 4.2, the nodes at distance 1 are still always successful and those at distance 2 fail if there is at least one transmission

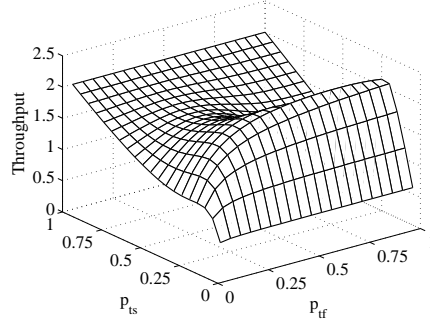


Figure 5-12: Throughput plot for deterministic locations case with $r_1 = 1$, $r_2 = 2$, $n_1 = 2$, $n_2 = 10$ and $z = 0.2$ using the Basic Approximate Model.

from distance 1 or if there are more than c transmissions from distance 2. As a result, we obtain;

$$p_{d1} = 0 \quad \text{and} \quad \tau_1 = p_{ts} \quad (5.12)$$

$$p_{d2} = P_1 + P_2 - P_1P_2, \text{ where} \quad (5.13)$$

$$P_1 = (1 - (1 - \tau_1)^{n_1})$$

$$P_2 = \sum_{k=c+1}^{n_2} \binom{n_2}{k} \tau_2^k (1 - \tau_2)^{n_2-k}$$

Where in (5.13), we used the fact that nodes at distance 2 can fail as a result of two independent events with probabilities P_1 and P_2 . Using equation (4.3), τ_2 is given by;

$$\tau_2 = \frac{p_{ts}}{1 - p_{d2} + \frac{p_{ts}}{p_{tf}} p_{d2}} \quad (5.14)$$

Finally, the throughput equation is given by;

$$S = n_1 p_{ts} + (1 - p_{ts})^{n_1} \sum_{k=1}^c \binom{n_2}{k} \tau_2^k (1 - \tau_2)^{n_2-k} \quad (5.15)$$

The reasoning in this equation is similar to what we had for (5.6) and (5.11).

We show the resulting plot of throughput in Fig. 5-12 for $n_1 = 2$, $n_2 = 10$ and $z = 0.2$. Comparing this figure with Fig. 5-7, the plots are different in the area where p_{ts} is small and p_{tf} is large. The reason for this difference is that there are multiple roots to the solution of (5.13) and (5.14) and hence in this region, the numerical equation solver (MATLAB in our case) converges to different solutions for τ_2 for different initial values. We observed that MATLAB converges to the correct root for some initial values of τ_2 . Other than this region, the values in the plot are very close to the exact values in Fig. 5-7.

Case 3: $n_1 > c$ and $n_2 > c$

In this case, failure events of faraway nodes are the same but nearby nodes also fail if there are more than c simultaneous transmissions from distance 1. This difference yields the following result in formulation:

$$p_{d1} = \sum_{k=c+1}^{n_1} \binom{n_1}{k} \tau_1^k (1 - \tau_1)^{n_1-k} \quad (5.16)$$

$$\tau_1 = \frac{p_{ts}}{1 - p_{d1} + \frac{p_{ts}}{p_{tf}} p_{d1}} \quad (5.17)$$

$$p_{d2} = P_1 + P_2 - P_1 P_2, \text{ where} \quad (5.18)$$

$$P_1 = (1 - (1 - \tau_1)^{n_1})$$

$$P_2 = \sum_{k=c+1}^{n_2} \binom{n_2}{k} \tau_2^k (1 - \tau_2)^{n_2-k}$$

$$\tau_2 = \frac{p_{ts}}{1 - p_{d2} + \frac{p_{ts}}{p_{tf}} p_{d2}} \quad (5.19)$$

In this case, we can solve for τ_1 and τ_2 , and hence for p_{d1} and p_{d2} numerically using (5.16), (5.17), (5.18) and (5.19). The throughput equation is given by:

$$S = \sum_{k=1}^c \binom{n_1}{k} \tau_1^k (1 - \tau_1)^{n_1-k} + (1 - \tau_1)^{n_1} \sum_{k=1}^c \binom{n_2}{k} \tau_2^k (1 - \tau_2)^{n_2-k} \quad (5.20)$$

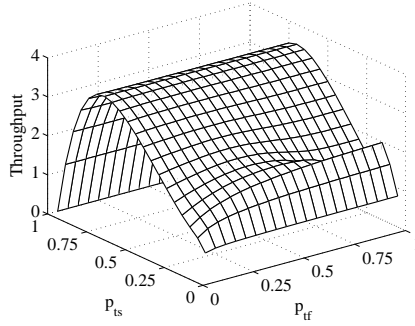


Figure 5-13: Throughput plot for deterministic locations case with $r_1 = 1$, $r_2 = 2$, $n_1 = 6$, $n_2 = 10$ and $z = 0.2$ using the Basic Approximate Model.

This throughput equation is again similar to (5.6) and (5.11) and can be understood in the same way.

The resulting 3-dimensional throughput plot is shown in Fig. 5-13 for $n_1 = 6$, $n_2 = 10$. Similar to what we had in case-2, when we compare this figure with Fig. 5-9, we observe that the approximation deviates from the exact results for $p_{ts} \cong 1$ or $p_{tf} \cong 1$. However, operating the protocol with such large p_{ts} or p_{tf} values is not practical and other than these two impractical regions, the values in the plot are very close to the exact values in Fig. 5-7.

We see that the basic approximate model of this section works well for most p_{ts} and p_{tf} values. Note that this approximate model is simple and general in the sense that it also applies to networks with random node locations as demonstrated in Section 4.3. However, if the locations of the nodes are deterministic, we can provide better approximations as shown in the next section.

5.2.3 Enhanced Approximate Model

In this section we provide a better approximation in order to be able to make general claims for all sets of probabilities. One observation from sections 5.2.1 and 5.2.2 is that under the limitation $n_2 < 2^\beta$, nodes at distance 1 are totally independent from the nodes at distance 2, however, they are not independent of each other. Furthermore, the dependence of faraway users on the nearby nodes for successful transmission is limited to the single event that “no transmission should occur from the nearby nodes”. As a result, approximating the nodes at different distances to be independent of each other and nodes at the same distance to be

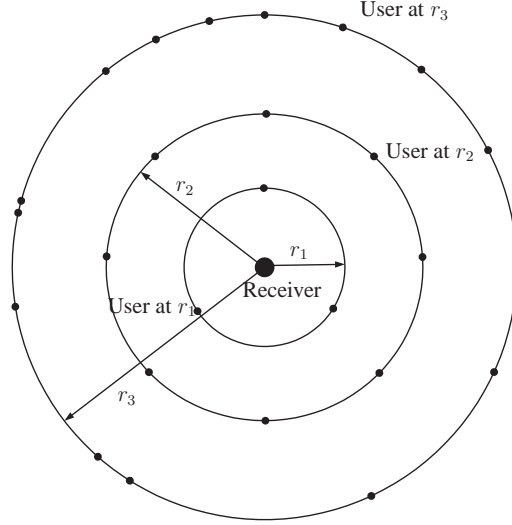


Figure 5-14: Network Structure, Enhanced Approximate Model.

dependent on each other is a reasonable idea in our setting. We apply this idea by having a separate Markov Chain for nodes at different distances in the network. The state of each Markov Chain is the number of failed nodes at the corresponding distance and the dependence⁴ between different Markov Chains is through the average transmission probabilities $\tau(i)$ denoted by τ_i of nodes at distance r_i from the base station for $i = 1, 2, 3, 4, \dots$. In order to have this idea of independence among different distances be a good approximation, we need to put some limitations on n_i , the number of users at distance r_i , i.e., we need to have users at distance r_i depend only on users whose distance is less than r_i and independent of the rest of the nodes. In sections 4.1, 5.2.1 and 5.2.2, we explained that when there are only two distances in the system, i.e., some nodes at distance 1 and some at distance 2, the condition that $n_2 < 2^\beta$ ensures that faraway nodes have no affect on nearby nodes, in other words, nearby nodes are independent of the faraway nodes. Now in order to generalize these results to more distances, we consider a network with nodes at one of three different distances from the receiver.

Consider the network setting shown in Fig. (5-14). We have n_1 users at distance r_1 , n_2 at r_2 and n_3 at r_3 . Next, consider the capture equation (3.3) and note that $R = 1$ here since there is no fading assumed in this section. In order to have nodes at r_2 independent of the

⁴The users at different distances are of course not totally independent since for example if there is at least one transmission from distance-1, the distance-2 nodes cannot be successful. This limited dependence is captured through the average probability of transmission from distance r_i , $\tau(i)$, in the model.

nodes at r_3 , using the capture equation (3.3) we have⁵;

$$Kr_2^{-\beta}P_T > z\left(\frac{1}{z} - 1\right)Kr_2^{-\beta}P_T + n_3Kr_3^{-\beta}P_T$$

simplifying we get

$$r_2^{-\beta} > r_2^{-\beta} - zr_2^{-\beta} + zn_3r_3^{-\beta}$$

and hence

$$n_3 < \left(\frac{r_3}{r_2}\right)^\beta \quad (5.21)$$

In order to have nodes at r_1 to be independent of nodes at r_2 and r_3 , and noting that in the most limiting case n_3 is equal to $\lceil\left(\frac{r_3}{r_2}\right)^\beta\rceil - 1$, we have;

$$Kr_1^{-\beta}P_T > z\left(\frac{1}{z} - 1\right)Kr_1^{-\beta}P_T + n_2Kr_2^{-\beta}P_T + n_3Kr_3^{-\beta}P_T$$

canceling the constants we obtain,

$$r_1^{-\beta} > z\left(\frac{1}{z} - 1\right)r_1^{-\beta} + n_2r_2^{-\beta} + n_3r_3^{-\beta}$$

this gives,

$$r_1^{-\beta} > r_1^{-\beta} - zr_1^{-\beta} + zn_2r_2^{-\beta} + zn_3r_3^{-\beta}$$

further simplifications yield,

$$n_2 < r_2^\beta(r_1^{-\beta} - n_3r_3^{-\beta})$$

and hence,

$$n_2 < \left(\frac{r_2}{r_1}\right)^\beta - \left(\frac{r_2}{r_3}\right)^\beta(\lceil\left(\frac{r_3}{r_2}\right)^\beta\rceil - 1) \quad (5.22)$$

Now consider $r_1 = 1$, $r_2 = 2$, $r_3 = 3$ and $\beta = 4$. We have $n_3 < \left(\frac{3}{2}\right)^4 = 5.063$ and $n_2 < \left(\frac{2}{1}\right)^4 - \left(\frac{2}{3}\right)^\beta(\lceil\left(\frac{3}{2}\right)^4\rceil - 1) = 15.012$, i.e., for the practical value of $\beta = 4$ assumed in our work, we need n_3 to be less than or equal to 5 while the condition on n_2 is that it should

⁵Similar to the explanation in Section 4.1 for the distance-1 users, the limiting case for the effect of distance-3 nodes on the success criteria of distance-2 nodes occurs when there are total c transmissions from distance 2 and hence $c - 1 = 1/z - 1$ interferers from distance 2.

be less than or equal to 15 if want to use this approximation model with a good reliability⁶. However, in a uniform spatial distribution of nodes on a disk, the number of nodes from the receiver increases proportionally to the distance from the receiver. Therefore this limitation on n_3 prevents us from obtaining practical results. As a result, we consider $r_3 = 4$ in our setting and get $n_2 < 15.063$ and $n_3 < 16$ from (5.21) and (5.22) respectively, allowing us to obtain results very close to the exact values. With a similar analysis for $r_1 = 1, r_2 = 2, r_3 = 4$ and $r_4 = 8$ one obtains $n_2 < 14.066, n_3 < 15.063$ and $n_4 < 16$.

When compared to the cumbersome exact analysis of Section 5.2.1 for two distances case, the *Enhanced Approximation* is much easier to formulate and it is easy to extend to more distances from the receiver as long as some constraints on n_i , the number of users at distance r_i are satisfied. In particular, note that we have three Markov Chains for three different distances representing the number of failed users at each distance and the formulation of these Markov Chains are very similar to each other. Furthermore, the dependence between the Markov Chain of each distance is through the average probabilities of transmission from those distances, which substantially simplifies the analysis. Namely, considering the nodes at distance-2, in Section 5.2.1 we had 3 different cases in analysis for each of the 3 different changes in the first dimension of the state (i.e., increase, decrease or the no change of the number of failed nodes at distance-1) yielding total of 9 cases. However, all the effects of distance-1 transmissions on distance-2 transmissions are through the single event that *there is at least one transmission from distance-1* which is covered well by the *Enhanced Approximation*.

Under the constraints for n_2 and n_3 for the 3 distances case ($r_1 = 1, r_2 = 2$ and $r_3 = 4$), we formulate the transition probabilities of the Markov Chains as follows.

Markov Chain for nodes at distance $r_1 = 1$:

We will denote the state transitions as going from state i to state l and note that the explanations of the equations are very similar to what we have in Section 5.2.1.

⁶Note that in Section 4.1 we showed that a single distance-1 transmission is enough to destruct a distance-2 transmission for $z = 0.2$. Here a similar calculation shows that this is also the case for distances 2 and 3. Namely, a single distance-2 transmission destructs a distance-3 transmission for $z = 0.2$.

Case 1: $l > i$

$$s \triangleq l - i$$

$$P_{i \rightarrow l} = \begin{cases} 0 & \text{if } l \leq c \\ \binom{n_1 - i}{s} p_{ts}^s (1 - p_{ts})^{n_1 - i - s} \sum_{v=c+1-s}^i \binom{i}{v} p_{tf}^v (1 - p_{tf})^{i-v} & \text{if } s \leq c \text{ and } l \geq c + 1 \\ \binom{n_1 - i}{s} p_{ts}^s (1 - p_{ts})^{n_1 - i - s} & \text{if } s \geq c + 1 \end{cases}$$

Case 2: $l < i$

$$s \triangleq i - l$$

$$P_{i \rightarrow l} = \begin{cases} 0 & \text{if } s \geq c + 1 \\ \binom{i}{s} p_{tf}^s (1 - p_{tf})^{i-s} \sum_{v=0}^{c-s} \binom{n_1 - i}{v} p_{ts}^v (1 - p_{ts})^{n_1 - i - v} & \text{if } s \leq c \text{ and } n_1 - i \geq c - s \\ \binom{i}{s} p_{tf}^s (1 - p_{tf})^{i-s} & \text{if } s \leq c \text{ and } n_1 - i < c - s \end{cases}$$

Case 3: $l = i$

$$P_{i \rightarrow l} = P_1 + P_2, \text{ where}$$

$$P_1 = \begin{cases} (1 - p_{\text{tf}})^i & \text{if } n_1 - i \leq c \\ (1 - p_{\text{tf}})^i \sum_{v=0}^c \binom{n_1 - i}{v} p_{\text{ts}}^v (1 - p_{\text{ts}})^{n_1 - i - v} & \text{if } n_1 - i \geq c + 1 \end{cases}$$

$$P_2 = \begin{cases} 0 & \text{if } i \leq c \\ (1 - p_{\text{ts}})^{n_1 - i} \sum_{v=c+1}^i \binom{i}{v} p_{\text{tf}}^v (1 - p_{\text{tf}})^{i - v} & \text{if } i > c \end{cases}$$

Calculating the steady state probabilities $p_1(i)$ of this Markov Chain numerically, we can obtain the average probability of transmission, τ_1 , for a node at distance 1 as

$$\tau_1 = p_1(i) \frac{i p_{\text{tf}} + (n_1 - i) p_{\text{ts}}}{n_1} \quad (5.23)$$

Markov Chain at Distance $r_2 = 2$:

The state transitions will be denoted as going from state j to state m and note that the explanations of the equations are still very similar to what we have in Case-1 and Section 5.2.1. There are two minor differences from Case-1 equations; first, in order to successfully receive a packet from the distance-2 users we need to have no transmissions from the distance-1 users $((1 - \tau_1)^{n_1})$ and second, distance-2 nodes can fail if there is at least one transmission from the distance-1 users $((1 - (1 - \tau_1)^{n_1}))$ or if there are more than c transmissions from the distance-2 users.

Case 1: $m > j$

$$k \triangleq m - j$$

$$P_{j \rightarrow m} = \begin{cases} (1 - (1 - \tau_1)^{n_1}) \binom{n_2 - j}{k} p_{\text{ts}}^k (1 - p_{\text{ts}})^{n_2 - j - k} & \text{if } m \leq c \\ (1 - (1 - \tau_1)^{n_1}) \binom{n_2 - j}{k} p_{\text{ts}}^k (1 - p_{\text{ts}})^{n_2 - j - k} + \\ + (1 - \tau_1)^{n_1} \binom{n_2 - j}{k} p_{\text{ts}}^k (1 - p_{\text{ts}})^{n_2 - j - k} \sum_{v=c+1-k}^j \binom{j}{v} p_{\text{tf}}^v (1 - p_{\text{tf}})^{j-v} & \text{if } k \leq c \text{ and } m \geq c + 1 \\ \binom{n_2 - j}{k} p_{\text{ts}}^k (1 - p_{\text{ts}})^{n_2 - j - k} & \text{if } k \geq c + 1 \end{cases}$$

Case 2: $m < j$

$$k \triangleq j - m$$

$$P_{j \rightarrow m} = \begin{cases} 0 & \text{if } k \geq c + 1 \\ (1 - \tau_1)^{n_1} \binom{j}{k} p_{\text{tf}}^k (1 - p_{\text{tf}})^{j-k} \sum_{v=0}^{c-k} \binom{n_2 - j}{v} p_{\text{ts}}^v (1 - p_{\text{ts}})^{n_2 - j - v} & \text{if } k \leq c \text{ and } n_2 - j \geq c - k \\ (1 - \tau_1)^{n_1} \binom{j}{k} p_{\text{tf}}^k (1 - p_{\text{tf}})^{j-k} & \text{if } k \leq c \text{ and } n_2 - j < c - k \end{cases}$$

Case 3: $m = j$

$$P_{j \rightarrow m} = P_1 + P_2 + P_3, \text{ where}$$

$$P_1 = (1 - (1 - \tau_1)^{n_1}) (1 - p_{\text{ts}})^{n_2 - j} \quad (5.24)$$

$$P_2 = \begin{cases} (1 - \tau_1)^{n_1} (1 - p_{\text{tf}})^j & \text{if } n_2 - j \leq c \\ (1 - \tau_1)^{n_1} (1 - p_{\text{tf}})^j \sum_{v=0}^c \binom{n_2 - j}{v} p_{\text{ts}}^v (1 - p_{\text{ts}})^{n_2 - j - v} & \text{if } n_2 - j \geq c + 1 \end{cases}$$

$$P_3 = \begin{cases} 0 & \text{if } j \leq c \\ (1 - \tau_1)^{n_1} (1 - p_{\text{ts}})^{n_2 - j} \sum_{v=c+1}^j \binom{j}{v} p_{\text{tf}}^v (1 - p_{\text{tf}})^{j - v} & \text{if } j > c \end{cases}$$

After calculating the steady state probabilities $p_2(j)$ of this Markov Chain numerically, we obtain the average probability of transmission, τ_2 , for a node at distance 2 to be

$$\tau_2 = p_2(j) \frac{j p_{\text{tf}} + (n_2 - j) p_{\text{ts}}}{n_2} \quad (5.25)$$

Markov Chain at Distance $r_3 = 4$:

We denote the state transitions as going from state h to state u . Throughout this case, let P_a , P_b and P_c denote;

$$P_a = (1 - \tau_1)^{n_1} \quad (5.26)$$

$$P_b = (1 - \tau_2)^{n_2} \quad (5.27)$$

$$P_c = (1 - P_a) + (1 - P_b) - (1 - P_a)(1 - P_b) \quad (5.28)$$

Note that, P_c denotes the event that there is at least one transmission either from distance 1 or distance 2. The equations in this case are very similar to those in Case-2. In particular, in order to have a successful transmission from the distance-4 users, we need no transmissions from the distance-1 and distance-2 users ($P_a P_b$) and nodes at distance 4 fail only if there is at least one transmission from the distance-1 or distance-2 users (P_c) or if there are more than c transmissions from the distance-4 users.

Case 1: $u > h$

$$g \triangleq u - h$$

$$P_{h \rightarrow u} = \begin{cases} P_c \binom{n_3 - h}{g} p_{ts}^g (1 - p_{ts})^{n_3 - h - g} & \text{if } u \leq c \\ P_c \binom{n_3 - h}{g} p_{ts}^g (1 - p_{ts})^{n_3 - h - g} + P_a P_b \binom{n_3 - h}{g} p_{ts}^g (1 - p_{ts})^{n_3 - h - g} \sum_{v=c+1-g}^h \binom{h}{v} p_{tf}^v (1 - p_{tf})^{h-v} & \text{if } g \leq c \text{ and } u \geq c + 1 \\ \binom{n_3 - h}{g} p_{ts}^g (1 - p_{ts})^{n_3 - h - g} & \text{if } g \geq c + 1 \end{cases}$$

Case 2: $u < h$

$$g \triangleq h - u$$

$$P_{h \rightarrow u} = \begin{cases} 0 & \text{if } g \geq c + 1 \\ P_a P_b \binom{h}{g} p_{tf}^g (1 - p_{tf})^{h-g} \sum_{v=0}^{c-g} \binom{n_3 - h}{v} p_{ts}^v (1 - p_{ts})^{n_3 - h - v} & \text{if } g \leq c \text{ and } n_3 - h \geq c - g \\ P_a P_b \binom{h}{g} p_{tf}^g (1 - p_{tf})^{h-g} & \text{if } g \leq c \text{ and } n_3 - h < c - g \end{cases}$$

Case 3: $u = h$

$P_{h \rightarrow u} = P_1 + P_2 + P_3$, where

$$P_1 = P_c (1 - p_{ts})^{n_3 - h} \quad (5.29)$$

$$P_2 = \begin{cases} P_1 P_2 (1 - p_{\text{tf}})^h & \text{if } n_3 - h \leq c \\ P_a P_b (1 - p_{\text{tf}})^h \sum_{v=0}^c \binom{n_3 - h}{v} p_{\text{ts}}^v (1 - p_{\text{ts}})^{n_3 - h - v} & \text{if } n_3 - h \geq c + 1 \end{cases}$$

$$P_3 = \begin{cases} 0 & \text{if } h \leq c \\ P_a P_b (1 - p_{\text{ts}})^{n_3 - h} \sum_{v=c+1}^h \binom{h}{v} p_{\text{tf}}^v (1 - p_{\text{tf}})^{h-v} & \text{if } h > c \end{cases}$$

We calculate the steady state probabilities $p_3(h)$ of this Markov Chain numerically and obtain the average probability of transmission, τ_3 , for a node at distance $n_3 = 4$ to be

$$\tau_3 = p_3(h) \frac{j p_{\text{tf}} + (n_3 - j) p_{\text{ts}}}{n_3} \quad (5.30)$$

We finally obtain the throughput equation as

$$S = \sum_{i=0}^{n_1} \sum_{j=0}^{n_2} \sum_{h=0}^{n_3} p_1(i) p_2(j) p_3(h) \left\{ \sum_{v=0}^{\min(c,i)} \binom{i}{v} p_{\text{tf}}^v (1 - p_{\text{tf}})^{i-v} \sum_{d=0}^{\min(c-v, n_1-i)} \binom{n_1-i}{d} p_{\text{ts}}^d (1 - p_{\text{ts}})^{n_1-i-d} + \right.$$

$$+ (1 - p_{\text{ts}})^{n_1-i} (1 - p_{\text{tf}})^i \left[\sum_{v=0}^{\min(c,j)} \binom{j}{v} p_{\text{tf}}^v (1 - p_{\text{tf}})^{j-v} \sum_{d=0}^{\min(c-v, n_2-j)} \binom{n_2-j}{d} p_{\text{ts}}^d (1 - p_{\text{ts}})^{n_2-j-d} \right] +$$

$$\left. + (1 - p_{\text{ts}})^{n_1+n_2-i-j} (1 - p_{\text{tf}})^{i+j} \left[\sum_{v=0}^{\min(c,h)} \binom{h}{v} p_{\text{tf}}^v (1 - p_{\text{tf}})^{h-v} \sum_{d=0}^{\min(c-v, n_3-h)} \binom{n_3-h}{d} p_{\text{ts}}^d (1 - p_{\text{ts}})^{n_3-h-d} \right] \right\} \quad (5.31)$$

This equation is very similar to (5.6) with the difference that we have 3 sources of throughput, namely throughput of distance-1, 2 and 4 users. In order to have a successful transmission from distance-2 we need to have no transmissions from distance-1 ($(1 - p_{\text{ts}})^{n_1-i} (1 - p_{\text{tf}})^i$). Similarly, for a successful transmission from distance-4, we need no transmissions from both distance 1 and 2 ($(1 - p_{\text{ts}})^{n_1+n_2-i-j} (1 - p_{\text{tf}})^{i+j}$). Finally, the steady state probabilities of the Markov Chains $p_1(i)$, $p_2(j)$ and $p_3(h)$ are multiplicative. This naturally results from the independence approximation that we make in this section between different distances⁷.

⁷As explained at the beginning of this section, the nodes at different distances are not totally independent

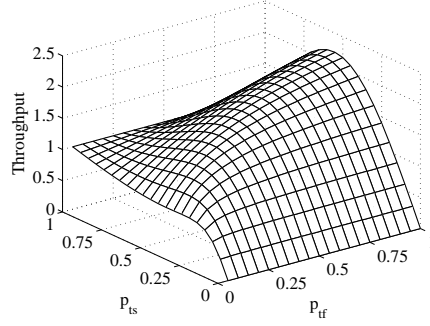


Figure 5-15: Throughput plot for deterministic locations case with $r_1 = 1$, $r_2 = 2$, $n_1 = 1$, $n_2 = 5$ and $z = 0.2$ using the Enhanced Approximate Model.

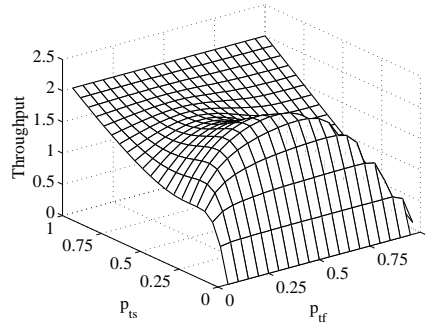


Figure 5-16: Throughput plot for deterministic locations case with $r_1 = 1$, $r_2 = 2$, $n_1 = 2$, $n_2 = 10$ and $z = 0.2$ using the Enhanced Approximate Model.

Note that in order to generate results for two locations case using this approximate model, all we have to do is to discard the Markov Chain of distance 4; this is because both users at distance 1 and distance 2 are independent of the users at distance 4. The resulting throughput equation would then be given by;

$$\begin{aligned}
 S = & \sum_{i=0}^{n_1} \sum_{j=0}^{n_2} p_1(i)p_2(j) \left\{ \sum_{v=0}^{\min(c,i)} \binom{i}{v} p_{\text{tf}}^v (1 - p_{\text{tf}})^{i-v} \sum_{d=0}^{\min(c-v, n_1-i)} (d+v) \binom{n_1-i}{d} p_{\text{ts}}^d (1 - p_{\text{ts}})^{n_1-i-d} + \right. \\
 & \left. + (1 - p_{\text{ts}})^{n_1-i} (1 - p_{\text{tf}})^i \left[\sum_{v=0}^{\min(c,j)} \binom{j}{v} p_{\text{tf}}^v (1 - p_{\text{tf}})^{j-v} \sum_{d=0}^{\min(c-v, n_2-j)} (d+v) \binom{n_2-j}{d} p_{\text{ts}}^d (1 - p_{\text{ts}})^{n_2-j-d} \right] \right\}
 \end{aligned} \tag{5.32}$$

The throughput plot for $n_1 = 1$, $n_2 = 5$ is shown in Fig. 5-15. The results are the same

but they have a very limited dependence. Namely, in order to have a successful transmission from a given user, we require no transmissions from users closer to the receiver than the given user.

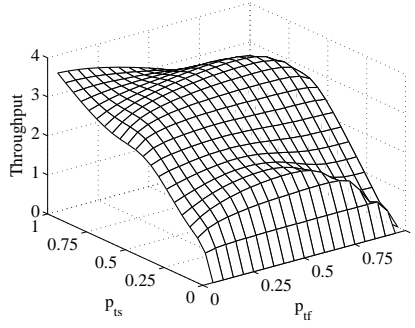


Figure 5-17: Throughput plot for deterministic locations case with $r_1 = 1$, $r_2 = 2$, $n_1 = 6$, $n_2 = 10$ and $z = 0.2$ using the Enhanced Approximate Model.

as the exact values in Fig. 5-5. This is expected since this approximation is better than the first one which already achieves the same exact values for the case of $n_1 \leq c$ and $n_2 \leq c$. Fig. 5-16 shows the throughput plot for $n_1 = 2$ and $n_2 = 10$. We observe that this case also yields the same values as the exact case in Fig. 5-7, and this is also expected since when $n_1 \leq c$, the nearby nodes are always successful, i.e., there is no Markov Chain for distance 1 and hence $\tau_1 = p_{ts}$ always. As a result, the input from the first Markov Chain to the second, i.e., $\tau_1 = p_{ts}$ is exact and therefore the Markov Chain of distance 2 describes the system completely. A similar observation was pointed out at the end of the Section 5.2.1, i.e., when $n_1 \leq c$, we observed that the two-dimensional Markov Chain collapsed to the 1-dimensional Markov Chain whose states denoted the number of failed users at distance 2 only. In Fig. 5-17 we show the throughput plot for the case of $n_1 = 6$ and $n_2 = 10$. The values are the same as the exact values in Fig. 5-9 except in the area $p_{ts} > 0.75$ and $p_{tf} < 0.35$ where the values are correct to two decimal places. As a result, we see that this approximation is very accurate and can provide results that are very close to exact, as long as some conditions on n_i , $i = 2, 3, 4, \dots$ are satisfied.

Figures 5-18, 5-19 and 5-20 show the overall throughput of the network, total throughput of the n_2 nodes at distance-2 and that of the n_3 nodes at distance-4 respectively for $z = 0.2$. In order to show the validity of these results, we plot the ratio of the throughput values obtained from simulations to those obtained from the Enhanced Approximate Model. These figures can be found in Chapter 7 (Figures 7-6, 7-7 and 7-8) demonstrating the accuracy of the Enhanced Approximate Model.

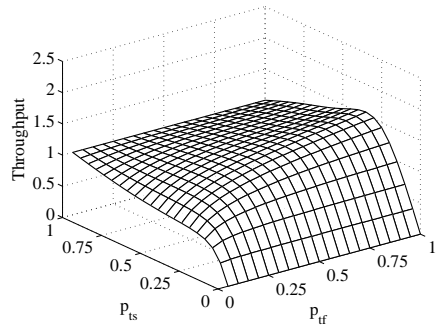


Figure 5-18: Throughput plot for deterministic locations case with $r_1 = 1$, $r_2 = 2$, $r_3 = 4$, $n_1 = 1$, $n_2 = 2$, $n_3 = 4$ and $z = 0.2$ using the Enhanced Approximate Model.

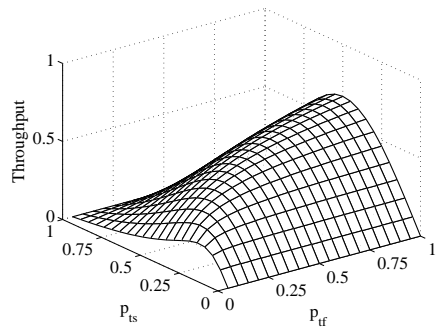


Figure 5-19: Throughput plot of the users at distance 2 for deterministic locations case with $r_1 = 1$, $r_2 = 2$, $r_3 = 4$, $n_1 = 1$, $n_2 = 2$, $n_3 = 4$ and $z = 0.2$ using the Enhanced Approximate Model.

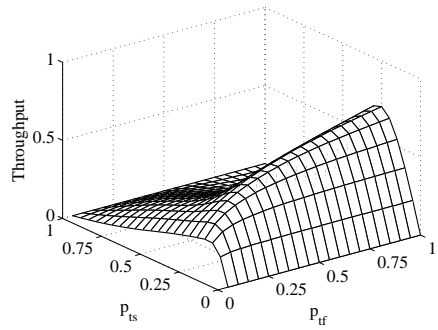


Figure 5-20: Throughput plot of the users at distance 4 for deterministic locations case with $r_1 = 1$, $r_2 = 2$, $r_3 = 4$, $n_1 = 1$, $n_2 = 2$, $n_3 = 4$ and $z = 0.2$ using the Enhanced Approximate Model.

The maximum throughput of 1.555 is obtained for $(p_{ts}, p_{tf}) = (0.35, 1)$ showing that the *backward model* is more favorable in this case. Furthermore, for this maximum point, the nodes at different distances are not starved for throughput since the throughput from distance 1 is 0.350, that from distance 2 is 0.589 and from distance 3 is 0.616 at the maximum overall throughput point. One other observation is that the aggregate throughput of nodes at distance r_3 is greater than that of nodes at distance r_2 which is greater than that of nodes at distance r_1 . This is in favor of fairness since the number of nodes is increasing with distance. We observe from Figures 5-19 and 5-20 that as the distance increases, the throughput increases with decreasing values of p_{ts} which supports the intuition that when p_{ts} is small, the nearby node, which uses the probability p_{ts} always since $n_1 < c$, has less chances of capturing the channel and the network can achieve more throughput by giving greater chances to the faraway nodes which outnumber the nearby nodes.

As a result of the different analysis and the various results considered in this section, i.e, when the locations of the users are known and no fading effect in the channel, we see that the *backward model* achieves better throughput and fairness results than the *forward model* in most cases considered. Note that when the number of nodes at distance 1 is comparable to c , the maximum throughput point is in favor of the *forward model* and this is because the distance-1 nodes use the probability p_{ts} most of the time (they use p_{ts} all the time if $n_1 \leq c$) and having a large value of p_{ts} lets them capture the channel all the time yielding a high throughput. The faraway nodes, however, get almost zero throughput in this case and therefore having a large p_{ts} value, especially when the number of nearby nodes is large, is catastrophic from a fairness perspective. In Chapter 6 we explain why having nearly c nearby nodes is not realistic in UWB systems and nevertheless provide an alternative protocol to alleviate this problem.

In the following two sections we continue analyzing the performance of the *backward model* in the case where there is fading effect in the channel.

5.3 Deterministic Locations-With Fading

In this subsection we assume the locations of the users are known and there is Rayleigh Fading in the channel, i.e., the Rayleigh fading term R_i in (3.1) is not a constant anymore but a Rayleigh distributed random variable and as explained in Chapter 3, the R_i^2 terms are exponentially distributed random variables of unit mean. The analysis in this section follows from the related work of Zorzi and Rao [61] which studies the power capture model given by (3.1) and (3.3) under a spatial distribution of nodes on a disk. The differences of the work in this section from previous work is that we assume multi-packet reception, i.e., z in (3.3) is less than 1, our received power model given by (3.1) does not include the shadowing term and most importantly we carry out the analysis for the *Backward Protocol* explained in previous sections thoroughly. First we obtain a general expression for the probability that a node at distance r captures the channel in the presence of k interferers by treating the distances of nodes as variables. Then we adopt the result into our setting by substituting the given values of the node distances. Note that the general expression for probability of capture will also be used in the next section where we have random node locations.

We define $p_{c,k}(r_0)$ to be the probability that the packet of a user at distance r_0 is received successfully in the presence of k other transmissions where k can at most be one less than the total number of nodes in the network, i.e., $k \in [0, n - 1]$ and there are n nodes in the system. From (3.1) and (3.3) we see that a transmission from a node at distance r_i is captured if its received power level is greater than the total interference factor times the threshold z . Therefore;

$$\begin{aligned} p_{c,k}(r_0) &= Pr \left\{ P_{R,0} > z \sum_{j=1}^k P_{R,j} \right\} \\ &= Pr \left\{ R_0^2 > z \sum_{j=1}^k R_j^2 \left(\frac{r_0}{r_j} \right)^\beta \right\} \end{aligned}$$

Now conditioning on the interferer distances r_1, r_2, \dots, r_k and the interferer Rayleigh fading terms R_1, R_2, \dots, R_k and denoting R_j^2 terms as a_j which are exponentially distributed

random variables of unit mean we obtain

$$p_{c,k}(r_0|r_{\{i:1\leq i\leq k\}}, a_{\{i:1\leq i\leq k\}}) = \exp \left\{ -z \sum_{j=1}^k a_j \left(\frac{r_0}{r_j}\right)^\beta \right\} \quad (5.33)$$

This expression follows from the fact that for an exponentially distributed random variable R_0^2 of unit mean, $Pr(R_0^2 > x)$ is given as $exp(-x)$. Removing the conditioning on $\{a_1, a_2, \dots, a_k\}$ by averaging (5.33) over $\{a_1, a_2, \dots, a_k\}$ we obtain

$$\begin{aligned} p_{c,k}(r_0|r_{\{i:1\leq i\leq k\}}) &= \int_0^\infty da_1 e^{-a_1} \dots \int_0^\infty da_k e^{-a_k} \exp \left\{ -z \sum_{j=1}^k a_j \left(\frac{r_0}{r_j}\right)^\beta \right\} \\ &= \prod_{j=1}^k \int_0^\infty \exp \left\{ -\left(1 + z\left(\frac{r_0}{r_j}\right)^\beta\right) a_j \right\} da_j \\ &= \prod_{j=1}^k \frac{1}{1 + z\left(\frac{r_0}{r_j}\right)^\beta} \end{aligned} \quad (5.34)$$

Now we apply this result to our setting by assuming that there are n_1, n_2, \dots, n_L nodes⁸ at distances r_1, r_2, \dots, r_L from the receiver respectively. We define $p_{ci}(k_1, k_2, \dots, k_i, \dots, k_L)$ to be the probability that a packet from a node at distance r_i is captured by the receiver given that there are $k_1, k_2, \dots, k_i, \dots, k_L$ interferers⁹ from distances $r_1, r_2, \dots, r_i, \dots, r_L$ respectively. Define the total number of interferers k as

$$k = \sum_{j=1}^L k_j \quad (5.35)$$

Therefore;

$$p_{ci}(k_1, k_2, \dots, k_i, \dots, k_L) = \prod_{j=1}^k \frac{1}{1 + z\left(\frac{r_i}{r_j}\right)^\beta} = \prod_{j=1}^L \left[\frac{1}{1 + z\left(\frac{r_i}{r_j}\right)^\beta} \right]^{k_j} \quad (5.36)$$

where the last equality follows from the fact that we can combine the terms with the same

⁸Note that $n_1 + n_2 + \dots + n_L = n$.

⁹Note that $p_{ci}(k_1, k_2, \dots, k_i, \dots, k_L)$ is the successful reception probability given the transmission of the user at distance r_i and $k_1, k_2, \dots, k_i, \dots, k_L$ interferers. Hence $k_j \in [0, n_j]$ for all j except $j = i$ for which $k_i \in [0, n_i - 1]$.

distance r_j from the receiver. Now, in order to formulate the throughput of the network, we apply the approximate model which was first introduced in Section 4.3 and then analyzed in sections 5.1 and 5.2.2, whereby a transmission from distance r_i is lost with constant and independent probability $p_d(r_i)$ regardless of its success history in the previous slots. We showed in sections 5.1 and 5.2.2 by numerical analysis that the approximation works well in most settings considered. The system can be analyzed as a system of non-linear equations. This is because the average transmission probability from distance r_i , $\tau(r_i)$, depends on $p_d(r_i)$ through the nonlinear equation (5.37) and the $p_d(r_i)$ on $\tau(r_i)$ for $i \in \{1, \dots, L\}$ through the nonlinear equation (5.38):

$$\tau(r_i) = \frac{p_{ts}}{1 - p_d(r_i) + \frac{p_{ts}}{p_{tf}} p_d(r_i)} \quad i \in \{1, \dots, L\} \quad (5.37)$$

$$p_d(r_i) = \sum_{k_1=0}^{n_1} \sum_{k_2=0}^{n_2} \dots \sum_{k_i=0}^{n_i-1} \dots \sum_{k_L=0}^{n_L} \binom{n_1}{k_1} \tau(r_1)^{k_1} (1 - \tau(r_1))^{n_1-k_1} \binom{n_2}{k_2} \tau(r_2)^{k_2} (1 - \tau(r_2))^{n_2-k_2} \dots \binom{n_i-1}{k_i} \tau(r_i)^{k_i} (1 - \tau(r_i))^{n_i-k_i-1} \binom{n_L}{k_L} \tau(r_L)^{k_L} (1 - \tau(r_L))^{n_L-k_L} (1 - p_{ci}(k_1, k_2, \dots, k_i, \dots, k_L)) \quad (5.38)$$

Where $p_{ci}(k_1, k_2, \dots, k_i, \dots, k_L)$ is as given in (5.36). Thus the aggregate throughput of nodes at distance r_i is given as

$$S(r_i) = n_i \tau(r_i) (1 - p_d(r_i)) \quad (5.39)$$

$$S = \sum_{i=1}^L S(r_i) \quad (5.40)$$

Fig. 5-21 shows the overall throughput of the network when we have 1 node at distance 1, 3 nodes at distance 2 and 9 nodes at distance 3. We observe that the largest throughput results are obtained for large values of p_{tf} and small values of p_{ts} . This result shows the better performance of the *backward model* compared to the *forward model* when we add multipath fading into the system.

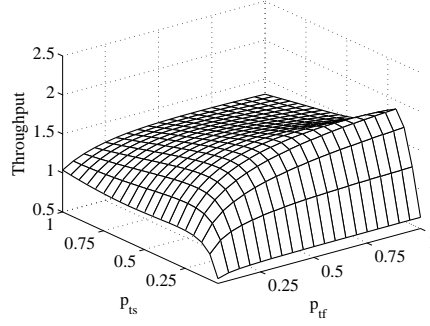


Figure 5-21: Throughput plot for the case of deterministic locations with fading in the channel. The number of nodes at distances $r_1 = 1$, $r_2 = 2$ and $r_3 = 3$ are $n_1 = 1$, $n_2 = 3$, $n_3 = 9$ respectively, and $z = 0.2$.

5.4 Random Locations With Fading

In this section we consider the most general network setting so far, i.e., the analysis is for random locations of the nodes when there is multipath fading in the network. Similar to Section 5.3, the analysis follows from related work of Zorzi and Rao in [61]. Consider n nodes distributed randomly on a disk at the center of which there is a receiver. Similar to the previous section, define $p_{c,k}(r_0)$ to be the probability that a packet transmitted from a node at distance r_0 is successfully received by the receiver given that there are k other transmissions where $k \leq n - 1$. Using (5.34), we obtain $p_{c,k}(r_0)$ after removing the conditioning (i.e., averaging over r_1, \dots, r_k) to be

$$p_{c,k}(r_0) = \left(\int_0^\infty \frac{f_r(r) dr}{1 + z \left(\frac{r_0}{r}\right)^\beta} \right)^k \quad (5.41)$$

For $\beta = 4$ and uniform spatial distribution as in (3.4), the integral in (5.41) can be evaluated analytically, yielding

$$p_{c,k}(r_0) = \left(1 - \sqrt{z} r_0^2 \tan^{-1} \left(\frac{1}{\sqrt{z} r_0^2} \right) \right)^k \quad (5.42)$$

Now similar to what we did for the deterministic locations with fading case, we apply the approximate analysis of the Section 4.3. We need to obtain the average probability of destruction, $p_d(r)$ from distance r (given that there is a transmission from distance r) and

using this quantity we find $\tau(r)$, the average probability of transmission from distance r as

$$\tau(r) = \frac{p_{ts}}{1 - p_d(r) + \frac{p_{ts}}{p_{tf}}(1 - p_d(r))} \quad (5.43)$$

where $p_d(r)$ is given as

$$p_d(r) = 1 - p_c(r) \quad (5.44)$$

and $p_c(r)$ is the average of $p_{c,k}(r)$ over all possible number of interferers k . The exact expression of $p_c(r)$ is given by

$$p_c(r) = \overline{p_{c,k}(r)} = \sum_{k=0}^{n-1} Pr\{\text{There are } k \text{ interferers}\} P_{c,k}(r) \quad (5.45)$$

Since the probability that there are k interferers depends on the dynamics of the *Backward Protocol*, there is no exact expression for $p_c(r)$. Therefore, we provide two approximations to $p_c(r) = \overline{p_{c,k}(r)}$.

5.4.1 Approximating $p_c(r)$ Using $\tau(r)$

Since we utilize $\tau(r)$ in the numerical analysis, we can approximate $\overline{p_{c,k}(r)}$ by calculating the average probability of transmission, τ , using $\tau(r)$;

$$\tau = \int_r \tau(r) f_r(r) dr \quad (5.46)$$

Using τ we can calculate $\overline{p_{c,k}(r)}$ (for $\beta = 4$ and uniform spatial distribution (3.4) as explained above) as

$$p_c(r) = \overline{p_{c,k}(r)} \cong \sum_{k=0}^{n-1} \binom{n-1}{k} \tau^k (1 - \tau)^{n-1-k} P_{c,k}(r)$$

$$= \sum_{k=0}^{n-1} \binom{n-1}{k} \tau^k (1 - \tau)^{n-1-k} \left(1 - \sqrt{z} r^2 \tan^{-1} \left(\frac{1}{\sqrt{z} r^2} \right) \right)^k \quad (5.47)$$

$$(5.48)$$

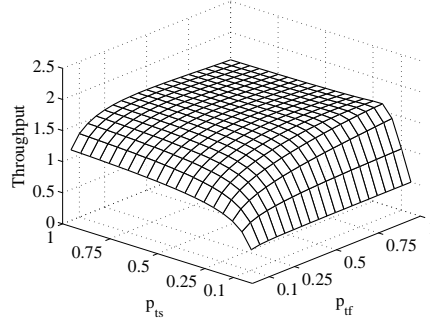


Figure 5-22: Throughput plot for random node locations case with fading in the channel for $n = 10$ and $z = 0.2$ using the Jensen's Inequality approximation to the average of $p_{c,k}(r)$.

Now (5.43) and (5.44) can be solved numerically to obtain the throughput of the network given as

$$S(r) = \bar{n} \int_{r=0}^1 p_c(r) f_r(r) dr = \bar{n} \int_{r=0}^1 p_c(r) 2r dr \quad (5.49)$$

where \bar{n} is equal to $n\tau$.

The overall throughput of the system is presented in Fig. 5-22 for $z = 0.2$ and $n = 10$. We see that the resulting throughput plot is very close to the throughput plot generated by simulation shown in Fig. 7-12 except for high p_{ts} values. The exact results in Fig. 7-12 suggest that in the most general network setting considered so far, i.e., random node locations and fading in the channel, the high throughput area results from utilizing high p_{tf} and low p_{ts} values suggesting ones more the better performance of the *backward model* over the *forward model*.

We observe that the approximate results for $n = 6$ are closer to simulation than $n = 10$ case, however, as we increase the number of nodes in the network, the approximate results start to diverge from the simulation results. The reason for this is that the numerical analysis gets more and more complicated to solve as we increase n . The number of possible solutions to $\tau(r)$ increases linearly with n and hence the numerical equation solver converges to a wrong root with higher probability as n is increased.

5.4.2 Approximating $p_c(r)$ Using Jensen's Inequality

A second way of approximating $p_c(r)$ is to assume that the average (over k) probability of capture of a packet transmitted from distance r is approximately the probability of capture of the packet when there are average number of interferers in the channel. Namely,

$$p_c(r) = \overline{p_{c,k}(r)} \cong p_{c,\bar{k}}(r) \quad (5.50)$$

where \bar{k} , the average number of interferers, is given by

$$\bar{k} = (n - 1) \int_r \tau(r) f_r(r) dr \quad (5.51)$$

Note from (5.41) that $p_{c,k}(r)$ is a convex function of the random variable k and from Jensen's Inequality we obtain

$$\overline{p_{c,k}(r)} \geq p_{c,\bar{k}}(r). \quad (5.52)$$

Hence the approximation that $\overline{p_{c,k}(r)} \cong p_{c,\bar{k}}(r)$ corresponds to using the lower bound obtained from Jensen's Inequality to the convex function $p_{c,k}(r)$. Moreover, the random variable k is defined in the range $[0, n - 1]$, therefore, Edmundson-Madansky Inequality gives us an upper bound to $\overline{p_{c,k}(r)}$. We give the Edmundson-Madansky Inequality with a simple proof in Appendix C. We apply Edmundson-Madansky Inequality to our setting ($g(k) = p_{c,k}(r)$, $a = 0$, $b = n - 1$) and denote $p_{c,k}(r) = \gamma(r, z)^k$ where $\gamma(r, z)$ for $\beta = 4$ and uniform spatial distribution as in (3.4) is given as

$$\gamma(r, z) = 1 - \sqrt{z}r^2 \tan^{-1} \left(\frac{1}{\sqrt{z}r^2} \right). \quad (5.53)$$

$\gamma(r, z)$ is a monotonically decreasing function of r for $r \in [0, 1]$. Applying the Edmundson-Madansky Inequality with the specified values we obtain

$$\overline{p_{c,k}(r)} \leq 1 - \frac{\bar{k}}{n - 1} (1 - \gamma(r, z)^{n-1}) \quad (5.54)$$

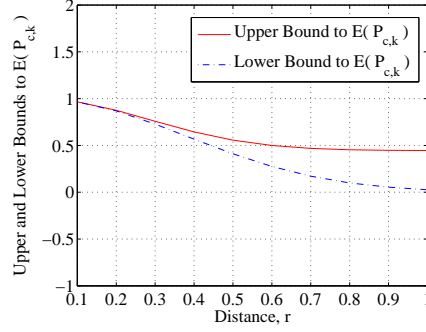


Figure 5-23: The upper and lower bounds to $\overline{p_{c,k}(r)}$ as a function of distance, r for $n = 10$ nodes in the system and $z = 0.2$. The figure corresponds to $\bar{k} = 5$.

Combining (5.52) and (5.54) we finally get

$$\gamma(r, z)^{\bar{k}} \leq \overline{p_{c,k}(r)} \leq 1 - \frac{\bar{k}}{n-1}(1 - \gamma(r, z)^{n-1}) \quad (5.55)$$

We observe from (5.55) that when $\gamma(r, z)$ is close to 1, the two bounds become tight, while for $\gamma(r, z)$ tending to 0 they are loose. However for $z = 0.2$ and $r = 0$, $\gamma(0, 0.2) = 1$ and for $z = 0.2$ and $r = 1$, $\gamma(1, 0.2) = 0.4856$, hence for practical values of z , we do not have to worry about very small values of $\gamma(r, z)$. When $n = 10$, $\bar{k} = 5$ and $z = 0.2$, Fig. 5-23 shows the values of the upper and the lower bounds as we vary r from 0 to 1. We obtain similar figures for different values of \bar{k} , and observe that the bounds get tighter as \bar{k} increases. We see that the two bounds are very close for $r \leq 0.5$. This means that approximating $\overline{p_{c,k}(r)}$ as $p_{c,\bar{k}}(r)$ works reasonably well for $r \leq 0.5$. For $r > 0.5$ the actual value of $\overline{p_{c,k}(r)}$ lies between these two curves. Applying the approximation, we obtain

$$p_c(r) = \overline{p_{c,k}(r)} \cong p_{c,\bar{k}}(r) = \left(1 - \sqrt{z}r^2 \tan^{-1} \left(\frac{1}{\sqrt{z}r^2} \right) \right)^{(n-1) \int_r \tau(r) f_r(r) dr} \quad (5.56)$$

Now we formulate the approximate model as given by equations (5.43) and (5.44). These equations are solved numerically to obtain the throughput of the network given in (5.49). We plot the overall network throughput as a function of p_{ts} and p_{tf} in Fig. 5-24 for $z = 0.2$ and $n = 10$. We see that the resulting throughput plot is very similar to the throughput plot generated by simulation shown in Fig. 7-12. Similar observations to the Fig. 5-22 are seen for this figure.

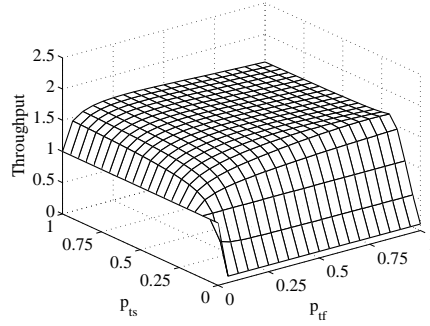


Figure 5-24: Throughput plot for random node locations case with fading in the channel for $n = 10$ and $z = 0.2$ using the Jensen's Inequality approximation to the average of $p_{c,k}(r)$.

We observed that as n increases, the results diverges from the simulation results for this approximate model also. The reason in this case is that for large values of n (e.g., $n \geq 20$ in our setting), we find more nodes faraway from the receiver and hence $\gamma(r, z)$ takes values that are not close to 1 more often, making the approximation $p_c(r) = \overline{p_{c,k}(r)} \cong p_{c,\bar{k}}(r)$ lose its validity.

Note that, in Section 7.3, we give various simulation results for this case and explain how the *backward* and *forward* models compare as we keep z constant and vary n and vice versa.

Chapter 6

New Protocols

In this section, we first provide a solution to the problem associated with the *backward model* when the number of nodes that are close to the receiver is comparable to c , the maximum number of successful receptions (see the discussion at the end of Section 5.2.1). Note that having the number of nearby nodes close to c may not be a realistic situation for some network configurations. First, we know that for spread spectrum systems, the receiver capture threshold z can be very small (in fact close to 0) with enough processing gain [42] making c a very large number. Moreover, for most practical spatial distributions of nodes, the number of users increases with the distance. Consequently, when there is a finite number of nodes in the network, the possibility of having nearly c nearby users is very low unless the total number of nodes is very large. Nevertheless, we modify the *Backward Protocol* and develop the *Backward Model with Forced Idle Periods* to remedy this problem.

Next we propose the *Backward Model with Dynamic Contention Windows*, which is potentially easier to implement compared to the original *Backward Protocol*, enabling nodes to adjust their transmission probability dynamically and still carrying the essence of the *backward model*. From Chapter 5, it is clear that the analysis regarding the simpler *Backward Protocol* is complex and it becomes considerably more difficult to analyze the *Backward Model with Dynamic Contention Windows*. Consequently, we will present the performance analysis of this protocol through simulations.

6.1 Backward Model with Forced Idle Periods

Now consider the problem outlined at the end of Section 5.2.1 where we assumed that the node locations were known and there was no fading in the system. As it was pointed out there, if the number of nodes that are close to the receiver is comparable to c , then having a large value of p_{ts} and a small value of p_{tf} yields the highest throughput as it gives more chances to the nearby nodes who are almost always successful¹. However as mentioned before, this approach amounts to the complete starvation of the faraway nodes and hence it is not fair. As a result, in this section, we are interested in modifying the backward protocol to be able to provide more fair results as well as high throughput values in cases where the number of nearby nodes is comparable to c .

The idea behind this new protocol comes from the following observation of the original protocol when the number of nearby nodes is comparable to c . Assume the settings of Section 5.2.1, i.e., there are two possible locations and the number of nodes at those distances are n_1 and n_2 . When n_1 is comparable to c in such a setting, even for a very small p_{ts} value, the channel is occupied most of the time by the nearby nodes. To see this, assume that the number of nodes at distance 1 is $n_1 = c = 5$ and those at distance 2 is $n_2 = 15$. As we know from Section 5.2.1, the nearby nodes are always successful in this case. Suppose $p_{ts} = 0.25$, a low value that seems to give enough chances for faraway users. However, as it was pointed out in Section 5.2.1, in order for a node at distance 2 to be successful, we need to have no transmissions from distance 1. Considering the complimentary event, we find that probability of having “at least 1 nearby node transmitting” is given by $1 - (1 - p_{ts})_1^n = 1 - (1 - 0.25)^5 = 0.763$. This means that more than 75 percent of the time there is a transmission from nearby users even when their probability of transmission is very low. The throughput plots of the original *Backward Protocol* in this network setting (i.e., $n_1 = 5$, $n_2 = 15$ and $z = 0.2$) are shown in Figures 6-1, 6-2 and 6-3. We see that the network is clearly dominated by the nearby users.

Considering the above example and the observation of the results in Figures 6-1, 6-2 and 6-3, the new protocol should give more chances to faraway nodes, and we want to

¹Nearby nodes are always successful if $n_1 \leq c$ and $n_2 < 2^\beta$ for $r_1 = 1$ and $r_2 = 2$.

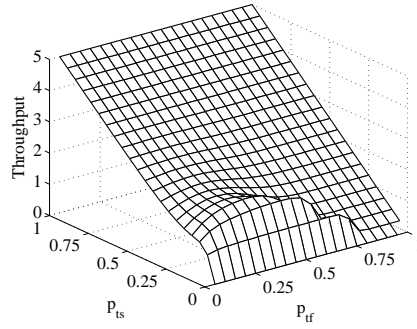


Figure 6-1: Throughput plot for deterministic locations case (no fading) with $r_1 = 1$, $r_2 = 2$, $n_1 = 5$, $n_2 = 15$ and $z = 0.2$ using the original model.

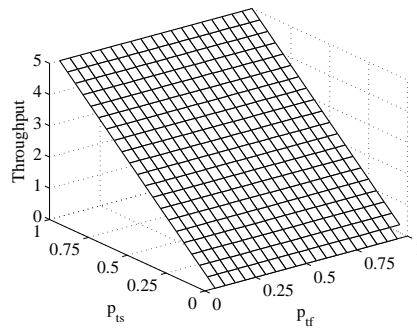


Figure 6-2: Throughput plot of the users at distance 1 for deterministic locations case (no fading) with $r_1 = 1$, $r_2 = 2$, $n_1 = 5$, $n_2 = 15$ and $z = 0.2$ using the original model.

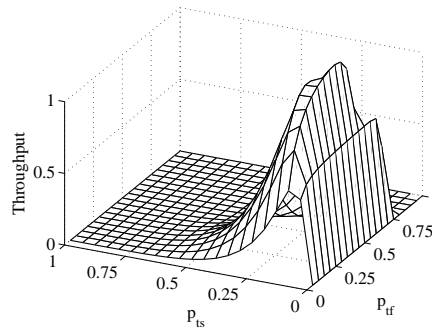


Figure 6-3: Throughput plot of the users at distance 2 for deterministic locations case (no fading) with $r_1 = 1$, $r_2 = 2$, $n_1 = 5$, $n_2 = 15$ and $z = 0.2$ using the original model.

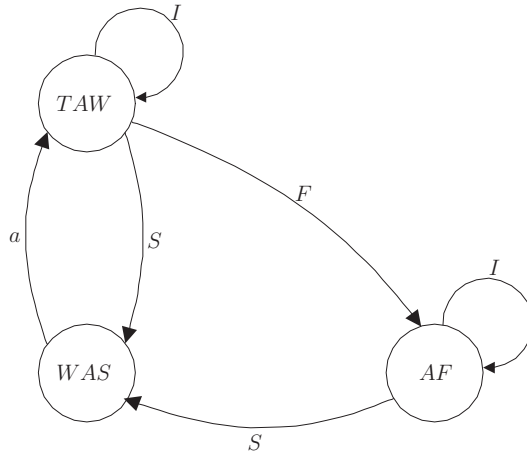


Figure 6-4: The single user state diagram for the *Backward Model with Forced Idle Periods*. This figure corresponds to having nodes stay idle for 1 slot after a successful transmission. *S*: Success, *I*: Idle, *F*: Failure, *WAS*: Wait After Success, *AF*: After Failure, *TAW*: Transmit After Waiting. The transition labeled by “*a*” occurs with probability 1.

achieve this without additional feedback from the receiver. We perform this by having the nodes that were successful in the previous slot stay idle for some slots (or for some random number of slots) and then letting them transmit again with the same probability p_{ts} in the next slot. The number of slots for which nodes wait silent after a successful transmission is a design parameter to be determined in the analysis. The state diagram associated with the new protocol when successful nodes wait for one slot before a transmission attempt with probability p_{ts} is shown in Fig. 6-4. After a successful transmission nodes stay in the *Wait After Success* (WAS) state for 1 slot and then move to the *Transmit After Waiting* (TAW) state where they attempt transmission with probability p_{ts} . Comparing this state diagram with that of the original *Backward Protocol* we see that nodes behave the same way when they are in the failed state in both protocols. Hence, the state diagram of the *Backward Model with Forced Idle Periods* is obtained from that of the *Backward Protocol* by dividing the *After Success* (AS) state of the *Backward Protocol* into WAS and TAW states.

We know that in the original *Backward Protocol*, when n_1 is close to c , the average number of successes from the nearby users is much greater than that of the faraway users. Hence, this idea of going idle after a successful transmission gives more chances to the distant users. Note that the distant nodes will also be silent after they complete a successful transmission. However, since the number of faraway nodes is larger than that of the nearby nodes (and hence larger than c), the probability that there are some distant nodes ready to

transmit in the next slot will be larger than the corresponding quantity for nearby nodes. Therefore, the aggregate throughput from nodes at distance 2 is expected to increase compared to the original *Backward Protocol*. We present the overall network throughput, the aggregate throughput of the nodes at distance 1 and that at distance 2 for the *Backward Model with Forced Idle Periods* in Figures 7-20, 7-21 and 7-22 in Section 7.4 for $n_1 = 5$, $n_2 = 15$ and $z = 0.2$ and hence $c = 5$. These figures are for the case where nodes stay idle for 2 slots after a successful transmission. Comparing figures 6-3 and 7-22 we see that the throughput of the distant nodes is greater in the *Backward Model with Forced Idle Periods* for almost all operating points as expected. Note that the spikes in Figures 7-20 and 7-22 are due to the synchronization issues that arise when p_{ts} is equal to 1. This is because the network operation becomes totally dependent on the number of successful nearby users in the first few slots². As an example, if all the nearby nodes transmit in the first slot, then every third slot will be occupied by the nearby nodes and the channel will be left free 66 percent of the time for distant users leaving a very high throughput for them. However, we will have a totally different situation if for example 2 nearby users transmit in the first slot, 2 in the second slot and 1 in the third slot. This configuration leaves zero throughput for the distant users. As a result, the $p_{ts} = 1$ case depends on the transient behavior of the simulation hence it should not be considered in the comparisons between protocols.

Figures 7-23, 7-24 and 7-22 show the throughput plots for the same network (i.e., for $n_1 = 5$, $n_2 = 15$ and $z = 0.2$) when the successful users stay idle for 8 slots. We see the advantage of the *Backward Model with Forced Idle Periods* clearly in these figures in the sense that for many operating points, faraway nodes have almost 12 percent more throughput than the maximum aggregate throughput obtained by distant nodes in the original protocol. Furthermore, distant users get even more aggregate throughput than nearby users for most of the operating points.

As a result, although the underlying network structure is not much probable in practice, we can still find easy ways to prevent throughput starvation of distant nodes in the network by a simple modification of the *Backward Protocol*.

²We start the simulation with every node in the failed state.

6.2 Backward Model with Dynamic Contention Windows

In this Section we propose a more practical protocol, *Backward Model with Dynamic Contention Windows*, compared to the original *Backward Protocol*. This protocol assigns different backoff windows to users according to their success history in the previous attempt as is done in IEEE. 802.11 (e.g., [6]) and it adopts the *backward model* idea into this setting. More clearly, the backoff window size of each node is a uniformly distributed random variable depending on the success history of the last transmission attempt of each node. If a node was successful in its last transmission, it chooses a number in the interval $[0, n_s]$ with probability $1/(n_s + 1)$ and starts to decrement its counter³ from the random number to 0. The node transmits with probability 1 when its counter decreases down to 0. Similarly, if a node's transmission was failed in the last attempt, it chooses a random number uniformly distributed over the integers in the interval $[0, n_f]$ and starts to decrement its counter down to 0. The node transmits with probability 1 when its counter reaches 0. Note that n_f and n_s are design parameters and the case where n_f is less than n_s corresponds to the case where p_{f} is greater than p_{t} in the *Backward Protocol*. Consequently, the *Backward Model with Dynamic Contention Windows* carries the essence of the *backward model*.

Note that the protocol we propose here is far from being a complete protocol such as IEEE 802.11 in the sense that many practical problems are not addressed here. It is rather aimed towards demonstrating a way of implementing the *backward model* under simplistic assumptions.

We refer to the results of the simulations of this protocol presented in Chapter 7. Fig. 7-26 shows the total network throughput as a function of n_s and n_f for $n_1 = 1$ and $n_2 = 5$ nodes at distances $r_1 = 1$ and $r_2 = 2$ for $z = 0.2$. We see from this figure that the maximum throughput value of 2.331 is obtained when $n_f < n_s$ ($n_s = 1$ and $n_f = 0$) suggesting that the *backward model* is preferable with the new implementation as well. Since we have small number of nodes, throughput values are larger when n_f and n_s takes small values. Fig. 7-28 shows the total throughput of the distant nodes for the same settings and we see that the distant nodes get more chances when $n_f < n_s$, in particular, the throughput of the

³The decrements are 1 in every slot.

distant nodes is maximized when $n_f = 0$ and $n_s = 2$. We present throughput plots for the same settings for $n_1 = 2$ and $n_2 = 10$ in Figures 7-29 and 7-31 where 7-29 shows the total network throughput and 7-31 the throughput of the distant nodes. We see that the maximum throughput value in Fig. 7-29 is obtained for $n_f = 2$ and $n_s = 6$ suggesting that the *backward model* achieves better results than the *forward model* as expected. Moreover, a similar behavior to $n_1 = 1$ and $n_2 = 5$ case is observed for the throughput of the distant nodes.

We then simulate the network where nodes can be at one of three possible distances $r_1 = 1$, $r_2 = 2$ and $r_3 = 3$. Figures 7-32, 7-34 and 7-35 show the total network throughput, total throughput of nodes at distance 2 and that of nodes at distance 3 for $n_1 = 1$, $n_2 = 3$, $n_3 = 9$ and $z = 0.2$. We observe from these plots that $n_f < n_s$ case yields high overall network throughput and prevents the throughput starvation of the distant nodes suggesting the better performance of the *backward model* than the *forward model*.

Chapter 7

Performance Evaluation and Simulations

We simulated various network scenarios in order to see the performance of the *Backward Protocol* for the network settings where the exact or the approximate analyses cannot be used to get accurate results. We start with the verification of the simulation model for deterministic locations and without fading case by comparing the results obtained from the theoretical analysis with those from simulation. Next we simulate networks with more nodes and various distances from the receiver. Then we simulate networks with randomly distributed nodes with and without fading in the system. We finally move onto the simulations of the new protocols proposed in Chapter 6.

The model utilized in the simulations is as characterized by (3.1) and (3.3). The effect of additive noise is neglected due to the reasons explained before, hence N is set to 0 in (3.1). P_T , K , and β are assumed to be constants throughout this section such that $P_T = 1$, $K = 1$, and $\beta = 4$. We will denote the number of trials for each experiment by t . As expected, increasing t results in better convergence of simulation results to the theoretical estimates¹. We start with the deterministic node locations case without fading and show that the simulation results are the same as the exact results presented before. Then we use the simulation model to produce results for larger network scenarios where the exact model no longer applies. We then make the model more general in that we first make the nodes

¹ t will be chosen as 100K unless otherwise stated.

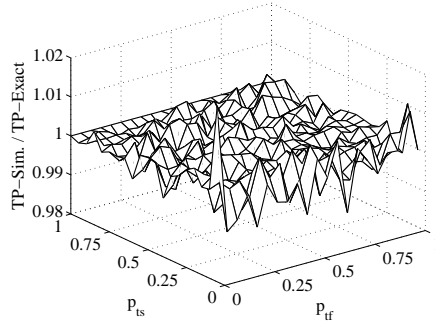


Figure 7-1: Comparison of the total network throughput in the simulation model and in the exact model for deterministic node locations and without fading in the channel where TP-Sim stands for throughput obtained by simulation and TP-Exact that from the exact analysis. We utilized $n_1 = 1$, $n_2 = 5$, $r_1 = 1$, $r_2 = 2$, $z = 0.2$ and $t = 100K$.

randomly distributed and then add multipath fading into the system and show that in all the cases, the *backward model* achieves higher throughput and more fair results as is clear from the previous analysis. Finally, we provide simulation results for two new protocols, the first aimed for as a solution to a specific network structure and the other being a more practical implementation of the *backward model*.

7.1 Deterministic Locations Without Fading

There is no fading in the channel, therefore the R term in (3.1) is set to 1. The choice of the start state is arbitrary, however, as the experiment proceeds the transient behavior vanishes and the system converges to some steady state operation.

We first consider the case $n_1 = 1$, $n_2 = 5$, $r_1 = 1$ and $r_2 = 2$ in Fig. 4-1 of Section 5.2.1. The results obtained were compared with those shown in Figures 5-5 and 5-6. The first comparisons for total network throughput are shown in Figures 7-1 and 7-3 for t equal to $100K$ and $1000K$ respectively. Figures 7-2 and 7-4 represents the comparison of the throughput of the faraway nodes under the same settings as above.

It can be observed that as t is increased, the simulation results gets closer to the ones predicted by the theoretical model, thus confirming its correctness. For $t = 100K$, the largest deviation is within 1.5% and as t is increased to $1000k$, the largest deviation gets bounded to within 0.4%.

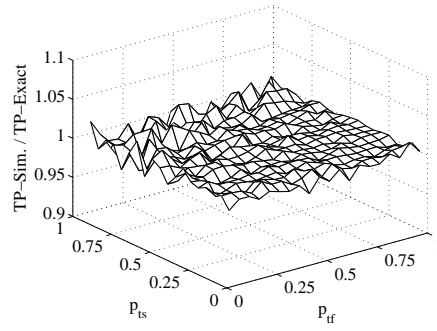


Figure 7-2: Comparison of the aggregate throughput of the distance-2 users in the simulation model and in the exact model for deterministic node locations and without fading in the channel where TP-Sim stands for throughput obtained by simulation and TP-Exact that from the exact analysis. We utilized $n_1 = 1$, $n_2 = 5$, $r_1 = 1$, $r_2 = 2$, $z = 0.2$ and $t = 100K$.

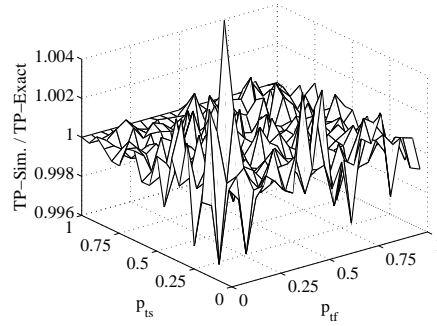


Figure 7-3: Comparison of the total network throughput in the simulation model and in the exact model for deterministic node locations and without fading in the channel where TP-Sim stands for throughput obtained by simulation and TP-Exact that from the exact analysis. We utilized $n_1 = 1$, $n_2 = 5$, $r_1 = 1$, $r_2 = 2$, $z = 0.2$ and $t = 1000k$.

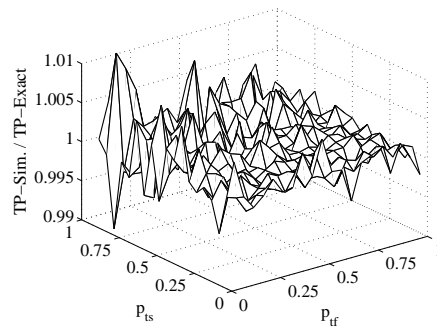


Figure 7-4: Comparison of the aggregate throughput of the distance-2 users in the simulation model and in the exact model for deterministic node locations and without fading in the channel where TP-Sim stands for throughput obtained by simulation and TP-Exact that from the exact analysis. We utilized $n_1 = 1$, $n_2 = 5$, $r_1 = 1$, $r_2 = 2$, $z = 0.2$ and $t = 1000k$.

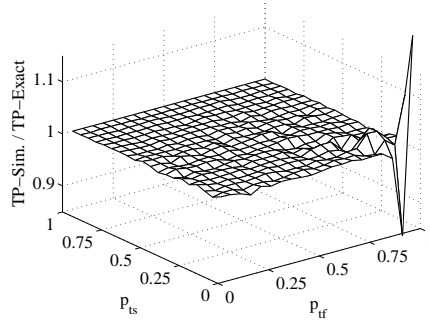


Figure 7-5: Comparison of the total network throughput in the simulation model and in the exact model for deterministic node locations and without fading in the channel where TP-Sim stands for throughput obtained by simulation and TP-Exact that from the exact analysis. We utilized $n_1 = 2$, $n_2 = 10$, $r_1 = 1$, $r_2 = 2$, $z = 0.2$ and $t = 100K$.

The comparison of the simulation and exact results for total network throughput for the case of $n_1 = 2$ and $n_2 = 10$ is in Fig. 7-5. We see that the simulation results are very close to the exact results for $n_1 = 2$ and $n_2 = 10$. This continues to hold for larger values of n_1 and n_2 conforming the accuracy of the simulations. The largest deviations from the theoretical results were found at the boundary values of p_{ts} and p_{tf} . These deviations were individually probed to explain possible causes. When p_{ts} is very low and p_{tf} is very high, we observed that the simulation takes longer to converge for some combinations of p_{ts} and p_{tf} values, e.g. $(p_{ts}, p_{tf}) = (0.05, 0.95)$. The peculiarity of these cases was due to the slow convergence of the system to some absorbing state (i.e., a state for which the system never gets out once this state happens). However, experimentation suggested that these problems could be solved by increasing t arbitrarily. As can be seen in Fig. 7-5, the other large deviations occurs when p_{ts} and p_{tf} are both very close to 1. This deviation is due to the synchronization issues associated with the simulation and it totally depends on the initial state with which the simulation is started. Overall, we see that the simulation model performs very close to the exact analysis and hence it will be used in network scenarios where the exact analysis is not sufficient.

Moreover, we compared the Enhanced Approximate Model results created in Section 5.2.3 with corresponding simulation results. Figures 7-6, 7-7, and 7-8 show the comparisons for the total network throughput, the throughput of the nodes at distance 2 and of those at distance 4. We see that the Enhanced Approximate Model works well in that the

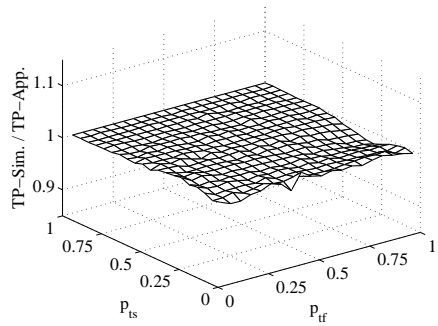


Figure 7-6: Comparison of the total network throughput in the simulation model and in Enhanced Approximate Model for deterministic node locations and without fading in the channel where TP-Sim stands for throughput obtained by simulation and TP-App. that from the approximate model. We utilized $n_1 = 1$, $n_2 = 2$, $n_3 = 4$, $r_1 = 1$, $r_2 = 2$, $r_3 = 4$, $z = 0.2$ and $t = 100K$.

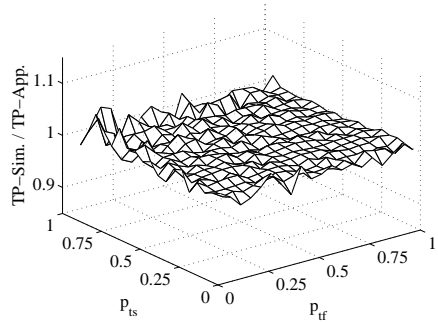


Figure 7-7: Comparison of the aggregate throughput of the distance-2 users in the simulation model and in Enhanced Approximate Model for deterministic node locations and without fading in the channel where TP-Sim stands for throughput obtained by simulation and TP-App. that from the approximate model. We utilized $n_1 = 1$, $n_2 = 2$, $n_3 = 4$, $r_1 = 1$, $r_2 = 2$, $r_3 = 4$, $z = 0.2$ and $t = 100K$.

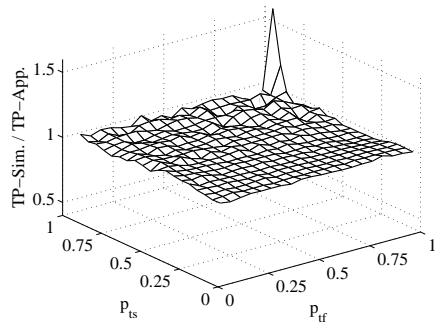


Figure 7-8: Comparison of the aggregate throughput of the distance 4 users in the simulation model and in Enhanced Approximate Model for deterministic node locations and without fading in the channel where TP-Sim stands for throughput obtained by simulation and TP-App. that from the approximate model. We utilized $n_1 = 1$, $n_2 = 2$, $n_3 = 4$, $r_1 = 1$, $r_2 = 2$, $r_3 = 4$, $z = 0.2$ and $t = 100K$.

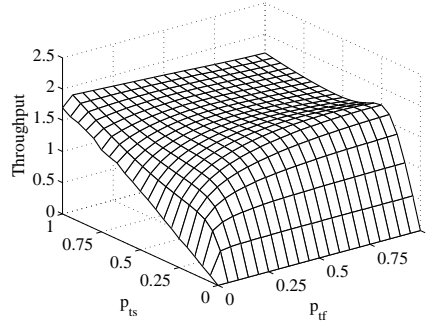


Figure 7-9: Total network throughput when there are 10 uniformly distributed nodes on a plane (no fading) with $z = 0.2$, $t = 100K$ and 40 iterations.

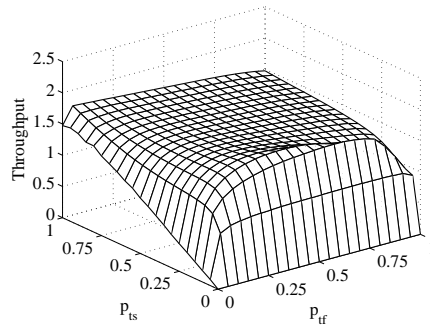


Figure 7-10: Total network throughput when there are 20 uniformly distributed nodes on a plane (no fading) with $z = 0.2$, $t = 100K$ and 40 iterations.

results produced from the model closely match the simulation results except for $p_{ts} = 1$ and $p_{tf} = 1$ for which some synchronization issues occur with the simulations as explained above.

7.2 Random Locations Without Fading

The transmitters are placed uniformly on a disk of radius 1 according to (3.4). With the introduction of randomness in node locations, it is essential to repeat each experiment of $100K$ slots 40 times with different random placement of nodes to get a good average over the distance.

Under these settings, Figures 7-9, 7-10 and 7-11 show the total network throughput when there are 10, 20 and 40 nodes in the network. We see that there are two areas of the plots that have the highest throughput; the first is for high p_{ts} and low p_{tf} area and the second

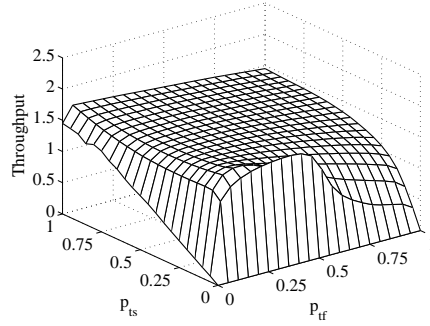


Figure 7-11: Total network throughput when there are 40 uniformly distributed nodes on a plane (no fading) with $z = 0.2$, $t = 100K$ and 40 iterations.

is the low p_{ts} and high (or moderate for $n = 40$) p_{tf} area. As we know from the previous analysis in Chapter 5, the former maximum area results in throughput starvation of the distant nodes whereas the latter gives much more chances for faraway users and prevents their throughput starvation. As a result, we see that the *Backward Protocol* achieves the same throughput as the traditional *forward models* while preventing the throughput starvation of the distant nodes. Comparing Figures 7-9 and 7-11 we observe that the maximum throughput area corresponding to low p_{ts} value tends to occur for lower p_{tf} values as the number of nodes increases. This is due to the fact that as n increases, the probability of failure increases for each node and hence transmitting with very high p_{tf} value causes considerable number of collisions.

7.3 Random Locations With Fading Simulation

We consider the same settings as the previous section except the Rayleigh fading term R_i^2 in the received power equation (3.1) is now an exponential random variable of unit mean. This random variable is generated from a uniform random variable that is independent of the random number generators of transmission probability and node locations. The results obtained by keeping z constant at 0.2 are given in Figures 7-12, 7-13, 7-14 and 7-15 for $n = 10, 20, 50$ and 100 respectively.

We see that there is only one maximum area in the throughput plots which is the low p_{ts} area. The reason for not having as high throughput as no fading case when p_{ts} is large is that

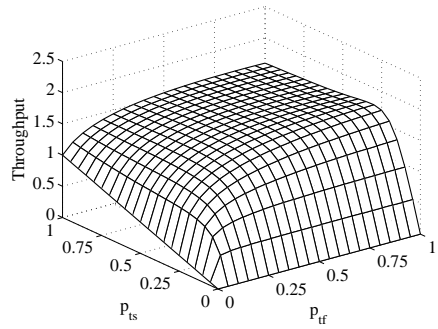


Figure 7-12: Total network throughput when there are 10 uniformly distributed nodes on a disk with fading in the system for $z = 0.2$, $t = 100K$ and 40 iterations.

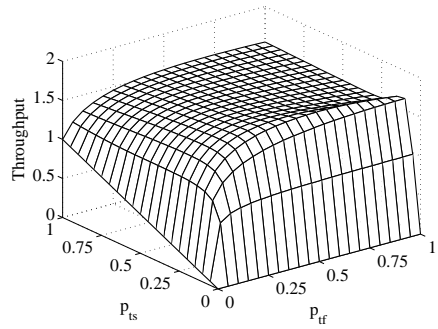


Figure 7-13: Total network throughput when there are 20 uniformly distributed nodes on a disk with fading in the system for $z = 0.2$, $t = 100K$ and 40 iterations.

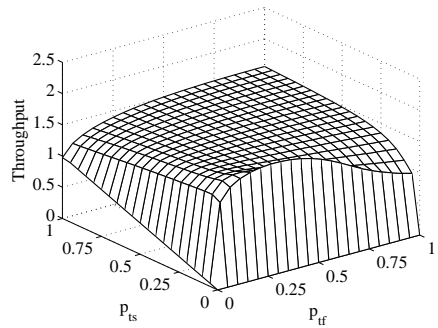


Figure 7-14: Total network throughput when there are 50 uniformly distributed nodes on a disk with fading in the system for $z = 0.2$, $t = 100K$ and 40 iterations.

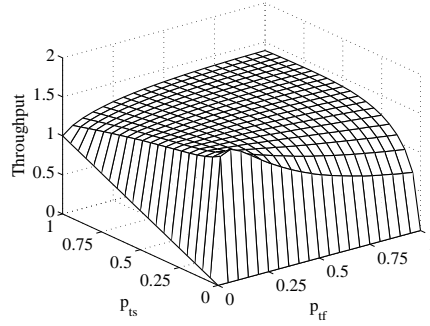


Figure 7-15: Total network throughput when there are 100 uniformly distributed nodes on a disk with fading in the system for $z = 0.2$, $t = 100K$ and 40 iterations.

when there is fading in the system, the nearby node signals also become weak (according to an exponentially distributed random variable in the signal amplitude). Hence the nearby nodes are not always successful anymore and the high throughput in the no fading case obtained by letting nearby nodes transmit with high probability does not happen here. As a result we see that in the most general settings, namely randomly distributed nodes together with multipath fading affect in the system, only low p_{ts} and high/moderate p_{tf} values produce the highest throughput value. Consequently we conclude that the *Backward Protocol* achieves higher throughput than the *forward protocols* in the most general network settings considered. Furthermore, we already know from Chapter 5 that the *Backward Protocol* is more fair than the *forward model*. This suggests that the *backward model* gives both high throughput and more fair results in the most realistic conditions considered in this thesis satisfying our initial claim.

Here we see a similar trend to what we observed in random locations without fading case as well. Namely, as we increase the number of nodes in the system, the maximum throughput point occurs for smaller p_{tf} values. The reason for this is the same as the no fading case. However, the maximum throughput point always occurs for $p_{ts} < p_{tf}$ suggesting that the *Backward Protocol* is preferable for the values of n considered.

Next we present the variation of throughput when we keep the number of nodes constant at $n = 10$ and vary the receiver power ratio threshold z . Figures 7-16, 7-17, 7-18 and 7-19 show the total network throughput for $z = 0.1, 0.3, 0.5$ and 0.7 respectively. We observe that as z gets close to 1, the total throughput of the system begins to have two maximum

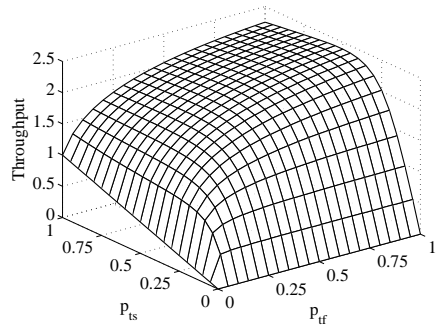


Figure 7-16: Total network throughput when there are 10 uniformly distributed nodes on a disk with fading in the system for $z = 0.1$, $t = 100K$ and 40 iterations.

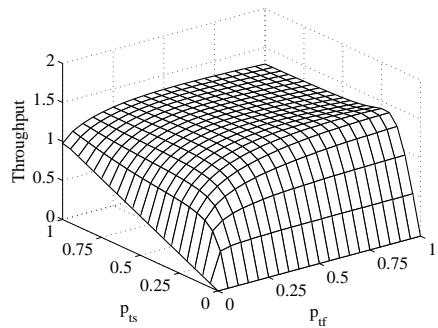


Figure 7-17: Total network throughput when there are 10 uniformly distributed nodes on a disk with fading in the system for $z = 0.3$, $t = 100K$ and 40 iterations.

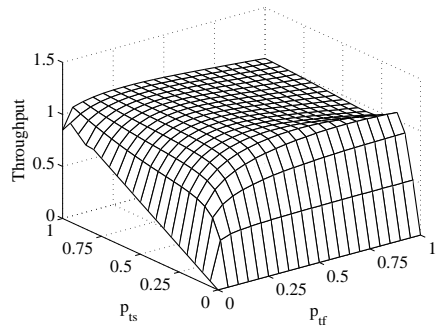


Figure 7-18: Total network throughput when there are 10 uniformly distributed nodes on a disk with fading in the system for $z = 0.5$, $t = 100K$ and 40 iterations.

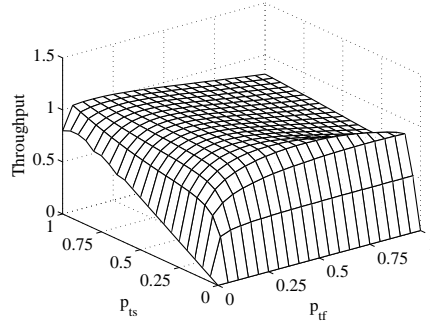


Figure 7-19: Total network throughput when there are 10 uniformly distributed nodes on a disk with fading in the system for $z = 0.7$, $t = 100K$ and 40 iterations.

areas as in the random locations without fading case. The reason for this is that as z gets close to 1, the receiver becomes capable of receiving only a single packet at a time. Hence giving more chances to the user with the strongest power level produces high throughput and this corresponds to having a high p_{ts} value in our system. Nevertheless, we see that low p_{ts} area also produces similar throughput values suggesting that the *Backward Protocol* has comparable throughput to *forward models* even when the receiver tends to a single packet reception capability.

7.4 Backward Model with Forced Idle Periods

As highlighted in Section 6.1, there is a limitation to the *Backward Protocol* when the number of nearby nodes is close to c . In such a scenario, there is a high probability that at least one of the nearby nodes will transmit, even for low values of p_{ts} and hence the throughput starvation of the faraway nodes occur with high probability. We suggested a new protocol *Backward Model with Forced Idle Periods* to remedy this issue. The state diagram according to which each node operates (for the case where nodes stay idle for one slot after each successful transmission) is shown in Fig. 6-4. In particular, this protocol is a modification of the *Backward Protocol* whereby after a successful transmission, a node becomes silent for some slots before becoming active again. The number of slots for which nodes wait idle after a successful transmission is a design parameter to be determined in the analysis. The assumptions in Section 6.1 apply here as well. Namely, there is no fading

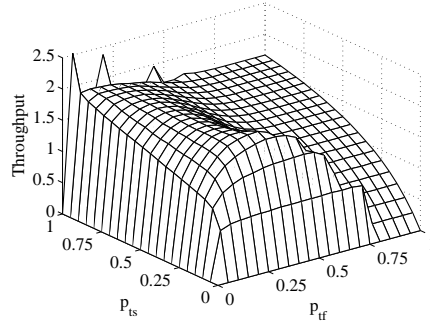


Figure 7-20: Total network throughput of the *Backward Model with Forced Idle Periods* for $r_1 = 1$, $r_2 = 2$, $n_1 = 5$, $n_2 = 15$, $z = 0.2$ and $t = 100K$ in the case where nodes stay idle for 2 slots after each successful transmission.

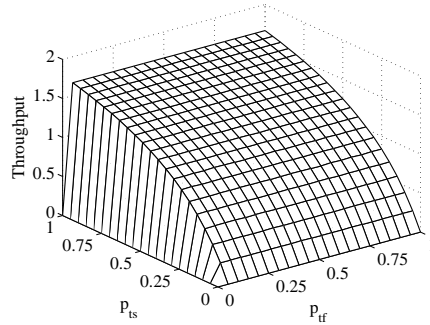


Figure 7-21: Throughput of the nodes at distance 1 for *Backward Model with Forced Idle Periods* for $r_1 = 1$, $r_2 = 2$, $n_1 = 5$, $n_2 = 15$, $z = 0.2$ and $t = 100K$ in the case where nodes stay idle for 2 slots after each successful transmission.

in the channel and there are $n_1 \simeq c$ nodes at distance $r_1 = 1$ and n_2 nodes at distance $r_2 = 2$. Figures 7-20, 7-21 and 7-22 show the total network throughput, the throughput of the nearby nodes and that of the distant nodes respectively, for $n_1 = 5$, $n_2 = 15$ and $z = 0.2$ ($c = 5$). The nodes stay idle for 2 slots after each successful transmission in these simulations.

The throughput plots for the same network settings but this time with nodes staying idle for 8 slots after a successful transmission are presented in Figures 7-23, 7-24 and 7-25.

7.5 Backward Model with Dynamic Contention Windows

As described in Section 6.2, *Backward Model with Dynamic Contention Windows* is a more practical protocol for implementing the *backward model* idea. Each node chooses a random

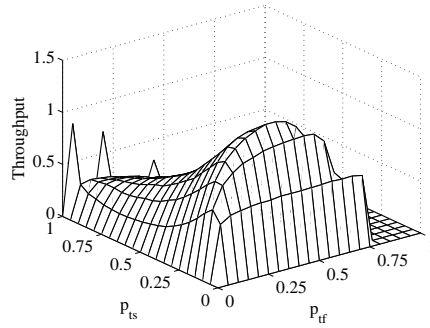


Figure 7-22: Throughput of the nodes at distance 2 for *Backward Model with Forced Idle Periods* for $r_1 = 1, r_2 = 2, n_1 = 5, n_2 = 15, z = 0.2$ and $t = 100K$ in the case where nodes stay idle for 2 slots after each successful transmission.

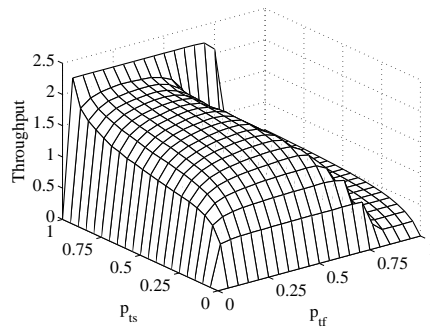


Figure 7-23: Total network throughput of the *Backward Model with Forced Idle Periods* for $r_1 = 1, r_2 = 2, n_1 = 5, n_2 = 15, z = 0.2$ and $t = 100K$ in the case where nodes stay idle for 8 slots after each successful transmission.

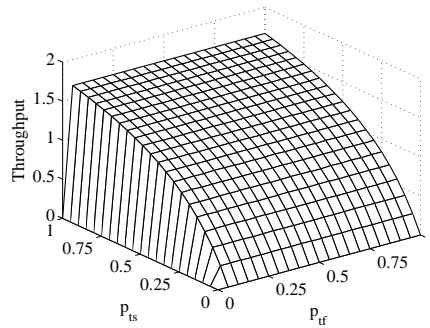


Figure 7-24: Throughput of the nodes at distance 1 for *Backward Model with Forced Idle Periods* for $r_1 = 1, r_2 = 2, n_1 = 5, n_2 = 15, z = 0.2$ and $t = 100K$ in the case where nodes stay idle for 8 slots after each successful transmission.

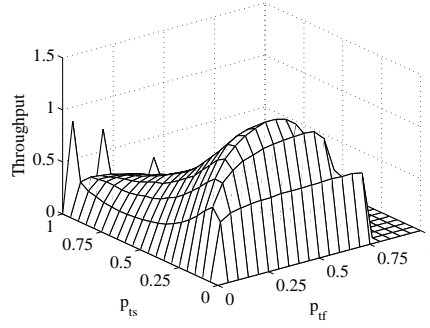


Figure 7-25: Throughput of the nodes at distance 2 for *Backward Model with Forced Idle Periods* for $r_1 = 1, r_2 = 2, n_1 = 5, n_2 = 15, z = 0.2$ and $t = 100K$ in the case where nodes stay idle for 8 slots after each successful transmission.

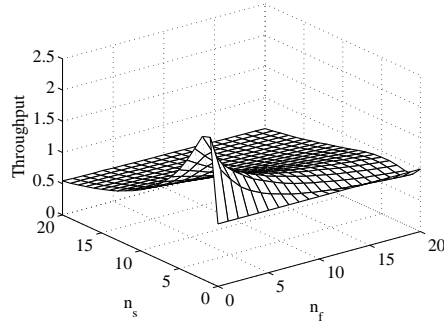


Figure 7-26: Total network throughput for *Backward Model with Dynamic Contention Windows* for $r_1 = 1, r_2 = 2, n_1 = 1, n_2 = 5, z = 0.2$ and $t = 100K$.

number uniformly distributed in the interval $[0, n_s]$ or $[0, n_f]$ if the last attempt of the node was a success or a failure respectively. Each node then decrements its counter by 1 in every slot and transmits with probability 1 when its counter reaches 0. We first evaluate the performance of this protocol when the node locations are deterministic and there is no fading in the system. The trials are repeated 100K times to have a good average over the randomness in the contention window sizes. We assume the settings of Section 5.2.1, namely, there are two possible distances from the receiver, $r_1 = 1$ and $r_2 = 2$ with n_1 and n_2 users at those distances respectively. The total network throughput, the total throughput of the nearby nodes and that of distant nodes as a function of several different n_s and n_f values for $n_1 = 1, n_2 = 5$ and $z = 0.2$ are displayed in Fig. 7-26, 7-27 and 7-28 respectively.

Figures 7-29, 7-30 and 7-31 respectively show the total network throughput, the total throughput of the nodes at distance 1 and that of the nodes at distance 2 for $n_1 = 2, n_2 = 10$

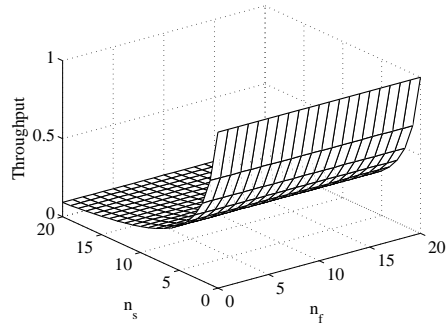


Figure 7-27: Total throughput of the nodes at distance 1 for *Backward Model with Dynamic Contention Windows* for $r_1 = 1, r_2 = 2, n_1 = 1, n_2 = 5, z = 0.2$ and $t = 100K$.

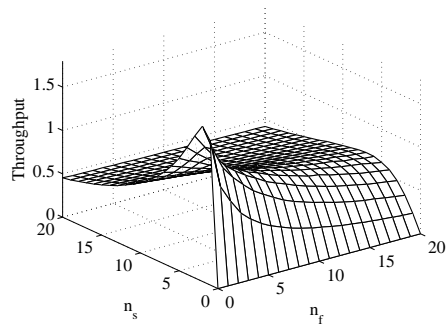


Figure 7-28: Total throughput of the nodes at distance 2 for *Backward Model with Dynamic Contention Windows* for $r_1 = 1, r_2 = 2, n_1 = 1, n_2 = 5, z = 0.2$ and $t = 100K$.

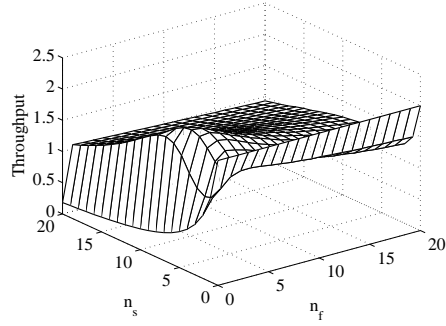


Figure 7-29: Total network throughput of the *Backward Model with Dynamic Contention Windows* for $r_1 = 1, r_2 = 2, n_1 = 2, n_2 = 10, z = 0.2$ and $t = 100K$.

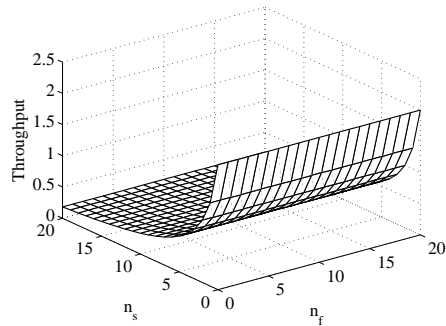


Figure 7-30: Total throughput of the nodes at distance 1 for *Backward Model with Dynamic Contention Windows* for $r_1 = 1, r_2 = 2, n_1 = 2, n_2 = 10, z = 0.2$ and $t = 100K$.

and $z = 0.2$.

Finally, we plot the total network throughput when there are 3 allowed distances from the receiver. Figures 7-32, 7-33, 7-34 and 7-35 show the total network throughput, the throughput of the node at distance 1, aggregate throughput of the nodes at distance 2 and that of the nodes at distance 3 respectively, for $n_1 = 1, n_2 = 3, n_3 = 9$ at distances $r_1 = 1, r_2 = 2$ and $r_3 = 9$.

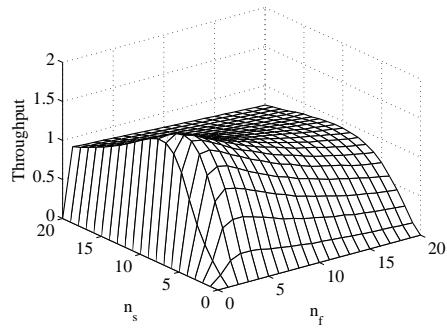


Figure 7-31: Total throughput of the nodes at distance 2 for *Backward Model with Dynamic Contention Windows* for $r_1 = 1, r_2 = 2, n_1 = 2, n_2 = 10, z = 0.2$ and $t = 100K$.

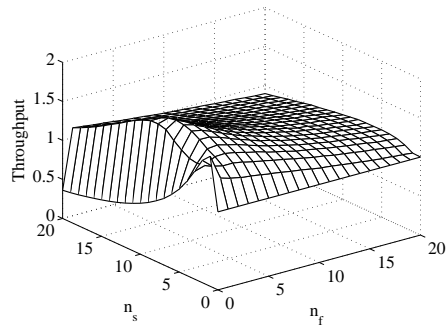


Figure 7-32: Total network throughput of the *Backward Model with Dynamic Contention Windows* for $r_1 = 1, r_2 = 2, r_3 = 3, n_1 = 1, n_2 = 3, n_3 = 9, z = 0.2$ and $t = 100K$.

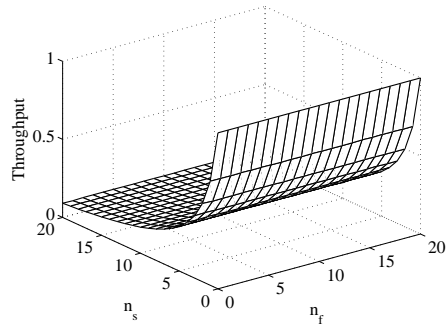


Figure 7-33: Throughput of the node at distance 1 for *Backward Model with Dynamic Contention Windows* for $r_1 = 1, r_2 = 2, r_3 = 3, n_1 = 1, n_2 = 3, n_3 = 9, z = 0.2$ and $t = 100K$.

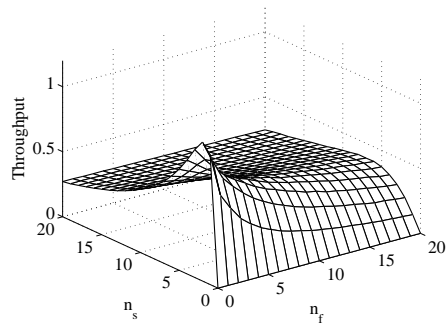


Figure 7-34: The aggregate throughput of the nodes at distance 2 for *Backward Model with Dynamic Contention Windows* for $r_1 = 1, r_2 = 2, r_3 = 3, n_1 = 1, n_2 = 3, n_3 = 9, z = 0.2$ and $t = 100K$.

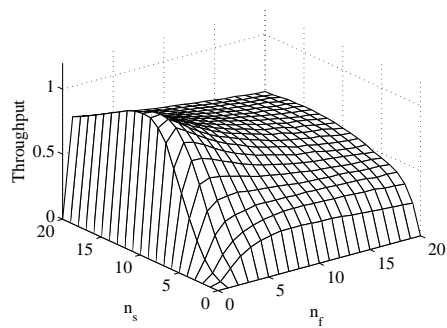


Figure 7-35: The aggregate throughput of the nodes at distance 3 for *Backward Model with Dynamic Contention Windows* for $r_1 = 1, r_2 = 2, r_3 = 3, n_1 = 1, n_2 = 3, n_3 = 9, z = 0.2$ and $t = 100K$.

Chapter 8

Conclusion and Future Work

Various different examples and analysis in this work illustrate the better performance of the so called *Backward Protocol* over the traditional MAC protocols for multipacket reception networks with spatially distributed nodes. We provide various analyses, approximate models and simulation results to show the validity of the idea that the *backward model* is preferable to the *forward model* in such networks. In particular we have given an exact analysis of the *Backward Protocol* when the node locations are known and no fading in the system. We proposed two different approximate models for this case and showed their validity through various results. We provided results using the approximate models for the cases where the exact analysis was cumbersome to formulate. Moreover, we provided simulation results for network settings where both the exact and the approximate analyses did not apply. We showed that the *Backward Protocol* achieves more fair results in all the cases and better throughput values in most of the cases considered. When there is multi-path fading in the system and the node locations are known in advance, we have proposed an approximate analysis and have shown the better performance of the *Backward Protocol* over the traditional *forward models*.

We formulated an approximate analysis when the nodes are randomly distributed on a plane without fading in the system and proved the validity of the approximation by comparing them with analytical results for specific cases. We were able to show that the *backward protocol* gives more chances to distant nodes and achieves similar throughput values even in the single packet capture case. We have given a different approximate model for the case

where the node locations are random and there is multipath fading in the system. We have demonstrated through simulations that in this general case the *backward model* achieves greater throughput than the *forward model*. We proposed a new protocol to remedy the throughput starvation of distant nodes when the node locations are deterministic and the number of nearby nodes is comparable to the maximum number of simultaneously successful transmissions. Finally, we proposed a more practical protocol than the *Backward Protocol* which carries the essence of the *backward model*. We showed through simulations that this protocol also achieves better throughput characteristics together with more fair results for most of the cases considered.

Our approach in this thesis is from a theoretical point of view, namely, the protocols we propose here are to show the validity of the idea behind them and more work is needed to come up with a full practical protocol. As a next step, we intend to develop and analyze more elaborate backoff mechanisms that will have several states and will utilize feedback from the receiver more efficiently. Furthermore, we intend to explore the option of using splitting (collision resolution) algorithms for the studied setting.

Finally, in most realistic scenarios a transmission can be received by more than one destination (multiple receivers). This provides diversity and flexibility that can be exploited by the MAC protocol. On the other hand, a transmission can interfere with other transmissions sent to a few different receivers. Thus, designing an efficient MAC protocol for such a setting is a challenging open problem. We would like to propose a protocol that will provide good performance (including fairness) in a situation in which there are multiple receivers with multi-packet reception capability.

Appendix A

Analytical solution of (4.3) and (4.4) in the case of two nodes

For $n = 2$ and $f_r(r) = 1$ we have;

$$\begin{aligned}\tau(r) &= \frac{p_{ts}}{1 + \left(\frac{p_{ts}}{p_{tf}} - 1\right) \int_0^{\alpha r} \tau(x) dx} \\ \frac{p_{ts}}{\tau(r)} &= 1 + \left(\frac{p_{ts}}{p_{tf}} - 1\right) \int_0^{\alpha r} \tau(x) dx \\ -\frac{p_{ts}}{\tau(r)^2} \frac{d\tau(r)}{dr} &= \left(\frac{p_{ts}}{p_{tf}} - 1\right) \tau(\alpha r) \alpha\end{aligned}\tag{A.1}$$

For $\alpha = 1$

$$\begin{aligned}\frac{d\tau(r)}{dr} &= -\frac{\left(\frac{p_{ts}}{p_{tf}} - 1\right) \tau(r)^3}{p_{ts}} \\ \tau(r) &= \frac{p_{ts}}{\sqrt{1 + 2p_{ts}\left(\frac{p_{ts}}{p_{tf}} - 1\right)r}}\end{aligned}\tag{A.2}$$

If $\alpha > 1$ a similar function can be obtained iteratively. Fig. A-1 shows that the results of numerical analysis are same as the analytical results.

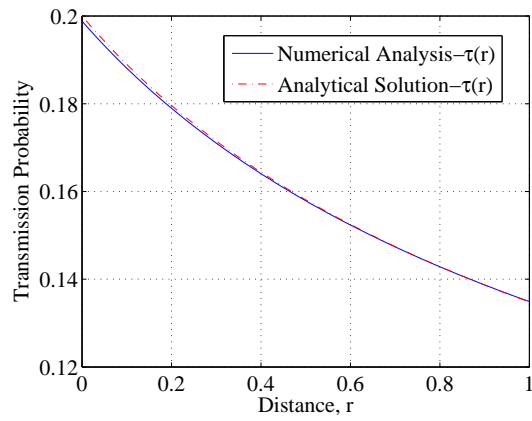


Figure A-1: The transmission probability obtained analytically and numerically as a function of distance for $p_{ts} = 0.2$, $p_{tf} = 0.05$, $\alpha = 1$ and uniform distribution of 2 nodes on a line.

Appendix B

The Transition Probabilities of The 1-Dimensional Markov Chain of Section

5.2.1

Denoting the probability of going from state (j) to (m) by $P_{j \rightarrow m}$ we have;

Case 1: $m > j$

$$\begin{aligned}
 & k \triangleq m - j \\
 P_{j \rightarrow m} = & \begin{cases} \left((1 - (1 - p_{ts})^{n_1}) \binom{n_2 - j}{k} p_{ts}^k (1 - p_{ts})^{n_2 - j - k} \right) & \text{if } m \leq c \\ \left((1 - (1 - p_{ts})^{n_1}) \binom{n_2 - j}{k} p_{ts}^k (1 - p_{ts})^{n_2 - j - k} + \right. \\ \left. + (1 - p_{ts})^{n_1} \binom{n_2 - j}{k} p_{ts}^k (1 - p_{ts})^{n_2 - j - k} \sum_{v=c+1-k}^j \binom{j}{v} p_{tf}^v (1 - p_{tf})^{j-v} \right) & \text{if } k \leq c \text{ and } m \geq c + 1 \\ \left(\binom{n_2 - j}{k} p_{ts}^k (1 - p_{ts})^{n_2 - j - k} \right) & \text{if } k \geq c + 1 \end{cases}
 \end{aligned}$$

Case 2: $m < j$

$$k \triangleq j - m$$

$$P_{j \rightarrow m} = \begin{cases} 0 & \text{if } k \geq c + 1 \\ (1 - p_{ts})^{n_1} \binom{j}{k} p_{tf}^k (1 - p_{tf})^{j-k} \sum_{v=0}^{c-k} \binom{n_2 - j}{v} p_{ts}^v (1 - p_{ts})^{n_2 - j - v} & \text{if } k \leq c \text{ and } n_2 - j \geq c - k \\ (1 - p_{ts})^{n_1} \binom{j}{k} p_{tf}^k (1 - p_{tf})^{j-k} & \text{if } k \leq c \text{ and } n_2 - j < c - k \end{cases}$$

Case 3: $m = j$

$$P_{j \rightarrow m} = P_1 + P_2 + P_3, \text{ where}$$

$$P_1 = (1 - (1 - p_{ts})^{n_1})(1 - p_{ts})^{n_2 - j} \quad (\text{B.1})$$

$$P_2 = \begin{cases} (1 - p_{ts})^{n_1} (1 - p_{tf})^j & \text{if } n_2 - j \leq c \\ (1 - p_{ts})^{n_1} (1 - p_{tf})^j \sum_{v=0}^c \binom{n_2 - j}{v} p_{ts}^v (1 - p_{ts})^{n_2 - j - v} & \text{if } n_2 - j \geq c + 1 \end{cases}$$

$$P_3 = \begin{cases} 0 & \text{if } j \leq c \\ (1 - p_{ts})^{n_1} (1 - p_{ts})^{n_2 - j} \sum_{v=c+1}^j \binom{j}{v} p_{tf}^v (1 - p_{tf})^{j-v} & \text{if } j > c \end{cases}$$

Appendix C

Edmundson-Madansky Inequality

Theorem 3 (*Edmundson-Madansky Inequality*) Let g be a convex function on $[a, b]$ and k a random variable that takes values in the interval $[a, b]$. Let \bar{k} be the expected value of k . Then

$$E[g(k)] \leq \frac{b - \bar{k}}{b - a}g(a) + \frac{\bar{k} - a}{b - a}g(b). \quad (\text{C.1})$$

Proof: We have $a \leq k \leq b$ and we can write k as

$$k = \frac{b - k}{b - a}a + \frac{k - a}{b - a}b \quad (\text{C.2})$$

Since g is convex, we have

$$g(k) \leq \frac{b - k}{b - a}g(a) + \frac{k - a}{b - a}g(b) \quad (\text{C.3})$$

Taking the expected values of both sides we obtain (C.1). \square

Bibliography

- [1] N. Abramson. The throughput of packet broadcasting channels. *IEEE Trans. Commun.*, 25(1):117–128, January 1977.
- [2] J. C. Arnbak and W. Blitterswijk. Capacity of slotted ALOHA in rayleigh-fading channels. *IEEE J. Sel. Areas Commun.*, 5(2):261–269, February 1987.
- [3] B. Bensaou, Y. Wang, and C. C. Ko. Fair medium access in 802.11 based wireless ad-hoc networks. In *Proc. ACM Mobihoc'00*, August 2000.
- [4] D. Bertsekas and R. Gallager. *Data Networks*. Prentice Hall, Englewood Cliffs, NJ, 1987.
- [5] Vaduvur Bharghavan, Alan Demers, Scott Shenker, and Lixia Zhang. MACAW: a media access protocol for wireless LAN's. In *Proc. ACM SIGCOMM'94*, August 1994.
- [6] G. Bianchi. Performance analysis of the IEEE 802.11 distributed coordination function. *IEEE J. Sel. Areas Commun.*, 18(3):535–547, March 2000.
- [7] M. M. Carvalho and J. J. Garcia-Luna-Aceves. A scalable model for channel access protocols in multihop ad hoc networks. In *Proc. ACM Mobicom'04*, Sept. 2004.
- [8] D.S. Chan and T. Berger. Performance and cross-layer design of CSMA for wireless networks with multipacket reception. In *Proc. IEEE Asilomar'04*, volume 2, pages 1917–1921, November 2004.
- [9] I. Chlamtac and A. Farago. An optimal channel access protocol with multiple reception capacity. *IEEE Trans. Comput.*, 43(4):480–484, April 1994.
- [10] Y. Chu and A. Ganz. A centralized MAC protocol for QoS support in UWB-based wireless networks. *Wireless Comm. and Mobile Comp.*, 34(1-2):45–66, July 2005.
- [11] I. Cidon, H. Kodesh, and M. Sidi. Erasure, capture and random power level selection in multi-access systems. *IEEE Trans. Commun.*, 36(3):263–271, March 1988.
- [12] M. Coupechoux, B. Baynat, T. Lestable, V. Kumar, and C. Bonnet. Improving the MAC layer of multi-hop networks. *Wirel. Pers. Commun.*, 29(1-2):71–100, 2004.

- [13] M. Coupechoux, T. Lestable, C. Bonnet, and V. Kumar. Throughput of the multi-hop slotted Aloha with multi-packet reception. in *Proc. WONS'04*, Lecture Notes in Computer Science, vol. 2928, pp. 301-314, 2004.
- [14] F. Cuomo, C. Martello, A. Baiocchi, and C. Fabrizio. Radio resource sharing for ad hoc networking with UWB. *IEEE J. Sel. Areas Commun.*, 20(9):1722–1732, December 2002.
- [15] J. del Prado Pavon, S. Shankar N, V. Gaddam, K. Challapali, and C-T. Chou. The MBOA-WiMedia specification for ultra wideband distributed networks. *IEEE Commun.*, 44(6):128–134, June 2006.
- [16] M.-G. Di Benedetto, L. De Nardis, M. Junk, and G. Giancola. (UWB)²: uncoordinated, wireless, baseborn, medium access control for UWB communication networks. *ACM/Springer MONET*, 10(5):663–674, October 2005.
- [17] M. Garetto, T. Salonidis, and E. Knightly. Modeling per-flow throughput and capturing starvation in CSMA multi-hop wireless networks. In *Proc. IEEE INFOCOM'06*, April 2006.
- [18] S. Ghez, S. Verdu, and S. C. Schwartz. Stability properties of Slotted Aloha with multipacket reception capability. *IEEE Trans. Autom. Control*, 33(7):640–649, July 1988.
- [19] S. Ghez, S. Verdu, and S. C. Schwartz. Optimal decentralized control in random-access multipacket channel. *IEEE Trans. Autom. Control*, 34:1153–1163, November 1989.
- [20] G. Giancola, C. Martello, F. Cuomo, and M.-G. Di Benedetto. Radio resource management in infrastructure-based and ad hoc UWB networks. *Wireless Comm. and Mobile Comp.*, 5(5):581–597, 2005.
- [21] P. Gupta and P. R. Kumar. The capacity of wireless networks. *IEEE Trans. Inf. Theory*, 46(2):388–404, March 2000.
- [22] Z. Hadzi-Velkov and B. Spasenovski. Capture effect in IEEE 802.11 basic service area under influence of rayleigh fading and near far effect. In *Proc. IEEE PIMRC'02*, Sept. 2002.
- [23] Z. Hadzi-Velkov and B. Spasenovski. On the capacity of IEEE 802.11 DCF with capture in multipath-faded channels. *Int. J. of Wireless Inf. Net.*, 9(3):191–199, July 2002.
- [24] Z. Hadzi-Velkov and B. Spasenovski. Capture effect with diversity in IEEE 802.11b DCF. In *Proc. IEEE ISCC'03*, June 2003.
- [25] B. Hajek, A. Krishna, and R. O. LaMaire. On the capture probability for a large number of stations. *IEEE Trans. Commun.*, 45(2):254–260, February 1997.

- [26] R. Jurdak, P. Baldi, and C. V. Lopes. U-MAC: a proactive and adaptive UWB medium access control protocol. *Wireless Comm. and Mobile Comp.*, 5(5):551–566, 2005.
- [27] A. Krishna and R. O. LaMaire. A comparison of radio capture models and their effect on wireless lan protocols. In *Proc. IEEE ICUPC'94*, Sept. 1994.
- [28] F. Kuperus and J. Arnbak. Packet radio in a rayleigh channel. *Electron. Lett.*, 18(12):506–507, 1982.
- [29] R. O. LaMaire, A. Krishna, and M. Zorzi. On the randomization of transmitter power levels to increase throughput in multiple access radio systems. *Wireless Networks*, 4(3):263–277, March 1998.
- [30] C. T. Lau and C. Leung. Capture models for model packet radio networks. *IEEE Trans. Commun.*, 40(5):917–925, May 1992.
- [31] N. Likhanov, E. Plotnik, Y. Shavitt, M. Sidi, and B. Tsybakov. Random access algorithms with multiple reception capability and N-Ary feedback channel. *Problemy Peredachi Informatsii*, 29(1):82–91, 1993.
- [32] J. P. Linnartz. *Narrowband Land-Mobile Radio Networks*. Artech House, Inc., Norwood, MA, 1993.
- [33] W. Luo and A. Ephremides. Power levels and packet lengths in random multiple access. *IEEE Trans. Inf. Theory*, 48(1):46–58, January 2002.
- [34] W. Luo and A. Ephremides. Power levels and packet lengths in random multiple access with multiple-packet reception capability. *IEEE Trans. Inf. Theory*, 52(2):414–420, February 2006.
- [35] A. B. MacKenzie and S. B. Wicker. Stability of multipacket Slotted Aloha with selfish users and perfect information. In *Proc. IEEE INFOCOM'03*, April 2003.
- [36] M.H. Manshaei, G. R. Cantieni, C. Barakat, and T. Turletti. Performance analysis of the IEEE 802.11 MAC and physical layer protocol. In *Proc. IEEE WoWMoM'05*, 2005.
- [37] G. Mergen and L. Tong. Receiver controlled medium access in multihop ad hoc networks with multipacket reception. In *Proc. IEEE MILCOM'01*, October 2001.
- [38] G. Mergen and L. Tong. Random scheduling medium access for wireless ad hoc networks. In *Proc. IEEE MILCOM'02*, October 2002.
- [39] R. Merz, J. Widmer, J.-Y. Le Boudec, and B. Radunovic. A joint PHY/MAC architecture for low-radiated power TH-UWB wireless ad-hoc networks. *Wireless Commun. and Mobile Comp.*, 5(5):567–580, August 2005.
- [40] J.J. Metzner. On improving utilization in ALOHA networks. *IEEE Trans. Commun.*, 24(4):447–448, April 1976.

- [41] T. Nandagopal, T. Kim, X. Gao, and V. Bhargavan. Achieving MAC layer fairness in wireless packet networks. In *Proc. ACM Mobicom'00*, August 2000.
- [42] G.D. Nguyen, A. Ephremides, and J.E. Wieselthier. Comments on “capture and re-transmission control in mobile radio”. *IEEE J. Sel. Areas Commun.*, 24(12):2340–2341, December 2006.
- [43] G.D. Nguyen, J.E. Wieselthier, and A. Ephremides. Accurate capture models and their impact on random access in multiple-destination networks. In *Proc. IEEE MIL-COM'06*, October 2006.
- [44] A. Nyandoro, L. Libman, and M. Hassan. Service differentiation in wireless LANs based on capture. In *Proc. IEEE GLOBECOM'05*, December 2005.
- [45] M. C. H. Peh, S. V. Hanly, and P. Whiting. Random access with multipacket reception over fading channels. In *Proc. Australian Commun. Theory Workshop'03*, February 2003.
- [46] B. Radunovic and J. Y. Le Boudec. Optimal power control, scheduling and routing in UWB networks. *IEEE J. Sel. Areas Commun.*, 22(7):1252–1270, Sept. 2004.
- [47] A. Rajeswaran, G. Kim, and R. Negi. A scheduling framework for UWB and cellular networks. In *Proc. Broadnets'05*, October 2005.
- [48] M. Realp and A. I. Perez-Neira. Multipacket MAC for multiple antenna systems: a cross-layer approach. In *Proc. IEEE SAM'02*, July 2004.
- [49] M. Realp and A.I. Perez-Neira. PHY-MAC dialogue with multi-packet reception. In *ETSI Workshop on Broadband Wireless Ad-hoc Networks and Services*, Sept. 2002.
- [50] Lawrence G. Roberts. ALOHA packet system with and without slots and capture. *SIGCOMM Comput. Commun. Rev.*, 5(2):28–42, 1975.
- [51] R. Rom and M. Sidi. *Multiple Access Protocols: Performance and Analysis*. Springer-Verlag, New York, 1990.
- [52] J. Sant and V. Sharma. Performance analysis of a Slotted-ALOHA protocol on a capture channel with fading. *Queueing Syst., Theory Applic.*, 34(1):1–35, 2000.
- [53] N. Shacham. Throughput-delay performance of packet-switching multiple access channel with power capture. *Perfor. Eval.*, 4(3):153–170, August 1984.
- [54] F. Shad, T. D. Todd, V. Kezys, and J. Litva. Dynamic slot allocation (dsa) in indoor sdma/tdma using a smart antenna basestation. *IEEE/ACM Trans. Netw.*, 9(1):69–81, February 2001.
- [55] Y. Shi, Y. T. Hou, H. D. Sherali, and S. F. Midkiff. Cross-layer optimization for routing data traffic in UWB-based sensor networks. In *Proc. ACM Mobicom'05*, August 2005.

- [56] L. Tong, Q. Zhao, and G. Mergen. Multipacket reception in random access wireless networks: From signal processing to optimal medium access control. *IEEE Commun.*, 39(11):108–112, November 2001.
- [57] M. Z. Win and R. A. Scholtz. Ultra-wide bandwidth time-hopping spread-spectrum impulse radio for wireless multiple-access communications. *IEEE Trans. Commun.*, 48:679–691, April 2000.
- [58] Y. Yu, X. Cai, and G. B. Giannakis. On the instability of Slotted Aloha with capture. In *Proc. IEEE WCNC'04*, March 2004.
- [59] Q. Zhao and L. Tong. A multiqueue service room MAC protocol for wireless networks with multipacket reception. *IEEE/ACM Trans. Netw.*, 11(1):125–137, February 2003.
- [60] Q. Zhao and L. Tong. A dynamic queue protocol for multiaccess wireless networks with multipacket reception. *IEEE Trans. Wireless Commun.*, 3(6):2221–2231, November 2004.
- [61] M. Zorzi. Mobile radio slotted ALOHA with capture, diversity and retransmission control in the presence of shadowing. *Wirel. Netw.*, 4(5):379–388, 1998.
- [62] M. Zorzi and R.R. Rao. Capture and retransmission control in mobile radio. *IEEE J. Sel. Areas Commun.*, 12(8):1289–1298, October 1994.
- [63] M. Zorzi and R.R. Rao. Reply to “comments on ‘capture and retransmission control in mobile radio’”. *IEEE J. Sel. Areas Commun.*, 24(12):2341–2342, December 2006.